

BSIM-BULK 107.2.0 Beta0_2 MOSFET Compact Model

Technical Manual

Authors:

**Yawar Hayat Zarkob, Ayushi Sharma, Dinesh Rajasekharan,
Chetan K. Dabhi, Girish Pahwa, Yogesh Singh Chauhan,
Sayeef Salahuddin and Chenming Hu**

Project Director:

Prof. Sayeef Salahuddin and Prof. Chenming Hu

**Department of Electrical Engineering and Computer Sciences
University of California, Berkeley, CA 94720**

Copyright © 2023 University of California

**This work is licensed under the Creative Commons Attribution 4.0
International License. To view a copy of this license, visit
<http://creativecommons.org/licenses/by/4.0/> or send a letter to Creative
Commons, PO Box 1866, Mountain View, CA 94042, USA.**

Past Developers :

Ravi Goel, IIT Kanpur
Harshit Agarwal, UC Berkeley
Chetan Gupta, IIT Kanpur
Sourabh Khandelwal, UC Berkeley
Huan-Lin Chang, UC Berkeley
Navid Paydavosi, UC Berkeley
Sriramkumar Venugopalan, UC Berkeley
Pankaj Thakur, UC Berkeley
Mohammed A. Karim, UC Berkeley

Contents

1	RELEASE NOTES	9
1.1	Updates made in BSIM-BULK107.2.0 Beta0_2	9
1.2	Updates made in BSIM-BULK107.2.0 Beta0_1	9
1.3	Updates made in BSIM-BULK107.1.0	10
1.4	Updates made in BSIM-BULK107.0.0	13
1.5	Updates made in BSIM-BULK106.2.0	16
2	BSIM-BULK Model Equations	20
2.1	Physical constants	20
2.2	Effective Channel Length & Width	21
2.3	Binning Calculations	21
2.4	Global geometrical scaling	22
2.5	Terminal Voltages	27
2.6	Pinch-off Potential and Normalized Charge Calculation	28
2.6.1	Pinch-off Potential with Poly Depletion	28
2.6.2	Normalized Charge Density	30
2.7	Short Channel Effects	34
2.8	Drain Saturation Voltage	36
2.9	Mobility degradation with vertical field	37
2.10	Parasitic series resistance	38
2.10.1	Bias Independent External Series Resistance, Bias Dependent Internal Resistance (RDSMOD=0)	38
2.10.2	Bias Dependent External Series Resistance ($R_s(V)$ & $R_d(V)$)	38
2.10.3	Bias Dependent Internal Resistance (RDSMOD=2)	39
2.10.4	Sheet resistance model	40
2.11	Output Conductance	40
2.12	Velocity Saturation	42

2.13	Effective Mobility	43
2.14	Drain Current Model	43
2.14.1	Without Velocity Saturation	43
2.14.2	Including Velocity Saturation	44
2.15	Threshold Voltage Model	46
2.15.1	Long Channel Threshold Voltage	46
2.16	MNUD model to increase $I_{DS} - V_{DS}$ Fitting Flexibility	47
2.17	MNUD1 model to increase $g_m - I_D$ Fitting Flexibility	47
2.18	AbulkIV model to increase $I_{DS} - V_{DS}$ Fitting Flexibility	48
2.19	Subthreshold Hump Module	48
2.20	Modeling of Sub-Surface Leakage Drain Current	49
2.21	Impact Ionization Model	49
2.22	GIDL/GISL Current Model	50
2.23	Gate Tunneling Current Model	51
2.23.1	Model Selectors	52
2.23.2	Equations for Tunneling Currents	53
2.24	Gate resistance and Body resistance network Model	55
2.24.1	Gate Electrode Electrode and Intrinsic-Input Resistance (IIR) Model	55
2.24.2	Substrate Resistance Network	57
2.25	Noise Modeling	61
2.25.1	Flicker Noise Models	61
2.25.2	Channel Thermal Noise	66
2.25.3	Gate Current Shot Noise	68
2.25.4	Resistor Noise	68
2.26	Self Heating Model	69
3	Asymmetric MOS Junction Diode Models	69
3.1	Junction Diode IV Model	69
3.2	Junction Diode CV Model	72

4 Layout dependent Parasitics Models	74
4.1 Layout-Dependent Parasitics Models	74
4.1.1 Geometry Definition	74
4.1.2 Model Formulation and Options	75
5 Temperature dependence Models	78
5.1 Temperature Dependence Model	78
5.1.1 Length Scaling of Temperature parameters	78
5.1.2 Temperature Dependence of Threshold Voltage	79
5.1.3 Temperature Dependence of Mobility	79
5.1.4 Temperature Dependence of Saturation Velocity	79
5.1.5 Temperature Dependence of LDD Resistance	80
5.1.6 Temperature Dependence of Junction Diode IV	80
5.1.7 Temperature Dependence of Junction Diode CV	82
5.1.8 Temperature Dependences of E_g and n_i	84
6 Stress effect Model Development	84
6.1 Stress Effect Model	84
6.1.1 Stress Effect Model Development	85
6.1.2 Effective SA and SB for Irregular LOD	88
7 Well Proximity Effect Model	89
7.1 Well Proximity Effect Model	89
8 High Voltage Model	91
8.1 High Voltage Model	91
8.2 Drift Resistance Model Equations	92
8.3 Decoupling Drain-side Drift Resistance	95
8.4 Substrate Resistance Network for HVMOS	95
8.5 Parameter Extraction for DC: Guideline	95

8.5.1	Id-Vg Sub-threshold region	96
8.5.2	Id-Vg Above threshold region, low drain bias	96
8.5.3	Id-Vd Characteristics	96
8.5.4	Capacitance Parameters and their impact	97
9	C-V Model	98
10	Parameter Extraction Procedure	107
10.1	Extraction of Geometry Independent Parameters	108
10.1.1	Gate Capacitance C_{GG} vs. V_G Analysis @ $V_S = 0 V$, $V_D = 0 V$ & $V_B = 0 V$	108
10.1.2	Drain Current I_D vs. V_G Analysis @ $V_D = [V_{D,lin}, V_{D,sat}]$, $V_S = 0 V$ & $V_B = 0 V$	109
10.1.3	Gate Current I_G vs. V_G Analysis @ various V_D , $V_S = 0 V$ & $V_B = 0 V$	110
10.1.4	Drain Current I_D vs. V_D Analysis @ various V_G , $V_S = 0 V$ & $V_B = 0 V$	111
10.1.5	Gate Capacitance C_{GG} vs. V_G Analysis @ $V_{DS} \neq 0 V$ & $V_B = 0 V$	111
10.1.6	Drain Current I_D vs. V_G Analysis @ $V_D = [V_{D,lin}, V_{D,sat}]$ & various V_B	111
10.1.7	Fitting Verification	112
10.2	Extraction of Short Channel Effects & Length Scaling Parameters	112
10.2.1	Gate Capacitance C_{GG} vs. V_G Analysis @ $V_S = 0 V$, $V_D = 0 V$ & $V_B = 0 V$	113
10.2.2	Drain Current I_D vs. V_G Analysis @ $V_D = [V_{D,lin}, V_{D,sat}]$, $V_S = 0 V$ & $V_B = 0 V$	113
10.2.3	I_G vs. V_G Analysis @ various V_D , $V_S = 0 V$ & $V_B = 0 V$	115
10.2.4	I_D vs. V_D Analysis @ various V_G , $V_S = 0 V$ & $V_B = 0 V$	115
10.2.5	C_{GG} vs. V_G Analysis @ $V_{DS} \neq 0 V$ & $V_B = 0 V$	116
10.2.6	I_D vs. V_G Analysis @ $V_D = [V_{D,lin}, V_{D,sat}]$ & various V_B (or various V_S)	116
10.2.7	Fitting Verification	117

10.3 Extraction of Narrow Channel Effects & Width Scaling Parameters	117
10.3.1 Gate Capacitance C_{GG} vs. V_G Analysis @ $V_S = 0 V$, $V_D = 0 V$ & $V_B = 0 V$	117
10.3.2 Drain Current I_D vs. V_G Analysis @ $V_D = [V_{D,lin}, V_{D,sat}]$, $V_S = 0 V$ & $V_B = 0 V$	118
10.3.3 Gate Current I_G vs. V_G Analysis @ various V_D , $V_S = 0 V$ & $V_B = 0 V$	119
10.3.4 Gate Capacitance C_{GG} vs. V_G Analysis @ $V_{DS} \neq 0 V$ & $V_B = 0 V$	119
10.3.5 Drain Current I_D vs. V_G Analysis @ $V_D = [V_{D,lin}, V_{D,sat}]$ & various V_B (or various V_S)	119
10.3.6 Fitting Verification	119
10.4 Extraction of Parameters for Narrow/Short Channel Devices	120
10.4.1 Gate Capacitance C_{GG} vs. V_G Analysis @ $V_S = 0 V$, $V_D = 0 V$ & $V_B = 0 V$	120
10.4.2 Drain Current I_D vs. V_G Analysis @ $V_D = [V_{D,lin}, V_{D,sat}]$, $V_S = 0 V$ & $V_B = 0 V$	120
10.4.3 C_{GG} vs. V_G Analysis @ $V_{DS} \neq 0 V$ & $V_B = 0 V$	121
10.4.4 Drain Current I_D vs. V_G Analysis @ $V_D = [V_{D,lin}, V_{D,sat}]$ & various V_B (or various V_S)	122
10.4.5 Fitting Verification	122
10.5 Extraction of Impact Ionisation parameters	122
10.5.1 Extraction in Intrinsic region	122
10.5.2 Extraction in Drift region	123
10.6 Extraction of Conductivity Modulation parameters for HV FETs	123
10.7 Extraction of Temperature Dependence Parameters	123
10.7.1 Wide & Long Channel Devices	123
10.7.2 Length Scaling of Wide Channel Devices	125
11 Instance Parameters	127
12 Model Controllers and Process Parameters	128

13 Basic Model Parameters	131
14 Both model and instance parameters	140
15 High-Speed/RF Model Parameters	141
16 Flicker and Thermal Noise Model Parameters	143
17 Layout-Dependent Parasitic Model Parameters	145
18 Asymmetric Source/Drain Junction Diode Model Parameters	146
19 Temperature Dependence and Self Heating Parameters	149
20 Stress Effect Model Parameters	151
21 Well-Proximity Effect Parameters	153
22 Parameters for Edge FET and Sub-Surface Leakage Current	154
23 Parameters for High Voltage Model	156
24 Parameter equivalence between BSIM-BULK & BSIM4	159
25 Appendix A : Smoothing Function	163
25.1 Polynomial Smoothing	163
26 Appendix B : Derivation of Bulk charge with poly-depletion effect	167
26.1 Bulk charge with polydepletion effect	167
27 Acknowledgements	187

1 RELEASE NOTES

1.1 Updates made in BSIM-BULK107.2.0 Beta0_2

- Flicker noise model enhancement
- Decoupling drain-side drift resistance for capacitance calculations
- Issue in C_{GD} reciprocity while exercising QM parameters
- MULT implementation correction
- Correction in units of binning parameters
- Removing variables that were superfluously assigned
- Addressing the bias-dependent \$strobe warnings reported by VAMPyRE

1.2 Updates made in BSIM-BULK107.2.0 Beta0_1

- Accuracy enhancement in Impact Ionization model of Intrinsic MOSFET
- Accuracy enhancement in Impact Ionization model of Drift region
- Modeling of conductivity modulation (Expansion) effect
- To improve reverse Vds impact ionization current
- Introduction of MULT parameters (MULT_I, MULT_Q, MULT_FN)
- Correction in substrate current flow

- Better implementation of ln_one_plus_ex()
- Code cleaning
- Negative C_{GD} in BSIM_BULK
- Typo in the bulk charge expression in manual
- Noise QA test results have values less than simulator tolerance
- Correction in exponent factor of Electric field expression in drift region

1.3 Updates made in BSIM-BULK107.1.0

- Abulk Implementation in I-V
- Flexibility in tuning C_{gg}
- Enhancing the fitting flexibility of C_{gd} at high V_{ds}
- Add the flicker noise for drain and source resistance
- Modeling of Drift region with back bias in HV extension
- New well proximity parameters for EDGEFET
- Flat band voltage scaling parameters for I-V
- Improvement to the implementation of body-drain diode
- Gate bias dependence in the depletion model of drift region

- Improved Modeling of $I_{ds} - V_{ds}$ at high V_{gs} and V_{ds} for HV model
- ‘gamCV’ instead of ‘gam’ in VdsatCV equation
- Manual Update (Temperature dependent parameter list update in BSIM-BULK 107 manual)
- Change default values of model parameters related to CVMOD = 1
- Minimize division by Rdrain and Rsource
- Issues raised by VAMPyRE
- Improved flexibility in Asymmetry mode
- IDEFF and ISEFF
- Convergence issue due to DVT2EDGE
- Clamping of Gate electrode resistance in RGATEMOD=2
- Limit XRCRG1 and XRCRG2 parameters
- Remove IIMOD mode selector
- Issues raised by VAMPyRE
- Revert IIMOD changes to BSIM-BULK 107.0.0.
- Missing multiplication factor in 2nd instance of T5 in Rdss=0
- Remove redundant calculation of Rdss in RDSSMOD =2

- Improved smoothing of drift resistance in HV module
- Correct the description of RBPD parameter
- Typo in the comment of Drain junction current(IBD).
- Node order correction in the body-drain diode for HV model.
- Removing extra contribution of Ibd in the HV model.
- Drain-body junction current splitting in RBODYHVMOD.
- Protection for junction capacitance grading coefficient (MJX) against 0/0 form.
- Smoothing function for psiph.
- Default values of body bias dependent parameters in HVMOD.
- Unit correction of source and drain resistances.
- Id-Vg shows spikes in transient simulation.
- Operating point should include charge Qbdj_ext from external diode.
- Changing lln to ln for junction capacitance calculation in VA code.
- Clamping Nsat for non-saturation effect.
- Correction in JunCap macro.
- VAMPyRE error in operating-point variable IDRIFTSATD.

- Limit model parameter MDRIFT.
- Add QA test to check the missing parameters
- Allow minr=0.
- Model parameter ABULK added for backward compatibility.
- keyLetter x is added for Smartspice/ELDO simulator in QA pearl script
- Encountered divide by zero error with node (g,b)
- Typo Correction in gspr
- Divide by zero error when parameters DMCG/(DMCG+DMCI) are zero
- Limit the layout-dependent parasitic model parameters
- Code cleaning

1.4 Updates made in BSIM-BULK107.0.0

- Resolved the Kink in the I_{DS} issue for large values of PSATB for $V_{BS} \neq 0$.
- Added a model to enhance the Tuning Flexibility of G_m/I_d .
- Added *ABULK* parameter to enhance the flexibility of Tuning C_{gg} in Strong Inversion for $V_{ds} \neq 0$.
- Negative Cbg issue for CVMOD =0
- Add temperature dependence for the parameter EU.

- Changed the default value of the parameter "LH".
- Improved Flicker noise model for L<=LH.
- Warning message for FNOIMOD=1
- Enhance the BSIMBULK flicker noise tuning flexibility.
- Evaluating K2_EDGE and ETA0_EDGE independent of STI stress model.
- Device Type implementation in sub-surface leakage model.
- Abnormal flicker noise performance when EDGEFET=1.
- Aligning BSIMBULK 1/f behavior with BSIM4 1/f behavior.
- Corrected implementation of sub-surface leakage model.
- Enhancing the tuning flexibility in the flicker noise model.
- Add flicker noise due to EDGEFET.
- Correction in description of parameters.
- Discrepancy in thermal noise model.
- Impact of non-zero C0 on thermal noise.
- Issue with the PSS (periodic state analysis).
- Implementation of ABULK is updated.

- ‘phib’ and ‘gam’ are replaced by ‘phibCV’ and ‘gamCV’ respectively in CVMOD=1.
- NDEPEDGE and its binning.
- Description of TNOIMOD=1 in manual.
- Code Cleaning.
- Node collapsing and minimum value of Rdrain/Rsource.
- GDS Op-pt definition.
- Incorrect IGBBACC behavior in the accumulation region.
- Enhancement for High Voltage modeling.
- Warning Message for $U_0 \leq 0$
- Range of model parameters.
- Default value of NDEPEDGE.
- Kink in DC current due to PSATB.
- Rollback MNUD and MNUD1 from thermal noise model.
- Addressing IGBACC issue.
- Add GMIN across D-B and S-B junctions.
- Missing type in sub-surface leakage model.

- External/Internal node issue in sub-surface leakage model.
- HVMOD issue - CV model.
- Secondary impact ionization in HVMOD.
- Implementing sigvds in flicker_noise.

1.5 Updates made in BSIM-BULK106.2.0

- Added a Modified Flicker noise model to model the low frequency noise for Halo transistors.
- Added modified function of $VDSX$ to avoid negative G_{DS} issue.
- $MNUD$ model to increase flexibility in I_{DS} - V_{DS} fitting.
- Removed kink around $V_{DS} = 0$ for $GIDLMOD = 1$.
- Improved Gamma behaviour in the linear Region for $TNOIMOD = 1$.
- Model for Sub-Surface leakage (between drain and source) added. $FLAG-SSLMOD$.
- Stress model has added to $EDGEFET$.
- Added parameters for $EDGEFET$ to control threshold voltage shift $KVTH0EDGE$, $STK2EDGE$ and $STETA0EDGE$ and kept their length and width parameters same as main BSIM-BULK.
- Sign correction in the charge calculations.

- Parameters *EDGEFET* and *DELVT0* have made instance parameter.
- *EDGEFET* SCE model made similar to main BSIM6 to avoid convergence at large L.
- Protection on *DLCIG* and *DLCIGD* from going negative.
- Hidden states during *PSS* have been resolved.
- Variables - *LOCALSCA*, *LOCALSCB* and *LOCALSCC* are initialized to avoid warnings.
- Removed clamping from *UCR*.
- Added protection to the following parameters: *LP1*, *LP2*, *NJS*, *NJD*, *XJBVS* and *XJBVD*.
- Added description for all the parameters in the Verilog-A code.
- Added *K2EDGE* parameter for V_{TH} shift with body bias for *EDGEFET*.
- Default values of Stress parameters for *EDGEFET* are set same as main parameters.
- Use limited log in fringe Capacitance Module.
- Removed hidden states in *EDGEFET* variables : *K2_EDGE*, *ETA0_EDGE*, *Eta_Stress_EDGE*.
- Added type="instance" for all instance parameters declaration in the macros definition just like in BSIM-CMG and BSIM-IMG.
- Modified Thermal noise model to tune *NF50* in Sub-threshold region and to achieve ideal trend of gamma for long channel transistors.

- Added Clamping in I_{GD} and I_{GS} .
- Added Self-Heating output variables.
- Deactivated node "T" when $RTH0$ or $SHMOD$ or both are zero.
- Used $SRCFLAG$ as the formal argument of $BSIM6RdsEndSha$ and $BSIM6RdseffGeo$ in place of $TYPE$.
- Modified Calculations of Geometry-dependent source/drain resistance.
- Multiplied with $DEVSIGN$ in the Operating point V_{TH} expression.
- Limit $(W_{eff} + W_{TH0})$ to $(W_{eff} + W_{TH0}) > 0$ in Self Heating module.
- Module name has changed from *bsim6* to *bsimbulk*.
- Added CLM and Velocity Saturation terms of the Charge Expressions in manual.
- Added binning in the $EDGEFET$ parameters.
- Removed all the "*ifdef*" statements from the code.
- Node collapsing has been done for " $SHMOD = 0$ " and " $TNOIMOD = 0$ ". Since we had removed '*define_TNOISW_*' and '*define_SHMOD_*' .
- Every "*IF*" and "*ELSE*" statement starts with "*begin*" and ends with the "*end*" statement.
- Modified the name of the parameter "*MULUO*" to "*MULU0*".
- Align the Stress module conditioning similar to *BSIM4*.

- SCA , SCB , SCC and SC are allowed to take real number, instead of integer.
- $DTEMP$, $MULU0$, $DELVTO$ and $IDS0MULT$ have modified to both instance and model parameters.
- Added units for all the parameters of $BSIM - BULK$ 106.2.0 Verilog-A code and manual.

2 BSIM-BULK Model Equations

2.1 Physical constants

Physical quantities are in M.K.S units unless specified otherwise.

$$q = 1.6 \times 10^{-19} C \quad (2.1)$$

$$\epsilon_0 = 8.8542 \times 10^{-12} \frac{F}{m} \quad (2.2)$$

$$\epsilon_{sub} = EPSRSUB \cdot \epsilon_0 \frac{F}{m} \quad (2.3)$$

$$\epsilon_{ox} = EPSROX \cdot \epsilon_0 \frac{F}{m} \quad (2.4)$$

$$C_{ox} = \frac{3.9 \cdot \epsilon_0}{TOXE} \frac{F}{m^2} \quad (2.5)$$

$$\epsilon_{ratio} = \frac{EPSRSUB}{3.9} \quad (2.6)$$

$$(2.7)$$

2.2 Effective Channel Length & Width

$$\Delta L = LINT + \frac{LL}{(L_{new})^{LLN}} + \frac{LW}{(W_{new})^{LWN}} + \frac{LWL}{(L_{new})^{LLN} \cdot (W_{new})^{LWN}} \quad (2.8)$$

$$\Delta W = WINT + \frac{WL}{(L_{new})^{WLN}} + \frac{WW}{(W_{new})^{WWN}} + \frac{WWL}{L_{new}^{WLN} \cdot (W_{new})^{WWN}} \quad (2.9)$$

$$\Delta L_1 = LINT + \frac{LL}{(L_{new} + DLBIN)^{LLN}} + \frac{LW}{(W_{new} + DWBIN)^{LWN}} + \frac{LWL}{(L_{new} + DLBIN)^{LLN} \cdot (W_{new} + DWBIN)^{LWN}} \quad (2.10)$$

$$\Delta W_1 = WINT + \frac{WL}{(L_{new} + DLBIN)^{WLN}} + \frac{WW}{(W_{new} + DWBIN)^{WWN}} + \frac{WWL}{(L_{new} + DLBIN)^{WLN} \cdot (W_{new} + DWBIN)^{WWN}} \quad (2.11)$$

$$\Delta W_1 = WINT + \frac{WL}{(L_{new} + DLBIN)^{WLN}} + \frac{WW}{(W_{new} + DWBIN)^{WWN}} + \frac{WWL}{(L_{new} + DLBIN)^{WLN} \cdot (W_{new} + DWBIN)^{WWN}} \quad (2.12)$$

$$L_{new} = L * LM LT + XL; \quad (2.14)$$

$$W_{new} = \frac{W}{NF} * WM LT + XW; \quad (2.15)$$

$$\Delta L_{CV} = DLC \quad (2.16)$$

$$\Delta W_{CV} = DWC \quad (2.17)$$

$$L_{eff} = L * LM LT + XL - 2\Delta L \quad (2.18)$$

$$W_{eff} = W * WM LT + XW - 2\Delta W \quad (2.19)$$

$$L_{eff,CV} = L * LM LT + XL - 2\Delta L_{CV} \quad (2.20)$$

$$W_{eff,CV} = W * WM LT + XW - 2\Delta W_{CV} \quad (2.21)$$

$$L_{eff,Bin} = L * LM LT + XL - 2\Delta L_1 \quad (2.22)$$

$$W_{eff,Bin} = W * WM LT + XW - 2\Delta W_1 \quad (2.23)$$

2.3 Binning Calculations

For a given L and W, each model parameter $PARAM_i$ is calculated as a function of PARAM, and length dependent term, LPARAM, width dependent term, WPARAM, area

dependent term, PPARAM:

$$PARAM_i = PARAM + LPARAM \cdot BINL + WPARAM \cdot BINW + PPARAM \cdot BINWL \quad (2.24)$$

BINUNIT is the binning unit selector. When BINUNIT=1,

$$BINL = \frac{1e^{-6}}{L_{eff} + DLBIN} \quad (2.25)$$

$$BINW = \frac{1e^{-6}}{W_{eff} + DWBIN} \quad (2.26)$$

when BINUNIT=0,

$$BINL = \frac{1.0}{L_{eff} + DLBIN} \quad (2.27)$$

$$BINW = \frac{1.0}{W_{eff} + DWBIN} \quad (2.28)$$

and

$$BINWL = BINL \cdot BINW \quad (2.29)$$

For the list of binal parameters, please refer to the complete parameter list at the end of this technical note.

2.4 Global geometrical scaling

Following scaling formulation is used in global scaling -

$$\begin{aligned} PARAM[L] &= PARAM \cdot \left[1 + PARAML \cdot \left(\frac{1}{L_{eff}^{PARAMLEXP}} - \frac{1}{LLONG^{PARAMLEXP}} \right) \right. \\ &\quad + PARAMW \cdot \left(\frac{1}{W_{eff}^{PARAMWEXP}} - \frac{1}{WWIDE^{PARAMWEXP}} \right) \\ &\quad \left. + PARAMWL \cdot \left(\frac{1}{(L_{eff} \cdot W_{eff})^{PARAMWLEXP}} \right) \right] \end{aligned} \quad (2.30)$$

LLONG is the length of extracted long channel device and WWIDE is the width for extracted wide device. They are used to ensure that scaling parameters do not affect long-wide fitting. We will not mention LLONG and WWIDE part again but all of the following scaling equation use above kind of formulation.

$$NDEP[L] = NDEP \cdot \left[1 + NDEPL1 \cdot \frac{1}{L_{eff}^{NDEPLEXP1}} + NDEPL2 \cdot \frac{1}{L_{eff}^{NDEPLEXP2}} \right. \\ \left. + NDEPW \cdot \frac{1}{W_{eff}^{NDEPWEXP}} + NDEPWL \cdot \frac{1}{(L_{eff} \cdot W_{eff})^{NDEPWLEXP}} \right] \quad (2.31)$$

$$+ VFBVW \cdot \frac{1}{W_{eff}^{VFBWEXP}} + VFBWL \cdot \frac{1}{(L_{eff} \cdot W_{eff})^{VFBWLEXP}} \quad (2.32)$$

$$NFACTOR[L] = NFACTOR \cdot \left[1 + NFACTORL \cdot \frac{1}{L_{eff}^{NFACTORLEXP}} \right. \\ \left. + NFACTORW \cdot \frac{1}{W_{eff}^{NFACTORWEXP}} + NFACTORWL \cdot \frac{1}{(L_{eff} \cdot W_{eff})^{NFACTORWLEXP}} \right] \quad (2.33)$$

$$CDSCD[L] = CDSCD \cdot \left[1 + CDSCDL \cdot \frac{1}{L_{eff}^{CDSCDLEXP}} \right] \quad (2.34)$$

$$CDSCB[L] = CDSCB \cdot \left[1 + CDSCBL \cdot \frac{1}{L_{eff}^{CDSCBLEXP}} \right] \quad (2.35)$$

$$(2.36)$$

if (MOBSCALE=0) (2.37)

$$U0[L] = \begin{cases} U0 \cdot \left[1 - U0L \cdot \frac{1}{L_{eff}^{U0LEXP}} \right] & U0LEXP > 0 \\ U0 \cdot [1 - U0L] & \text{Otherwise} \end{cases} \quad (2.38)$$

else (2.39)

$$U0[L] = U0 \cdot [1 - UP1 \cdot \exp^{\frac{-L_{eff}}{L^{UP1}}} - UP2 \cdot \exp^{\frac{-L_{eff}}{L^{UP2}}}] \quad (2.40)$$

$$UA[L] = UA \cdot \left[1 + UAL \cdot \frac{1}{L_{eff}^{UALEXP}} + UAW \cdot \frac{1}{W_{eff}^{UAWEXP}} + UAWL \cdot \frac{1}{(L_{eff} \cdot W_{eff})^{UAWLEXP}} \right] \quad (2.41)$$

$$EU[L] = EU \cdot \left[1 + EUL \cdot \frac{1}{L_{eff}^{EULEXP}} + EUW \cdot \frac{1}{W_{eff}^{EUWEXP}} + EUWL \cdot \frac{1}{(L_{eff} \cdot W_{eff})^{EUWLEXP}} \right] \quad (2.42)$$

$$UD[L] = UD \cdot \left[1 + UDL \cdot \frac{1}{L_{eff}^{UDLEXP}} \right] \quad (2.43)$$

$$UC[L] = UC \cdot \left[1 + UCL \cdot \frac{1}{L_{eff}^{UCLEXP}} + UCW \cdot \frac{1}{W_{eff}^{UCWEXP}} + UCWL \cdot \frac{1}{(L_{eff} \cdot W_{eff})^{UCWLEXP}} \right] \quad (2.44)$$

$$ETA0[L] = ETA0 \cdot \left[\frac{1}{L_{eff}^{DSUB}} \right] \quad (2.45)$$

$$ETAB[L] = ETAB \cdot \left[\frac{1}{L_{eff}^{ETABEXP}} \right] \quad (2.46)$$

$$PDIBLC[L] = PDIBLC \cdot \left[1 + PDIBLCL \cdot \frac{1}{L_{eff}^{PDIBLCLEXP}} \right] \quad (2.47)$$

$$DELTA[L] = DELTA \cdot \left[1 + DELTAL \cdot \frac{1}{L_{eff}^{DELTALEXP}} \right] \quad (2.48)$$

$$FPROUT[L] = FPROUT \cdot \left[1 + FPROUTL \cdot \frac{1}{L_{eff}^{FPROUTLEXP}} \right] \quad (2.49)$$

$$PCLM[L] = PCLM \cdot \left[1 + PCLML \cdot \frac{1}{L_{eff}^{PCLMLEXP}} \right] \quad (2.50)$$

$$\begin{aligned} VSAT[L] &= VSAT \cdot \left[1 + VSATL \cdot \frac{1}{L_{eff}^{VSATLEXP}} + VSATW \cdot \frac{1}{W_{eff}^{VSATWEXP}} \right. \\ &\quad \left. + VSATWL \cdot \frac{1}{(L_{eff} \cdot W_{eff})^{VSATWLEXP}} \right] \end{aligned} \quad (2.51)$$

$$PSAT[L] = PSAT \cdot \left[1 + PSATL \cdot \frac{1}{L_{eff}^{PSATLEXP}} \right] \quad (2.52)$$

$$PTWG[L] = PTWG \cdot \left[1 + PTWGL \cdot \frac{1}{L_{eff}^{PTWGLEXP}} \right] \quad (2.53)$$

$$ALPHA0[L] = ALPHA0 \cdot \left[1 + ALPHA0L \cdot \frac{1}{L_{eff}^{ALPHA0LEXP}} \right] \quad (2.54)$$

$$AGIDL[L] = AGIDL \cdot \left[1 + AGIDLL \cdot \frac{1}{L_{eff}} + AGIDLW \cdot \frac{1}{W_{eff}} \right] \quad (2.55)$$

$$AGISL[L] = AGISL \cdot \left[1 + AGISLL \cdot \frac{1}{L_{eff}} + AGISLW \cdot \frac{1}{W_{eff}} \right] \quad (2.56)$$

$$AIGC[L] = AIGC \cdot \left[1 + AIGCL \cdot \frac{1}{L_{eff}} + AIGCW \cdot \frac{1}{W_{eff}} \right] \quad (2.57)$$

$$AIGS[L] = AIGS \cdot \left[1 + AIGSL \cdot \frac{1}{L_{eff}} + AIGSW \cdot \frac{1}{W_{eff}} \right] \quad (2.58)$$

$$AIGD[L] = AIGD \cdot \left[1 + AIGDL \cdot \frac{1}{L_{eff}} + AIGDW \cdot \frac{1}{W_{eff}} \right] \quad (2.59)$$

$$PIGCD[L] = PIGCD \cdot \left[1 + PIGCDL \cdot \frac{1}{L_{eff}} \right] \quad (2.60)$$

$$\begin{aligned} NDEPCV[L] &= NDEPCV \cdot \left[1 + NDEPCVL1 \cdot \frac{1}{L_{eff}^{NDEPCVLEXP1}} \right. \\ &\quad + NDEPCVL2 \cdot \frac{1}{L_{eff}^{NDEPCVLEXP2}} + NDEPCVW \cdot \frac{1}{W_{eff}^{NDEPCVWEXP}} \\ &\quad \left. + NDEPCVWL \cdot \frac{251}{(L_{eff} \cdot W_{eff})^{NDEPCVWLEXP}} \right] \end{aligned} \quad (2.61)$$

$$VFBCV[L] = VFBCV \cdot \left[1 + VFBCVL \cdot \frac{1}{L_{eff}^{VFBCVLEXP}} \right. \\ \left. + VFBCVW \cdot \frac{1}{W_{eff}^{VFBCVWEXP}} + VFBCVWL \cdot \frac{1}{(L_{eff} \cdot W_{eff})^{VFBCVWLEXP}} \right] \quad (2.62)$$

$$VSATCV[L] = VSATCV \cdot \left[1 + VSATCVL \cdot \frac{1}{L_{eff}^{VSATCVLEXP}} \right. \\ \left. + VSATCVW \cdot \frac{1}{W_{eff}^{VSATCVWEXP}} + VSATCVWL \cdot \frac{1}{(L_{eff} \cdot W_{eff})^{VSATCVWLEXP}} \right] \quad (2.63)$$

$$PCLMCV[L] = PCLMCV \cdot \left[1 + PCLMCVL \cdot \frac{1}{L_{eff}^{PCLMCVLEXP}} \right] \quad (2.64)$$

$$K2[L] = K2 \cdot \left[1 + K2L \cdot \frac{1}{L_{eff}^{K2LEXP}} + K2W \cdot \frac{1}{W_{eff}^{K2WEXP}} + K2WL \cdot \frac{1}{(L_{eff} \cdot W_{eff})^{K2WLEXP}} \right] \quad (2.65)$$

$$PRWB[L] = PRWB \cdot \left[1 + PRWBL \cdot \frac{1}{L_{eff}^{PRWBLEXP}} \right] \quad (2.66)$$

$$RSW[L] = RSW \cdot \left[1 + RSWL \cdot \frac{1}{L_{eff}^{RSWLEXP}} \right] \quad (2.67)$$

$$RDW[L] = RDW \cdot \left[1 + RDWL \cdot \frac{1}{L_{eff}^{RDWLEXP}} \right] \quad (2.68)$$

$$RDSW[L] = RDSW \cdot \left[1 + RDSWL \cdot \frac{1}{L_{eff}^{RDSWLEXP}} \right] \quad (2.69)$$

2.5 Terminal Voltages

BSIM6 is a body referenced model [1].

$$V_t = \frac{K.T}{q} \quad (2.70)$$

$$V_g = V_g - V_b \quad (2.71)$$

$$V_d = V_d - V_b \quad (2.72)$$

$$V_s = V_s - V_b \quad (2.73)$$

$$V_{gs} = V_g - V_s \quad (2.74)$$

$$V_{gd} = V_g - V_d \quad (2.75)$$

$$V_{gb} = V_g - V_b \quad (2.76)$$

$$V_{ds} = V_d - V_s \quad (2.77)$$

$$V_{sb_noswap} = V_s \quad (2.78)$$

$$V_{dsx} = \left[\frac{2}{AVDSX} \cdot \ln(1 + \exp^{AVDSX \cdot V_{DS}}) - V_{DS} - \frac{2}{AVDSX} \cdot \ln(2) \right] \quad (2.79)$$

$$V_{bsx} = - \left[V_s + \frac{1}{2} (V_{ds} - V_{dsx}) \right] \quad (2.80)$$

2.6 Pinch-off Potential and Normalized Charge Calculation

2.6.1 Pinch-off Potential with Poly Depletion

$$\phi_b = \ln \left(\frac{n_{body}}{n_i} \right) \quad (2.81)$$

$$\gamma_0 = \frac{\sqrt{2 \cdot q \cdot \epsilon_{si} \cdot NDEP}}{C_{ox} \sqrt{nV_t}} \quad (2.82)$$

$$\gamma_g = \frac{\sqrt{2 \cdot q \cdot \epsilon_{si} \cdot NGATE}}{C_{ox} \sqrt{nV_t}} \quad (2.83)$$

$$\gamma' = \gamma_0 \cdot \sqrt{nV_t} \quad (2.84)$$

$$\gamma'_g = \gamma_g \cdot \sqrt{nV_t} \quad (2.85)$$

$$\delta_{PD} = \frac{NDEP}{NGATE} \quad (2.86)$$

$$\left(\frac{\gamma_0}{\gamma_g} \right)^2 = \left(\frac{\frac{\sqrt{2 \cdot q \cdot \epsilon_{si} \cdot NDEP}}{C_{ox} \sqrt{nV_t}}}{\frac{\sqrt{2 \cdot q \cdot \epsilon_{si} \cdot NGATE}}{C_{ox} \sqrt{nV_t}}} \right)^2 = \frac{NDEP}{NGATE} = \delta_{PD} \quad (2.87)$$

$$\gamma = \frac{\gamma_0}{1 + \delta_{PD}} \quad (2.88)$$

In accumulation and inversion under depletion approximation, the bulk charge is given as [2]

$$Q_b = -sign(\psi_s) \cdot \gamma' \cdot C_{ox} \cdot \sqrt{V_t \cdot (e^{-\frac{\psi_s}{V_t}} - 1) + \psi_s} \quad (2.89)$$

From potential balance equation including poly depletion,

$$V_G = V_{FB} + \psi_S - \frac{Q_i + Q_b}{C_{ox}} + \left(\frac{Q_i + Q_b}{\gamma'_g \cdot C_{ox}} \right)^2 \quad (2.90)$$

At pinch off, $\psi_S = \psi_P$ and $Q_i = 0$. Substituting in (2.89) and (2.90),

$$V_G - V_{FB} = \psi_P + \gamma' \cdot \sqrt{V_t \cdot (e^{-\frac{\psi_P}{V_t}} - 1) + \psi_P} + \left(\frac{\gamma'}{\gamma'_g} \right)^2 \left(V_t \cdot (e^{-\frac{\psi_P}{V_t}} - 1) + \psi_P \right) \quad (2.91)$$

$$= \psi_P + \gamma' \cdot \sqrt{V_t \cdot (e^{-\frac{\psi_P}{V_t}} - 1) + \psi_P} + \delta_{PD} \left(V_t \cdot (e^{-\frac{\psi_P}{V_t}} - 1) + \psi_P \right) \quad (2.92)$$

Normalizing it,

$$v_g - v_{fb} = \psi_p + \gamma_0 \cdot \sqrt{e^{-\psi_p} + \psi_p - 1} + \delta_{PD} \left(e^{-\psi_p} - 1 + \psi_p \right) \quad (2.93)$$

Explicit expression for ψ_p can be derived from above relation in the asymptotic form by inspecting the behavior in three different regions. First consider the depletion and inversion region of operation where $\psi_p \gg 0$ so that $e^{-\psi_p}$ is very small. Let $\zeta_1 = e^{-\psi_p}$

$$v_g - v_{fb} = \psi_p + \gamma_0 \cdot \sqrt{\psi_p + \zeta_1 - 1} + \delta_{PD} \left(\zeta_1 - 1 + \psi_p \right) \quad (2.94)$$

Let

$$\sqrt{\psi_p + \zeta_1 - 1} = x \quad (2.95)$$

or

$$\psi_p = x^2 + 1 - \zeta_1 \quad (2.96)$$

Thus

$$v_g - v_{fb} = x^2 + 1 - \zeta_1 + \gamma_0 \cdot x + \delta_{PD} \cdot x^2 \quad (2.97)$$

or

$$x^2 + \frac{\gamma_0}{1 + \delta_{PD}} \cdot x + \frac{1 - \zeta_1}{1 + \delta_{PD}} - \frac{v_g - v_{fb}}{1 + \delta_{PD}} = 0 \quad (2.98)$$

This gives

$$x = \left[\sqrt{\frac{v_g - v_{fb} - 1 + \zeta_1}{1 + \delta_{PD}}} + \left(\frac{\gamma_0}{2 \cdot (1 + \delta_{PD})} \right)^2 - \frac{\gamma_0}{2 \cdot (1 + \delta_{PD})} \right] \quad (2.99)$$

$$\begin{aligned} \psi_p &= x^2 + 1 - \zeta_1 = \left[\sqrt{\frac{v_g - v_{fb} - 1 + \zeta_1}{1 + \delta_{PD}}} + \left(\frac{\gamma_0}{2 \cdot (1 + \delta_{PD})} \right)^2 - \frac{\gamma_0}{2 \cdot (1 + \delta_{PD})} \right]^2 + 1 - \zeta_1 \\ &\quad (2.100) \end{aligned}$$

$$= \left[\sqrt{\frac{v_g - v_{fb} - 1 + \zeta_1}{1 + \delta_{PD}}} + \left(\frac{\gamma}{2} \right)^2 - \frac{\gamma}{2} \right]^2 + 1 - \zeta_1 \quad (2.101)$$

where $\gamma = \frac{\gamma_0}{1+\delta_{PD}}$

Similarly,

when ψ_p is close to 0

$$\psi_{p0} = \left[\frac{v_g - v_{fb}}{2} - 3\left(1 + \frac{\gamma}{\sqrt{2}}\right) \right] + \sqrt{\left[\frac{v_g - v_{fb}}{2} - 3\left(1 + \frac{\gamma}{\sqrt{2}}\right) \right]^2 + 6(v_g - v_{fb})} \quad (2.102)$$

and in accumulation where $\psi_p \ll 0$ ($\zeta_2 = \psi_p$),

$$\psi_p = -\ln \left[1 - \zeta_2 + \left(\frac{v_g - v_{fb} - \zeta_2}{\gamma} \right)^2 \right] \quad (2.103)$$

Thus the pinch off potential is expressed as

$$\psi_p = \begin{cases} -\ln \left[1 - \psi_{p0} + \left(\frac{v_g - v_{fb} - \psi_{p0}}{\gamma} \right)^2 \right] & \text{if } v_g - v_{fb} < 0 \\ 1 - e^{-\psi_{p0}} + \left[\sqrt{v_g - v_{fb} - 1 + e^{-\psi_{p0}} + \left(\frac{\gamma}{2} \right)^2} - \frac{\gamma}{2} \right]^2 & \text{otherwise} \end{cases} \quad (2.104)$$

Note : Derivatives of ψ_p are continuous in all regions.

2.6.2 Normalized Charge Density

Inversion Charge [3], [4] : Normalized inversion charge density at source/drain is newly derived for BSIM6 and can be obtained as follows.

Charge sheet model approximates inversion charge density as

$$Q_i = -\gamma' \cdot C_{ox} \cdot \sqrt{V_t} \left[\sqrt{\frac{\psi_S}{V_t} + e^{\frac{\psi_S - 2\phi_F - V_{ch}}{V_t}}} - \sqrt{\frac{\psi_S}{V_t}} \right] \quad (2.105)$$

Using inversion charge linearization [4],

$$Q_i = n_q \cdot C_{ox} \cdot (\psi_S - \psi_P) \quad (2.106)$$

or

$$\psi_S = \psi_P + \frac{Q_i}{n_q \cdot C_{ox}} \quad (2.107)$$

Substituting ψ_S from (2.107) in (2.105),

$$-\frac{Q_i}{\gamma' \cdot C_{ox} \cdot \sqrt{V_t}} = \left[\sqrt{\frac{\psi_P + \frac{Q_i}{n_q \cdot C_{ox}}}{V_t}} + e^{\frac{\psi_P + \frac{Q_i}{n_q \cdot C_{ox}} - 2 \cdot \phi_F - V_{ch}}{V_t}} - \sqrt{\frac{\psi_P + \frac{Q_i}{n_q \cdot C_{ox}}}{V_t}} \right] \quad (2.108)$$

rearranging,

$$\left[-\frac{Q_i}{\gamma' \cdot C_{ox} \cdot \sqrt{V_t}} + \sqrt{\frac{\psi_P + \frac{Q_i}{n_q \cdot C_{ox}}}{V_t}} \right]^2 = \left[\sqrt{\frac{\psi_P + \frac{Q_i}{n_q \cdot C_{ox}}}{V_t}} + e^{\frac{\psi_P + \frac{Q_i}{n_q \cdot C_{ox}} - 2 \cdot \phi_F - V_{ch}}{V_t}} \right]^2 \quad (2.109)$$

$$e^{\frac{\psi_P + \frac{Q_i}{n_q \cdot C_{ox}} - 2 \cdot \phi_F - V_{ch}}{V_t}} = \left(-\frac{Q_i}{\gamma' \cdot C_{ox} \cdot \sqrt{V_t}} \right)^2 - 2 \cdot \left(\frac{Q_i}{\gamma' \cdot C_{ox} \cdot \sqrt{V_t}} \right) \cdot \sqrt{\frac{\psi_P + \frac{Q_i}{n_q \cdot C_{ox}}}{V_t}} \quad (2.110)$$

This reduces to

$$\frac{\psi_P + \frac{Q_i}{n_q \cdot C_{ox}} - 2 \cdot \phi_F - V_{ch}}{V_t} = \ln \left[\left(-\frac{Q_i}{\gamma' \cdot C_{ox} \cdot \sqrt{V_t}} \right)^2 - 2 \cdot \left(\frac{Q_i}{\gamma' \cdot C_{ox} \cdot \sqrt{V_t}} \right) \cdot \sqrt{\frac{\psi_P + \frac{Q_i}{n_q \cdot C_{ox}}}{V_t}} \right] \quad (2.111)$$

$$= \ln \left[-\frac{Q_i}{\gamma' \cdot C_{ox} \cdot \sqrt{V_t}} \left(-\frac{Q_i}{\gamma' \cdot C_{ox} \cdot \sqrt{V_t}} + 2 \cdot \sqrt{\frac{\psi_P + \frac{Q_i}{n_q \cdot C_{ox}}}{V_t}} \right) \right] \quad (2.112)$$

Normalizing inversion charge to $-2V_t \cdot n_q \cdot C_{ox}$, all voltages to V_t ,

$$\psi_p - 2 \cdot q_i - 2 \cdot \phi_f - v_{ch} = \ln \left[\frac{2n_q \cdot q_i}{\gamma_0} \left(\frac{2 \cdot n_q \cdot q_i}{\gamma_0} + 2 \cdot \sqrt{\psi_p - 2q_i} \right) \right] \quad (2.113)$$

which gives

$$\ln(q_i) + \ln \left[\frac{2n_q}{\gamma_0} \left(q_i \frac{2n_q}{\gamma_0} + 2 \sqrt{\psi_p - 2q_i} \right) \right] + 2q_i = \psi_p - 2\phi_f - v_{ch} \quad (2.114)$$

This is a general equation which can be solved to give normalized inversion charge density. The procedure of obtaining initial guess for the solution of above equation for weak inversion is described below [5]. Note that to generalize the process, subscript "i" is dropped from the term q_i

Let $v = \psi_p - 2\phi_f - v_{ch} - \ln(\frac{4n_q\sqrt{\psi_p}}{\gamma}) = \ln q + 2q$

$$v = \ln q + 2q \quad (2.115)$$

$$= \ln q + 2e^{\ln q} \quad (2.116)$$

$$= \ln q + \frac{1}{F(\ln q)} \quad (2.117)$$

Here in second term q has been used as $\ln(e^q)$. The function F is defined as

$$F = \frac{1}{2e^{\ln q}} \quad (2.118)$$

$$= \frac{1}{2e^{(\ln q + \ln q_t - \ln q_t)}} \quad (2.119)$$

$$= \frac{1}{2q_t e^{\ln \frac{q}{q_t}}} \quad (2.120)$$

$$= \frac{1}{2q_t} e^{-\Delta} \quad (2.121)$$

Where $\Delta = \ln \frac{q}{q_t}$. Expanding (2.121) around $\Delta = 0$ using Taylor series expansion (as $|2q| << |\ln q|$),

$$F = \frac{1}{2q_t} \cdot [1 - e^{-0} \cdot \Delta] \quad (2.122)$$

$$= \frac{1}{2q_t} \left(1 - \ln \frac{q}{q_t}\right) \quad (2.123)$$

substituting in (2.117),

$$v = \ln q + \frac{2q_t}{1 - \ln q + \ln q_t} \quad (2.124)$$

This equation is solved for q. Let,

$$\ln q = x \quad (2.125)$$

$$v = x + \frac{2q_t}{1 + \ln q_t - x} \quad (2.126)$$

$$v(1 + \ln q_t) - vx - x(1 + \ln q_t) + x^2 - 2q_t = 0 \quad (2.127)$$

$$x = \frac{v + (1 + \ln q_t) - \sqrt{(v + (1 + \ln q_t))^2 - 4v(1 + \ln q_t) + 8q_t}}{2} \quad (2.128)$$

For subthreshold region, normalized inversion charge density will be $|q| << 1$ and $|\ln q| >> |2q|$. The initial value is taken at a point where $|\ln q| = 2.|2q|$ which gives

$$q_t = 0.301 \quad (2.129)$$

$$1 + \ln q_t = -0.201491 \quad (2.130)$$

substituting in (2.128),

$$x = \frac{v - 0.201491 - \sqrt{(v - 0.201491)^2 - 4v(-0.201491) + 8(0.301)}}{2} \quad (2.131)$$

$$x = \ln q = \frac{v - 0.201491 - \sqrt{(v + 0.402982)v + 2.446562}}{2} \quad (2.132)$$

Once the initial guess is known, the final value is obtained by using analytical method as shown below

$$n_{q0} = 1 + \frac{\gamma}{2\sqrt{\psi_p}} \quad (2.133)$$

$$v = \psi_p - 2\phi - v_{ch} - \ln \left(4.0 \cdot \frac{n_{q0}}{\gamma} \cdot \sqrt{\psi_p} \right) \quad (2.134)$$

$$\ln_{q0} = \frac{1}{2} \left[v - 0.201491 - \sqrt{v \cdot (v + 0.402982) + 2.446562} \right] \quad (2.135)$$

$$q_0 = e^{\ln_{q0}} \quad (2.136)$$

if $\ln_{q0} \leq -80.0$

$$q_{s/d} = f = q_0 \cdot \left[1 + \psi_p - 2\phi - v_{ch} - \ln_{q0} - \ln \left(2 \cdot \frac{n_{q0}}{\gamma} \left(2 \cdot q_0 \cdot \frac{n_{q0}}{\gamma} + 2 \cdot \sqrt{\psi_p} \right) \right) \right] \quad (2.137)$$

In this equation, if \ln_{q0} becomes very large and negative then $q_0 = e^{\ln_{q0}}$ may be out of range of precision limit of the simulator. Therefore it is approximated as follows

if $\ln_{q0} < -110$, $q_0 = e^{-100}$

if $\ln_{q0} > -90$, $q_0 = e^{\ln_{q0}}$

else $q_0 = \exp(-100 + 20(\frac{5}{64} + \frac{z}{2} + z^2(\frac{15}{16} - z^2)))$

where $z = \frac{\ln_{q0} + 100}{20}$.

The above polynomial provides smooth derivatives for q. For the derivation of polynomial coefficients, refer to Appendix A.

For $\ln q_0 > -80$

$$f = 2q_0 + \ln \left(2q_0 \frac{n_q}{\gamma} \left(2q_0 \frac{n_q}{\gamma} + 2\sqrt{\psi_p} \right) - (v_p - 2\phi_f - v_{ch}) \right) \quad (2.138)$$

$$f' = 2 + \frac{1}{q_0} + \frac{\frac{n_{q0}}{\gamma} - \frac{1}{\sqrt{\psi_p}}}{\frac{n_{q0}}{\gamma} \cdot q_0 + \sqrt{\psi_p}} \quad (2.139)$$

$$q_1 = q_0 - \frac{f}{f'} \quad (2.140)$$

The accuracy of this initial guess is further improved by following procedure

$$f = 2q_1 + \ln \left(2q_1 \frac{n_q}{\gamma} \left(2q_1 \frac{n_q}{\gamma} + 2\sqrt{\psi_p} \right) - (v_p - 2\phi_f - v_{ch}) \right) \quad (2.141)$$

$$f' = 2 + \frac{1}{q_1} + \frac{\frac{n_{q1}}{\gamma} - \frac{1}{\sqrt{\psi_p}}}{\frac{n_{q1}}{\gamma} \cdot q_1 + \sqrt{\psi_p}} \quad (2.142)$$

Applying Halley's method,

$$f'' = -\frac{1}{q_1^2} - \frac{1}{\left[(\psi_p)^{\frac{3}{2}} \right] \cdot \left[\frac{n_{q0}}{\gamma} \cdot q_1 + \sqrt{\psi_p} \right]} - \left[\frac{\frac{n_{q0}}{\gamma} - \frac{1}{\sqrt{\psi_p}}}{\frac{n_{q0}}{\gamma} \cdot q_1 + \sqrt{\psi_p}} \right]^2 \quad (2.143)$$

$$q_{s/d} = q_1 - \frac{f}{f'} \cdot \left(1 + \frac{f \cdot f''}{2 \cdot f'^2} \right) \quad (2.144)$$

2.7 Short Channel Effects

Asymmetry Mode

There are some devices with asymmetric drain and source structures. This is modeled as follows:

Weighting Function for forward and reverse modes

$$T_0 = \tanh(ASYMP * q * Vds_{noswap}/K \cdot T); \quad (2.145)$$

$$wf = 0.5 + 0.5 * T_0; \quad (2.146)$$

$$wr = 1.0 - wf; \quad (2.147)$$

$$if(ASYMMOD! = 0) \quad (2.148)$$

$$PARAM_A = PARAM_I * wr + PARAM_I * wf \quad (2.149)$$

$$else \quad (2.150)$$

$$PARAM_A = PARAM_I \quad (2.151)$$

$$(2.152)$$

ASYMP is a model parameter and its default value is 0.6. This parameter improves flexibility in asymmetry mode.

Asymmetry mode affect following parameters: CDSCD, ETA0, PDIBLC, PCLM, PSAT, VSAT, PTWG, U0, UA, UC, UD, UCS, ALPHA0, BETA0

Vt Roll-off, DIBL, and Subthreshold Slope Degradation (Ref.: BSIM4 Model)

$$\psi_{st} = 0.4 + PHIN + \frac{kT}{q} \cdot \ln \frac{NDEP}{n_i} \quad (2.153)$$

$$PhistVbs = \psi_{st} - V_{bsx} \quad (2.154)$$

$$X_{dep} = \sqrt{\frac{2 \cdot \epsilon_{sub} \cdot PhistVbs}{q \cdot NDEP}} \quad (2.155)$$

$$n = 1 + \frac{CIT + NFACTOR + CDSCD \cdot V_{dsx} - CDSCB \cdot V_{bsx}}{C_{ox}} \quad (2.156)$$

$$V_t = \frac{k_b \cdot T}{q} \quad (2.157)$$

$$nV_t = n \cdot V_t \quad (2.158)$$

$$\Delta V_{th,VDNUD} = K1 \cdot (\sqrt{\phi_{st} - V_{bs}} - \sqrt{\phi_{st}}) - K2 \cdot V_{bsx} \quad (2.159)$$

$$\Delta V_{th,DIBL} = -(ETA0 + ETAB \cdot V_{bsx}) \cdot V_{dsx} \quad (2.160)$$

$$\begin{aligned} \Delta V_{th,DITS} = & -n \frac{KT}{q} \cdot \ln \left(\frac{L_{eff}}{L_{eff} + DVTP0 \cdot (1 + \exp(-DVTP1 \cdot V_{ds}))} \right) \\ & - \left(DVTP5 + \frac{DVTP2}{L_{eff}^{DVTP3}} \right) \cdot \tanh(DVTP4 \cdot V_{dsx}) \end{aligned} \quad (2.161)$$

$$\Delta V_{th,all} = \Delta V_{th,VDNUD} + \Delta V_{th,DIBL} + \Delta V_{th,DITS} \quad (2.162)$$

$$V_{gfb} = V_g - V_{fb} - \Delta V_{th,all} \quad (2.163)$$

Note: Short channel effect and Reverse short channel effect are modeled using NDEPL1, NDELEXP1, NDEPL2 and NDEPLEXP2 parameters. Width scaling of V_{th} is modeled using NDEPW and NDEPWEXP parameters.

2.8 Drain Saturation Voltage

The drain saturation voltage model is calculated after the source-side charge (q_s) has been calculated. V_{dseff} is subsequently used to compute the drain-side charge (q_d).

Electric Field Calculations

Electric Field is in MV/cm

$$\eta = \begin{cases} \frac{1}{2} \cdot ETAMOB & \text{for NMOS} \\ \frac{1}{3} \cdot ETAMOB & \text{for PMOS} \end{cases} \quad (2.164)$$

$$E_{effs} = 10^{-8} \cdot \left(\frac{q_{bs} + \eta \cdot q_{is}}{\epsilon_{ratio} \cdot TOXE} \right) \quad (2.165)$$

Drain Saturation Voltage (V_{dsat}) Calculations (Ref. BSIM4 & EKV Model)

$$D_{mobs} = 1 + (UA + UC \cdot V_{bsx}) \cdot (E_{effs})^{EU} + \frac{UD}{\left[\frac{1}{2} \cdot \left(1 + \frac{q_{is}}{q_{bs}} \right) \right]^{UCS}} \quad (2.166)$$

$$T_{11} = PSATB \cdot V_{bsx}$$

$$T_{12} = \sqrt{0.1 + T_{11} \cdot T_{11}}$$

$$T_0 = 0.5 * (1 - T_{11} + \sqrt{(1 - T_{11}) \cdot (1 - T_{11}) + T_{12}}) \quad (2.167)$$

$$\lambda_C = \frac{2 \cdot U0 \cdot nV_t}{(D_{mobs})^{PSAT} \cdot VSAT \cdot L_{eff}} \cdot [1 + PTWG \cdot \frac{10 \cdot PSATX \cdot qs \cdot T_0}{10 \cdot PSATX + qs \cdot T_0}] \quad (2.168)$$

$$q_{dsat} = \frac{\lambda_C}{2} \cdot \frac{q_s^2 + q_s}{1 + \frac{\lambda_C}{2} \cdot (1 + q_s)} \quad (2.169)$$

$$v_{dsat} = \psi_p - \frac{2\phi_b}{n} - 2q_{dsat} - \ln \left[\frac{2q_{dsat} \cdot n_q}{gam} \cdot \left(\frac{2q_{dsat} \cdot n_q}{gam} + \frac{gam}{n_q - 1} \right) \right] \quad (2.170)$$

2.9 Mobility degradation with vertical field

(Ref. BSIM4 Model)

$$E_{effm} = 10^{-8} \cdot \left(\frac{q_{ba} + \eta \cdot q_{ia}}{\epsilon_{ratio} \cdot TOXE} \right) \quad (2.171)$$

Where q_{ia} and q_{ba} are the average inversion charge and bulk charge densities respectively.

$$D_{mob} = 1 + (UA + UC \cdot V_{bsx}) \cdot (E_{effm})^{EU} + \frac{UD}{\left[\frac{1}{2} \cdot \left(1 + \frac{q_{ia}}{q_{ba}} \right) \right]^{UCS}} \quad (2.172)$$

The D_{mob} goes into denominator of mobility expression.

2.10 Parasitic series resistance

BSIM6 offers three ways to model parasitic resistance of the MOSFET as shown below

- (a) RDSMOD=0, External resistance are bias independent while internal resistance is bias dependent.
- (b) RDSMOD=1, No internal resistance. Both bias dependent and independent resistor are kept externally.
- (c) RDSMOD=2, No external resistance. Both bias dependent and independent resistor are kept internally.

2.10.1 Bias Independent External Series Resistance, Bias Dependent Internal Resistance (RDSMOD=0)

$$T_0 = 1 + PRWG \cdot q_{ia} \quad (2.173)$$

$$T_1 = PRWB \cdot (\sqrt{\phi_s - V_{bs}} - \sqrt{\phi_s}) \quad (2.174)$$

$$T_2 = \frac{1}{T_0} + T_1 \quad (2.175)$$

$$T_3 = \frac{1}{2} [T_2 + \sqrt{T_2^2 + 0.01}] \quad (2.176)$$

$$R_{ds}(V) = NF \cdot \left(W_{eff}^{WR} \left[RDSWMIN + RDSW \cdot T_3 \right] \right) \quad (2.177)$$

$$D_r = 1.0 + \frac{\mu_0}{D_{mob} \cdot D_{vsat}} \cdot C_{ox} \cdot \frac{W_{eff}}{L_{eff}} \cdot q_{ia} \cdot R_{ds} \quad (2.178)$$

$$R_{source} = R_{s,geo} \quad (2.179)$$

$$R_{drain} = R_{d,geo} \quad (2.180)$$

$R_{s,geo}$ and $R_{d,geo}$ are the source and drain diffusion resistances, which are described later. And, D_r goes into the denominator of the final I_{ds} expression.

2.10.2 Bias Dependent External Series Resistance ($R_s(V)$ & $R_d(V)$)

The bias-dependent external resistance model is adopted from BSIM4 and can be invoked by setting model selector RDSMOD=1. BSIM4 and BSIM6 allow the source

extension resistance $R_s(V)$ and the drain extension resistance $R_d(V)$ to be external and asymmetric (i.e. here when HVMOD = 1, $R_s(V)$ is connected between nodes S and S_{i1} and $R_d(V)$ is connected between nodes D and D_{i1}). When HVMOD = 0, S_{i1} and S_i (D_{i1} and D_i) will be shorted. Furthermore, $R_s(V)$ does not have to be equal to $R_d(V)$. This feature makes accurate RF CMOS simulation possible.

The source/drain series resistance is the sum of a bias-independent component and a bias-dependent component.

$$\begin{aligned} V_{s1} &= V(si1, bi) \\ V_{d1} &= V(di1, bi) \end{aligned} \quad (2.181)$$

$$V_{gs1_noswap} = V_g - V_{s1} \quad (2.182)$$

$$V_{gd1_noswap} = V_g - V_{d1} \quad (2.183)$$

$$V_{sb1_noswap} = V_{s1} \quad (2.184)$$

$$V_{db1_noswap} = V_{d1} \quad (2.185)$$

$$V_{gs,eff} = \frac{1}{2} \left[V_{gs1} - V_{fbsdr} + \sqrt{(V_{gs1_noswap} - V_{fbsdr})^2 + 10^{-2}} \right] \quad (2.186)$$

$$V_{gd,eff} = \frac{1}{2} \left[V_{gd1} - V_{fbsdr} + \sqrt{(V_{gd1_noswap} - V_{fbsdr})^2 + 10^{-2}} \right] \quad (2.187)$$

$$\begin{aligned} R_{source} &= \frac{1}{W_{eff}^{WR} \cdot NF} \cdot \left(RSWMIN + RSW \cdot \left[-PRWB \cdot V_{sb1_noswap} + \frac{1}{1 + PRWG_i \cdot V_{gs,eff}} \right] \right) \\ &\quad + R_{s,geo} \end{aligned} \quad (2.188)$$

$$\begin{aligned} R_{drain} &= \frac{1}{W_{eff}^{WR} \cdot NF} \cdot \left(RDWMIN + RDW \cdot \left[-PRWB \cdot V_{db1_noswap} + \frac{1}{1 + PRWG_i \cdot V_{gd,eff}} \right] \right) \\ &\quad + R_{d,geo} \end{aligned} \quad (2.189)$$

$R_{s,geo}$ and $R_{d,geo}$ are the source and drain diffusion resistances.

2.10.3 Bias Dependent Internal Resistance (RDSMOD=2)

$$R_{ds}(V) = R_{s,geo} + NF \cdot \left(W_{eff}^{WR} \left[RDSWMIN + RDSW \cdot T_3 \right] \right) + R_{d,geo} \quad (2.190)$$

$$D_r = 1.0 + \frac{\mu_0}{D_{mob} \cdot D_{vsat}} \cdot C_{ox} \cdot \frac{W_{eff}}{L_{eff}} \cdot q_{ia} \cdot R_{ds} \quad (2.191)$$

where T3 is given by (2.176).

2.10.4 Sheet resistance model

The resistances $R_{s,geo}$ and $R_{d,geo}$ are simply calculated as the sheet resistances ($RSHS, RSHD$) times the number of squares (NRS, NRD):

$$\begin{aligned} R_{s,geo} &= NRS \cdot RSHS \\ R_{d,geo} &= NRD \cdot RSHD \end{aligned} \quad (2.192)$$

2.11 Output Conductance

The Output conductance model is taken from BSIM4 [6]

Channel Length Modulation (CLM)

$$E_{sat} = \frac{2 \cdot VSAT}{\frac{U_0}{D_{mob}}} \quad (2.193)$$

$$F = \begin{cases} 1 & \text{for } FPROUT \leq 0 \\ \frac{1}{1 + \frac{FPROUT \cdot \sqrt{L_{eff}}}{q_{ia} + 2 \cdot nV_t}} & \text{for } FPROUT > 0 \end{cases} \quad (2.194)$$

$$C_{clm} = \begin{cases} PCLM \cdot \left(1 + PCLMG \cdot \frac{q_{ia}}{E_{sat} \cdot L_{eff}}\right) \frac{1}{F} & \text{for } PCLMG > 0 \\ \frac{PCLM}{\left(1 - PCLMG \cdot \frac{q_{ia}}{E_{sat} \cdot L_{eff}}\right)} \frac{1}{F} & \text{for } PCLMG < 0 \end{cases} \quad (2.195)$$

$$V_{asat} = V_{dssat} + E_{satL} \quad (2.196)$$

$$M_{CLM} = 1 + C_{clm} \ln \left[1 + \frac{V_{ds} - V_{dseff}}{V_{asat}} \cdot \frac{1}{C_{clm}} \right] \quad (2.197)$$

Drain Induced Barrier Lowering (DIBL)

$$PVAG factor = \begin{cases} 1 + PVAG \cdot \frac{q_{im}}{E_{sat} L_{eff}} & \text{for } PVAG > 0 \\ \frac{1}{1 - PVAG \cdot \frac{q_{im}}{E_{sat} L_{eff}}} & \text{for } PVAG < 0 \end{cases} \quad (2.198)$$

$$\theta_{rout} = PDIBLC \quad (2.199)$$

$$V_{ADIBL} = \frac{q_{ia} + 2kT/q}{\theta_{rout}} \cdot \left(1 - \frac{V_{dssat}}{V_{dssat} + q_{ia} + 2kT/q}\right) \cdot PVAGfactor \cdot \frac{1}{1 + PDIBLCB \cdot V_{bsx}} \quad (2.200)$$

$$M_{DIBL} = \left(1 + \frac{V_{ds} - V_{dseff}}{V_{ADIBL}}\right) \quad (2.201)$$

Note: Length scaling parameters for PDIBLC are PDIBLCL and PDIBLCLEXP.

Drain Induced Threshold Shift (DITS)

$$V_{ADITS} = \frac{1}{PDITS} \cdot F \cdot [1 + (1 + PDITSL \cdot L_{eff}) \exp(PDITSD \cdot V_{ds})] \quad (2.202)$$

$$M_{DITS} = \left(1 + \frac{V_{ds} - V_{dseff}}{V_{ADITS}}\right) \quad (2.203)$$

Substrate Current induced Body Effect (SCBE)

$$litl = \sqrt{(\epsilon_{sub}/\epsilon_{ox}) \cdot TOXE \cdot XJ} \quad (2.204)$$

$$V_{ASCBE} = \frac{L_{eff}}{PSCBE2} \cdot \exp\left(\frac{PSCBE1 \cdot litl}{V_{ds} - V_{dseff}}\right) \quad (2.205)$$

$$M_{SCBE} = \left(1 + \frac{V_{ds} - V_{dseff}}{V_{ASCBE}}\right) \quad (2.206)$$

$$M_{oc} = M_{DIBL} \cdot M_{CLM} \cdot M_{DITS} \cdot M_{SCBE} \quad (2.207)$$

M_{oc} is multiplied to I_{ds} in the final drain current expression.

2.12 Velocity Saturation

Current Degradation Due to Velocity Saturation

$$T_1 = 2 \cdot \lambda_C \cdot (q_s - q_{deff}) \quad (2.208)$$

$$\lambda_C = \frac{2 \cdot U_0 \cdot nV_t}{(D_{mobs})^{\frac{1}{PSAT}} \cdot VSAT \cdot L_{eff}} \cdot [1 + PTWG \cdot \frac{10 \cdot PSATX \cdot qs \cdot T_0}{10 \cdot PSATX + qs \cdot T_0}] \quad (2.209)$$

$$D_{vsat} = \frac{1}{2} \left[\sqrt{1 + T_1^2} + \frac{1}{T_1} \cdot \ln(T_1 + \sqrt{1 + T_1^2}) \right] \quad (2.210)$$

$$D_{ptwg} = D_{vsat} \quad (2.211)$$

$$D_{tot} = D_{mob} \cdot D_{vsat} \cdot D_r \quad (2.212)$$

where D_r is the effect of internal resistance (R_{dsi}) on current, defined as

$$D_r = \begin{cases} 1 & \text{if } RDSDMOD = 1 \\ 1 + U_0 \cdot C_{ox} \cdot \frac{W_{eff}}{L_{eff}} \cdot q_{ia} \cdot R_{dsi} & \text{if } RDSDMOD = 0 \end{cases} \quad (2.213)$$

Non-Saturation Effect Some devices do not exhibit prominent or abrupt velocity saturation. The parameters A1 and A2 are used to tune this non-saturation effect to better the $I_{d,sat}$ or $g_{m,sat}$ fitting.

$$T_0 = A_1 + A_2 / (q_{ia} + 2.0 * n * V_{tm}) \quad (2.214)$$

$$dq_i = q_s - q_{deff} \quad (2.215)$$

$$T_1 = T_0 * dq_i * dq_i \quad (2.216)$$

$$T_2 = T_1 + 1.0 - 0.001 \quad (2.217)$$

$$T_3 = -1.0 + 0.5 * (T_2 + \sqrt{T_2 * T_2 + 0.004}) \quad (2.218)$$

$$N_{sat} = 0.5 * (1.0 + \sqrt{1.0 + T_3}) \quad (2.219)$$

$$N_{sat} = 0.5 * [(N_{sat} + 1.0) - \sqrt{(N_{sat} - 1.0)^2 + 0.25 * 0.01^2}] + 0.25 * 0.01 \quad (2.220)$$

$$I_{ds} = I_{ds} / N_{sat} \quad (2.221)$$

2.13 Effective Mobility

$$\mu_{eff} = \frac{U0}{D_{tot}} \quad (2.222)$$

2.14 Drain Current Model

2.14.1 Without Velocity Saturation

The drain current expression is derived as follows,

$$I_{ds} = I_{drift} + I_{diff} \quad (2.223)$$

$$I_{ds} = -W_{eff}.Q_i \cdot \mu_{eff} \frac{d\psi_s}{dx} + W \cdot \mu_{eff} \cdot V_t \frac{dQ_i}{dx} \quad (2.224)$$

from charge linearization, $\psi_s = \psi_p + \frac{Q_i}{n_q.C_{ox}}$. Thus

$$I_{ds} = \mu_{eff}.W_{eff} \cdot \left[-\frac{Q_i}{n_q.C_{ox}} + V_t \right] \frac{dQ_i}{dx} \quad (2.225)$$

normalizing inversion charge to $-2n_qC_{ox}V_t$ and using $\xi = \frac{x}{L}$,

$$I_{ds} = \mu_{eff} \cdot \frac{W_{eff}}{L_{eff}} \cdot \left[-\frac{(-2.n_q.C_{ox}.V_t.q)}{n_q.C_{ox}} + V_t \right] \frac{d(-2.n_q.C_{ox}.V_t.q)}{d\xi} \quad (2.226)$$

$$= -2 \cdot n_q \cdot \mu_{eff} \cdot \frac{W_{eff}}{L_{eff}} \cdot C_{ox} \cdot nV_t^2 \cdot (2q+1) \frac{dq}{d\xi} \quad (2.227)$$

Total drain current,

$$I_{DS} = \int_0^1 I_{ds} d\xi = -2 \cdot n_q \cdot \mu_{eff} \cdot \frac{W_{eff}}{L_{eff}} \cdot C_{ox} \cdot nV_t^2 \cdot \int_{q_s}^{q_d} (2q+1) dq \quad (2.228)$$

which gives

$$I_{DS} = 2 \cdot n_q \cdot \mu_{eff} \cdot \frac{W_{eff}}{L_{eff}} \cdot C_{ox} \cdot nV_t^2 \cdot [(q_s - q_{deff})(q_s + q_{deff} + 1)] \quad (2.229)$$

n_q is the slope factor in charge based model and nV_t is $n \cdot \frac{KT}{q}$ with n given by (2.156).

$$I_{DS} = 2 \cdot n_q \cdot \mu_{eff} \cdot \frac{W_{eff}}{L_{eff}} \cdot C_{ox} \cdot nV_t^2 \cdot [(q_s - q_{deff})(q_s + q_{deff} + 1)] \quad (2.230)$$

2.14.2 Including Velocity Saturation

As the device is getting smaller and smaller, the lateral electric field strength and therefore kinetic energy of the carriers increases. On reaching optical phonon energy levels, they releases optical phonon by virtue of reduction in kinetic energy and therefore loses velocity [7]. The effect of velocity saturation on mobility is captured as follows

$$\mu = \frac{\mu_{eff}}{\sqrt{1 + (\frac{E}{E_c})^2}} \quad (2.231)$$

$$= \frac{\mu_{eff}}{\sqrt{1 + (\frac{1}{E_c} \cdot \frac{d\psi_s}{dx})^2}} \quad (2.232)$$

from (2.227) and (2.232),

$$I_{ds} = -2 \cdot n_q \cdot \frac{\mu_{eff}}{\sqrt{1 + (\frac{1}{E_c} \cdot \frac{d\psi_s}{dx})^2}} \cdot \frac{W_{eff}}{L_{eff}} \cdot C_{ox} \cdot nV_t^2 \cdot (2q + 1) \frac{dq}{d\xi} \quad (2.233)$$

$$= z \cdot \frac{(2q + 1) \frac{dq}{d\xi}}{\sqrt{1 + (\frac{1}{E_c} \cdot \frac{d\psi_s}{dx})^2}} \quad (2.234)$$

with $z = -2\mu_{eff} \cdot n_q \cdot \frac{W_{eff}}{L_{eff}} \cdot C_{ox} \cdot nV_t^2$

Total current,

$$I_{DS} = \int_0^1 I_{ds} d\xi = z \cdot \int_{q_s}^{q_d} \frac{(2q + 1)}{\sqrt{1 + (\frac{1}{E_c} \cdot \frac{d\psi_s}{dx})^2}} dq \quad (2.235)$$

$$I_{DS} \int_0^1 \sqrt{1 + \left(\frac{1}{E_c} \cdot \frac{d\psi_s}{dx}\right)^2} dq = z \cdot \int_{q_s}^{q_d} (2q + 1) dq \quad (2.236)$$

from (2.262),

$$\int_{q_s}^{q_d} (2q + 1) dq = -(q_s - q_{deff})(q_s + q_{deff} + 1) \quad (2.237)$$

Now consider the LHS of (2.236). Using charge linearization, $\psi_s = \psi_p + \frac{Q_i}{n_q \cdot C_{ox}}$,

$$\frac{1}{E_c} \frac{d\psi_s}{dx} = \frac{1}{E_c \cdot n_q \cdot C_{ox}} \frac{Q_i}{dx} = -\frac{2V_t}{E_c \cdot L} \frac{dq}{d\xi} = -\lambda_c \cdot \frac{dq}{d\xi} \quad (2.238)$$

Let

$$D_{vsat} = \int \sqrt{1 + \left(\frac{1}{E_c} \cdot \frac{d\psi_s}{dx} \right)^2} d\xi$$

It is evaluated by assuming that lateral electric field ($-\frac{d\psi_s}{d\xi}$) increases linearly from 0 at source to $2 \cdot \left(\frac{\psi_{s,D} - \psi_{s,S}}{L} \right)$ at drain [8] i.e.

$$-\frac{d\psi_s}{dx} = 2 \cdot \frac{\psi_{s,D} - \psi_{s,S}}{L} \cdot \frac{x}{L} = 2 \cdot \frac{\psi_{s,D} - \psi_{s,S}}{L} \cdot \xi \quad (2.239)$$

From charge linearization (2.107),

$$\psi_{s,S} = \psi_P + \frac{Q_S}{n_q \cdot C_{ox}} = \psi_P - 2V_t \cdot q_s \quad (2.240)$$

$$\psi_{s,D} = \psi_P + \frac{Q_D}{n_q \cdot C_{ox}} = \psi_P - 2V_t \cdot q_d \quad (2.241)$$

$$\psi_{s,D} - \psi_{s,S} = 2 \cdot V_t (q_s - q_d) \quad (2.242)$$

substituting in (2.239),

$$-\frac{d\psi_s}{dx} = 2 \cdot \frac{2 \cdot V_t (q_s - q_d)}{L^2} \cdot x = 2 \cdot \frac{2 \cdot V_t (q_s - q_d)}{L} \cdot \xi \quad (2.243)$$

$$-\frac{1}{E_c} \frac{d\psi_s}{dx} = 2 \cdot \frac{2 \cdot V_t}{E_c L} \cdot (q_s - q_d) \xi = 2 \lambda_c (q_s - q_d) \xi \quad (2.244)$$

where $\lambda_c = \frac{2V_t}{E_c \cdot L}$. Thus D_{vsat} can be given as

$$D_{vsat} = \int \sqrt{1 + \left(\frac{1}{E_c} \cdot \frac{d\psi_s}{dx} \right)^2} d\xi \quad (2.245)$$

$$= \int \sqrt{1 + (2 \lambda_c (q_s - q_d) \xi)^2} d\xi = \int \sqrt{1 + (2 \lambda_c \Delta q \cdot \xi)^2} d\xi \quad (2.246)$$

$$= \frac{1}{2} \left[\sqrt{1 + (2 \lambda_c \Delta q)^2} + \frac{1}{2 \lambda_c \Delta q} \cdot \ln \left(2 \lambda_c \Delta q + \sqrt{1 + (2 \lambda_c \Delta q)^2} \right) \right] \quad (2.247)$$

with $\Delta q = q_s - q_d$. From (2.236), (2.237) and (2.247),

$$I_{DS} = 2 \cdot n_q \cdot \mu_{eff} \cdot \frac{W_{eff}}{L_{eff}} \cdot C_{ox} \cdot nV_t^2 \cdot [(q_s - q_{deff})(q_s + q_{deff} + 1)].M_{oc} \quad (2.248)$$

where $\mu_{eff} = \frac{U_0}{D_{tot}}$ and $D_{tot} = D_{mod} \cdot D_{vsat} \cdot D_r$

2.15 Threshold Voltage Model

2.15.1 Long Channel Threshold Voltage

The drain current under the standard drift-diffusion formalism can be represented as

$$I_{ds} = I_{drift} + I_{diff} \quad (2.249)$$

$$I_{ds} = -W.Q_i \cdot \mu \frac{d\psi_s}{dx} + W \cdot \mu \cdot V_t \frac{dQ_i}{dx} \quad (2.250)$$

Defining threshold voltage as the gate voltage at which $I_{drift} = I_{diff}$, which leads to $q_i = \frac{1}{2}$. Here, we define threshold voltage as the gate voltage at which normalized inversion charge density at the source is $q_s = \frac{1}{2}$. Pinch-off potential corresponding to $q_s = \frac{1}{2}$, $\psi_{p,th}$, is calculated using $q_s = \frac{1}{2}$ in (2.114) leading to

$$\psi_{p,th} = \left[\ln(0.5) + 1 \right] + \ln \left[\frac{2n_q}{\gamma_0} \left(\frac{n_q}{\gamma_0} + 2\sqrt{\psi_{p,th} - 1} \right) \right] + 2\phi_f + v_s \quad (2.251)$$

To obtain $\psi_{p,th}$ in explicit form, we make an assumption that at threshold voltage,

$$\psi_{p,th} - 1 = 2\phi_f + v_s \quad (2.252)$$

The other bias dependent term n_q is also approximated by

$$n_q = 1 + \frac{\gamma}{2\sqrt{2\phi_f}} \quad (2.253)$$

This gives,

$$\begin{aligned} \psi_{p,th} = & \left[\ln(0.5) + 1 \right] + \ln \left[\frac{2n_q}{\gamma_0} \left(\frac{n_q}{\gamma_0} + 2\sqrt{2\phi_f - v_b} \right) \right] + 2\phi_f \\ & + v_s \end{aligned} \quad (2.254)$$

After $\psi_{p,th}$ is obtained, next step is to calculate threshold voltage. The potential balance equation in conjunction with Poisson's equation and Gauss law for the MOSFET is given as ()

$$V_G = V_{FB} + \psi_S - \frac{Q_{in} + Q_{dep}}{C_{ox}} \quad (2.255)$$

At pinch-off, $\psi_S = \psi_P$, and $Q_{in} = 0$

$$V_G = V_{FB} + \psi_P + \gamma\sqrt{\psi_P} \quad (2.256)$$

Thus [9]

$$V_{TH,long} = V_{FB} + \psi_{p,th}.V_t - \gamma\sqrt{\psi_{p,th}.V_t} \quad (2.257)$$

Short Channel Threshold Voltage

$$V_{TH} = V_{TH,long} - \Delta V_{th,all} \quad (2.258)$$

2.16 MNUD model to increase $I_{DS} - V_{DS}$ Fitting Flexibility

$$MNUD = 1 + K_0 \left[\frac{(q_s - q_{deff})}{(M_0 + q_s + q_{deff})} \right]^2 \quad (2.259)$$

$$I_{DS} = 2 \cdot n_q \cdot \mu_{eff} \cdot \frac{W_{eff}}{L_{eff}} \cdot C_{ox} \cdot nV_t^2 \cdot [(q_s - q_{deff})(q_s + q_{deff} + 1)].M_{oc}/MNUD \quad (2.260)$$

2.17 MNUD1 model to increase $g_m - I_D$ Fitting Flexibility

$$MNUD1 = \exp \left[- \frac{C0}{[(C0SI + C0SISAT \cdot (q_s - q_{deff})^2)(q_s + q_{deff}) + 2 \cdot n \cdot V_t]} \right] \quad (2.261)$$

$$I_{DS} = 2 \cdot n_q \cdot \mu_{eff} \cdot \frac{W_{eff}}{L_{eff}} \cdot C_{ox} \cdot nV_t^2 \cdot [(q_s - q_{deff})(q_s + q_{deff} + 1)].M_{oc}/MNUD \cdot MNUD1 \quad (2.262)$$

2.18 AbulkIV model to increase $I_{DS} - V_{DS}$ Fitting Flexibility

$$T1 = \frac{Leff}{Leff + sqrt(XJ_i * Xdep)} \quad (2.263)$$

$$AbulkIV = 1 + \frac{A0 * T1 - AGS * q_s^{AGS1} * V_T * T1}{1 + KETA * V_{bsx}} \quad (2.264)$$

$$Vdssat = Vdssat / AbulkIV \quad (2.265)$$

$$T7 = pow(Vds / Vdssat, 1 / Delta_t) \quad (2.266)$$

$$T8 = pow(1 + T7, -Delta_t) \quad (2.267)$$

$$Vdseff = Vds * T8 \quad (2.268)$$

$$Vdeff = (Vdseff + Vs) * inv_Vt \quad (2.269)$$

Calculate qdeff using new Vdeff

2.19 Subthreshold Hump Module

The Edge FET Model current is added to the main current I_{ds} , when the parameter EDGEFET is 1 [10].

$$\begin{aligned} Ids, EDGE &= 2 \cdot NF \cdot nq \cdot \mu_{eff} \cdot WEDGE / Leff \cdot C_{ox} \cdot \\ &nV_t \cdot ((q_s - q_{deff}) \cdot (1 + q_s + q_{deff})) \cdot M_{oc} \end{aligned} \quad (2.270)$$

Now the total current will be $I_{Total} = Ids_{EDGE} + I_{ds}$. The parameters associated with subthreshold hump model are: WEDGE, DGAMMA, DGAMMAL, DGAMMAEXP, DVTEDGE, NFACTOREDGE, CITEDGE, CDSCDEDGE, CDSCBEDGE, ETA0EDGE, ETABEDGE, KT1EDGE, KT1LEDGE, KT2EDGE, KT1EXPEDGE, TNFACTOREDGE, TETA0EDGE, DVT0EDGE, DVT1EDGE, DVT2EDGE.

2.20 Modeling of Sub-Surface Leakage Drain Current

The flag for the sub-surface leakage model is SSLMOD [11].

$$T1 = \left(\frac{NDEP}{1e23} \right)^{SSLEXP1} \quad T2 = \left(\frac{300}{T} \right)^{SSLEXP2} \quad (2.271)$$

$$T3 = \frac{devsign.SSL5.V_{bs}}{Vt} \quad (2.272)$$

$$SSL0_NT = SSL0.exp(-T1T2) \quad SSL0_NT = SSL1.T2.T1 \quad (2.273)$$

$$T5 = SSL3.tanh\left(\exp(devsign.SSL4.(V_{gb} - VTH - V_{sb}))\right) \quad (2.274)$$

$$\begin{aligned} I_{ssl} = & sigvds.NF.W_{eff}.SSL0_NT.\exp(T3). \\ & \exp(-SSL1_NT.L + \frac{T5}{Vt}) \left[\exp(SSL2.\frac{V_{dsx}}{Vt}) - 1 \right] \end{aligned} \quad (2.275)$$

2.21 Impact Ionization Model

The impact ionization current model in intrinsic region for HVMOD=0 in BSIM-BULK is the same as that in BSIM4, and is modeled by

$$I_{ii} = ALPHA0 \cdot (V_{ds} - V_{dseff}) \cdot \exp\left(-\frac{BETA0}{V_{ds} - V_{dseff}}\right) \cdot \frac{I_{ds}}{M_{SCBE}} \quad (2.276)$$

where parameters *ALPHA0* and *BETA0* are impact ionization coefficients. *ALPHA0L* and *ALPHA0LEXP* are length scaling parameters for *ALPHA0*.

Note: The order of *ALPHA0* in BSIM6 = 10^6 X order of *ALPHA0* in BSIM4.

The impact ionization current model in intrinsic region for HVMOD=1 in BSIM-BULK is modeled by

$$I_{ii} = ALPHA0_{eff} \cdot (V_{ds} - V_{dseffii}) \cdot \exp\left(-\frac{BETA0_{eff}}{V_{ds} - V_{dseffii}}\right) \cdot \frac{I_{ds}}{M_{SCBE}} \quad (2.277)$$

$$ALPHA0_{eff} = ALPHA0 \cdot (1 + ALPHA1 \cdot V_{bsx} + ALPHA2 \cdot V_{bsx}^2) \quad (2.278)$$

$$V_{dseffii} = V_{ds} \cdot \left(1 + \left(\frac{V_{ds}}{(1 + BETA1 \cdot V_{ds}) \cdot V_{dssat}} \right)^{\frac{1}{BETA1}} \right)^{-BETA1} \quad (2.279)$$

$$BETA0_{eff} = \frac{BETA0}{2} \cdot \left(1 + V_{dseffii}^{BETA2} \right) \quad (2.280)$$

The secondary impact ionization current model in the drift region is modeled by

$$I_{subDR} = ALPHADR_{eff} \cdot E_m \cdot I_{ds} \cdot \exp\left(-\frac{BETADR}{E_m}\right) \quad (2.281)$$

$$E_m = \left[\left(\frac{2 \cdot q \cdot N_{extra}}{\epsilon} * VDDROP \right) \right]^{0.5} \quad (2.282)$$

$$VDDROP = V(d, s) - DRII3 \cdot V_{dseffii} - DRII2 - CMD1 \cdot (V_{bcm})^{DRII4} \quad (2.283)$$

$$\text{where } V_{bcm} = \sqrt{V(bi, b)^2 + 10^{-6}}$$

$$ALPHADR_{eff} = ALPHADR \cdot (1 + ALPHADR1 \cdot V_{bsx} + ALPHADR2 \cdot V_{bsx}^2) \quad (2.284)$$

2.22 GIDL/GISL Current Model

GIDL/GISL currents are set using model selector GIDLMOD=1. The GIDL/GISL current and its body bias effect are modeled by

$$\begin{aligned} I_{GIDL} &= AGIDL \cdot W_{eff} \cdot NF \cdot \frac{V_{ds} - V_{gse} - EGIDL}{3 \cdot T_{oxe}} \\ &\cdot \exp\left(-\frac{3 \cdot T_{oxe} \cdot BGIDL}{V_{ds} - V_{gse} - EGIDL}\right) \cdot \frac{V_{db}^3}{CGIDL + V_{db}^3} \end{aligned} \quad (2.285)$$

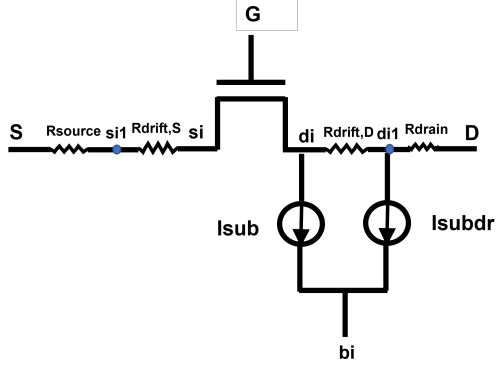


Figure 1: Equivalent circuit diagram of substrate current for intrinsic and drift region.

$$\begin{aligned}
 I_{GISL} = & AGISL \cdot W_{eff} \cdot NF \cdot \frac{-V_{ds} - V_{gde} - EGISL}{3 \cdot T_{oxe}} \\
 & \cdot \exp\left(-\frac{3 \cdot T_{oxe} \cdot BGISL}{-V_{ds} - V_{gde} - EGISL}\right) \cdot \frac{V_{sb}^3}{CGISL + V_{sb}^3}
 \end{aligned} \quad (2.286)$$

where $AGIDL$, $BGIDL$, $CGIDL$ and $EGIDL$ are model parameters for the drain side and $AGISL$, $BGISL$, $CGISL$ and $EGISL$ are the model parameters for the source side. $CGIDL$ and $CGISL$ account for the body-bias dependence of I_{GIDL} and I_{GISL} respectively. W_{eff} and NF are the effective width of the source/drain diffusions and the number of fingers. Further explanation of W_{eff} and NF can be found in the chapter of the layout-dependence model. Check scaling parameters in the parameter list at the end.

I_{GIDL}/I_{GISL} can be switched off by setting $GIDLMOD = 0$.

2.23 Gate Tunneling Current Model

As the gate oxide thickness is scaled down to $3nm$ and below, gate leakage current due to carrier direct tunneling becomes important. This tunneling happens between the gate and silicon beneath the gate oxide. To reduce the tunneling current, high-k dielectrics are being used in place of gate oxide. In order to maintain a good interface with substrate, multi-layer dielectric stacks are being used. The BSIM6 gate tunneling model (taken from BSIM4) has been shown to work for multi-layer gate stacks as well. The tunneling carriers can be either electrons or holes, or both, either from the conduction band or

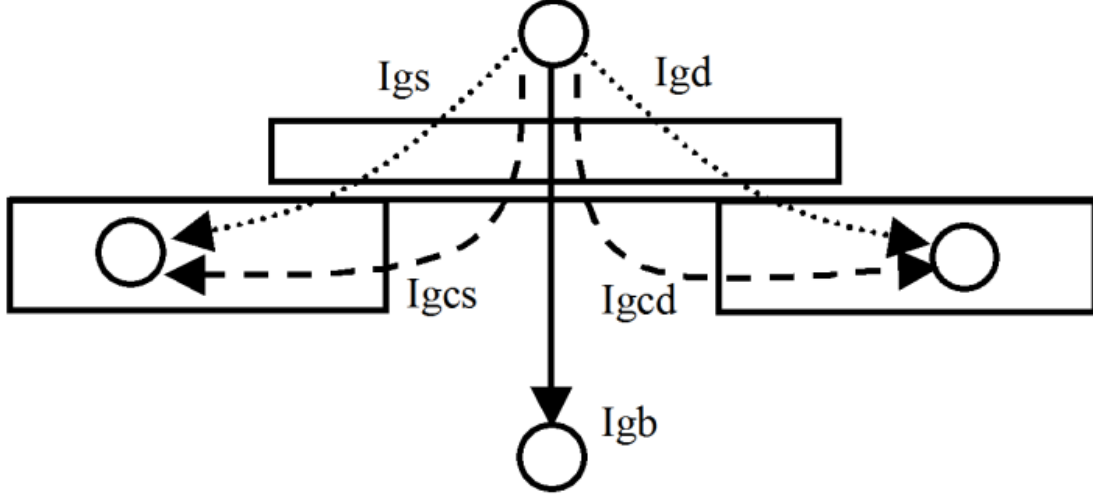


Figure 2: Schematic gate current components flowing between MOSFET terminals.

valence band, depending on (the type of the gate and) the bias regime. In BSIM6, the gate tunneling current components include the tunneling current between gate and substrate (I_{gb}), and the current between gate and channel (I_{gc}), which is partitioned between the source and drain terminals by $I_{gc} = I_{gcs} + I_{gcd}$. The third component happens between gate and source/drain diffusion regions (I_{gs} and I_{gd}). Figure 2 shows the schematic gate tunneling current flows.

2.23.1 Model Selectors

Two global selectors are provided to turn on or off the tunneling components. **IGCMOD** = 1 turns on I_{gc} , I_{gs} , and I_{gd} ; **IGBMOD** = 1 turns on I_{gb} . When the selectors are set to zero, no gate tunneling currents are modeled.

$$V_{ox} = nVt \cdot (v_g - v_{fb} - \psi_p + q_s + q_{deff}) \quad (2.287)$$

$$V_{oxacc} = \frac{1}{2} \left(-V_{ox} + \sqrt{V_{ox}^2 + 10^{-4}} \right) \quad (2.288)$$

$$V_{oxdepinv} = \frac{1}{2} \left(V_{ox} + \sqrt{V_{ox}^2 + 10^{-4}} \right) \quad (2.289)$$

Eq. (2.288) and (2.289) are valid and continuous from accumulation through depletion to inversion.

2.23.2 Equations for Tunneling Currents

Note: All gate tunneling current equations use operating temperature in the calculations.

Gate-to-Substrate Current ($I_{gb} = I_{gbacc} + I_{gbinv}$): I_{gbacc} , determined by ECB (Electron tunneling from Conduction Band), is significant in accumulation and given by

$$I_{gbacc} = NF \cdot W_{eff}L_{eff} \cdot A \cdot T_{oxRatio} \cdot V_{gb} \cdot V_{aux} \cdot i_{gttemp} \\ \cdot \exp[-B \cdot TOXE(AIGBACC - BIGBACC \cdot V_{oxacc}) \cdot (1 + CIGBAC \cdot V_{oxacc})] \quad (2.290)$$

where the physical constants $A = 4.97232e - 7 \text{ A/V}^2$, $B = 7.45669e11(g/F - s^2)^{0.5}$, and

$$T_{oxRatio} = \left(\frac{TOXREF}{TOXE} \right)^{NTOX} \cdot \frac{1}{TOXE^2} \quad (2.291)$$

$$V_{aux} = NIGBACC \cdot V_t \cdot \log \left(1 + \exp \left(- \frac{V_{ox}}{NIGBACC \cdot V_t} \right) \right) \quad (2.292)$$

I_{gbinv} , determined by EVB (Electron tunneling from Valence Band), is significant in inversion and given by

$$I_{gbinv} = NF \cdot W_{eff}L_{eff} \cdot A \cdot T_{oxRatio} \cdot V_{gb} \cdot V_{aux} \cdot i_{gttemp} \\ \cdot \exp[-B \cdot TOXE(AIGBINV - BIGBINV \cdot V_{oxdepinv}) \cdot (1 + CIGBINVV_{oxdepinv})] \quad (2.293)$$

where $A = 3.75956e-7 \text{ A/V}^2$, $B = 9.82222e11 (g/F - s^2)^{0.5}$, and

$$V_{aux} = NIGBINV \cdot V_t \cdot \log \left(1 + \exp \left(\frac{V_{ox} - EIGBINV}{NIGBINV \cdot V_t} \right) \right) \quad (2.294)$$

$$I_{gb} = I_{gbacc} + I_{gbinv} \quad (2.295)$$

Gate-to-Channel Current (I_{gc0}) and Gate-to-S/D (I_{gs} and I_{gd}): I_{gc0} , determined by ECB for NMOS and HVB (Hole tunneling from Valence Band) for PMOS at $V_{ds} = 0$, is formulated as

$$\begin{aligned} I_{gc0} = & NF \cdot W_{eff} L_{eff} \cdot A \cdot T_{oxRatio} \cdot V_{gse} \cdot V_{aux} \cdot i_{gtemp} \\ & \cdot \exp[-B \cdot TOXE(AIGC - BIGC \cdot V_{oxdepinv}) \cdot (1 + CIGCV_{oxdepinv})] \end{aligned} \quad (2.296)$$

where $A = 4.97232 \text{ A/V}^2$ for NMOS and 3.42537 A/V^2 for PMOS, $B = 7.45669e11 (g/F - s^2)^0.5$ for NMOS and $1.16645e12 (g/F - s^2)^0.5$ for PMOS.

$$V_{aux} = n_q \cdot nVt \cdot (q_s + q_{deff}) \quad (2.297)$$

Partition of I_{gc} : To consider the drain bias effect, I_{gc} is split into two components, I_{gcs} and I_{gcd} , that is $I_{gc} = I_{gcs} + I_{gcd}$, and

$$I_{gcs} = I_{gc0} \cdot \frac{PIGCD \cdot V_{dseffx} + \exp(-PIGCD \cdot V_{dseffx}) - 1 + 10^{-4}}{PIGCD \cdot V_{dseffx}^2 + 2 \cdot 10^{-4}} \quad (2.298)$$

and

$$I_{gcd} = I_{gc0} \cdot \frac{1 - (PIGCD \cdot V_{dseffx} + 1) \cdot \exp(-PIGCD \cdot V_{dseffx}) + 10^{-4}}{PIGCD \cdot V_{dseffx}^2 + 2 \cdot 10^{-4}} \quad (2.299)$$

where

$$V_{dseffx} = \sqrt{V_{dseff} + 0.01} - 0.1 \quad (2.300)$$

At $V_{ds} = 0$, $I_{gcs} = I_{gcd} = \frac{1}{2}I_{gc0}$. Thus I_{gc0} is the gate to channel current I_{gc} at $V_{ds} = 0$.

I_{gs} and I_{gd} : I_{gs} represents the gate tunneling current between the gate and the source diffusion region, while I_{gd} represents the gate tunneling current between the gate and the drain diffusion region. I_{gs} and I_{gd} are determined by ECB for NMOS and HVB for PMOS, respectively.

$$\begin{aligned} I_{gs} = & NF \cdot W_{eff} DLCIG \cdot A \cdot T_{oxRatioEdge} \cdot V_{gs} \cdot V'_{gs} \cdot i_{gtemp} \\ & \cdot \exp[-B \cdot TOXE \cdot POXEDGE \cdot (AIGS - BIGS \cdot V'_{gs}) \cdot (1 + CIGSV'_{gs})] \end{aligned} \quad (2.301)$$

and

$$\begin{aligned} I_{gd} = & NF \cdot W_{eff} DLCIGD \cdot A \cdot T_{oxRatioEdge} \cdot V_{gd} \cdot V'_{gd} \cdot i_{gtemp} \\ & \cdot \exp[-B \cdot TOXE \cdot POXEDGE \cdot (AIGD - BIGD \cdot V'_{gd}) \cdot (1 + CIGDV'_{gd})] \end{aligned} \quad (2.302)$$

where $A = 4.97232 A/V^2$ for NMOS and $3.42537 A/V^2$ for PMOS, $B = 7.45669e11 (g/F - s^2)^{0.5}$ for NMOS and $1.16645e12 (g/F - s^2)^{0.5}$ for PMOS, and

$$T_{oxRatioEdge} = \left(\frac{TOXREF}{TOXE \cdot POXEDGE} \right)^{NTOX} \cdot \frac{1}{(TOXE \cdot POXEDGE)^2} \quad (2.303)$$

$$V'_{gs} = \sqrt{(V_{gs} - V_{fbsd})^2 + 10^{-4}} \quad (2.304)$$

$$V'_{gd} = \sqrt{(V_{gd} - V_{fbsd})^2 + 10^{-4}} \quad (2.305)$$

V_{fbsd} is the flat-band voltage between gate and S/D diffusions calculated as

If $NGATE > 0.0$

$$V_{fbsd} = -devsign \cdot \frac{k_B T}{q} \log \left(\frac{NGATE}{NSD} \right) + VFBSDOFF \quad (2.306)$$

Else $V_{fbsd} = 0.0$.

2.24 Gate resistance and Body resistance network Model

2.24.1 Gate Electrode Electrode and Intrinsic-Input Resistance (IIR) Model

General Description: BSIM6 provides four options for modeling gate electrode resistance (bias-independent) and intrinsic-input resistance (IIR, bias-dependent). The IIR model considers the relaxation-time effect due to the distributive RC nature of the channel region, and therefore describes the first-order non-quasi-static effect. Thus, the IIR model should not be used together with the charge-deficit NQS model at the same time. The model selector RGATEMOD is used to choose different options.

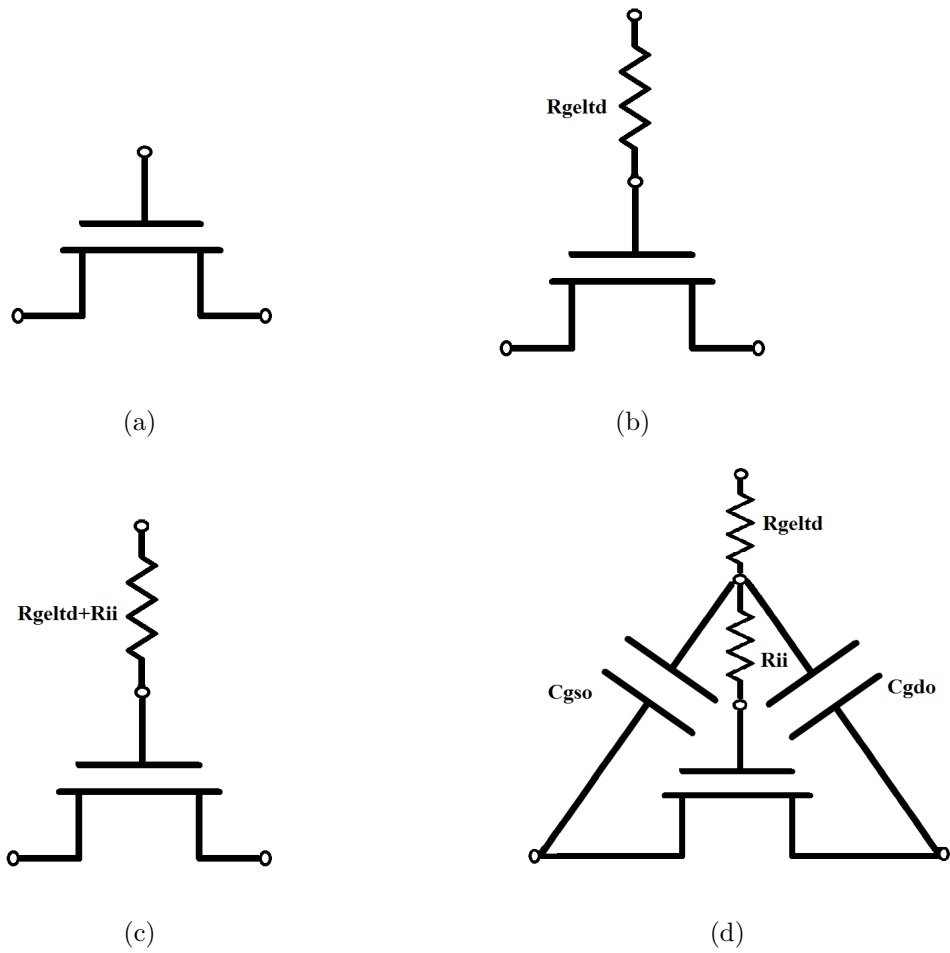


Figure 3: Gate resistance network for (a) $RGATEMOD = 0$ (b) $RGATEMOD = 1$
 (c) $RGATEMOD = 2$ (d) $RGATEMOD = 3$.

Model Option and Schematic: There are four model selectors for gate resistance network.

RGATEMOD = 0 (zero-resistance): In this case, no gate resistance is generated (see Figure 3).

RGATEMOD = 1 (constant-resistance): In this case, only the electrode gate resistance (bias-independent) is generated by adding an internal gate node. R_{geltd} is given by

$$R_{geltd} = \frac{RSHG \cdot (XGW + \frac{W_{effci}}{3 \cdot NGCON})}{NGCON \cdot (L_{drawn} - XGL) \cdot NF} \quad (2.307)$$

RGATEMOD = 2 (IIR model with variable resistance): In this case, the gate resistance is the sum of the electrode gate resistance R_{geltd} (2.307) and the intrinsic-input resistance R_{ii} as given by (2.308).

$$\frac{1}{R_{ii}} = XRCRG1.NF \cdot \left(\frac{I_{ds}}{V_{dseff}} + XRCRG2 \cdot \frac{W_{eff}\mu_{eff}C_{oxeff}V_t}{L_{eff}} \right)$$

or

$$\frac{1}{R_{ii}} \approx XRCRG1.NF \cdot \left(\mu_{eff} \left(\frac{W_{eff}}{L_{eff}} \right) C_{ox} \cdot q_{ia} + XRCRG2 \cdot \frac{W_{eff}\mu_{eff}C_{oxeff}V_t}{L_{eff}} \right) \quad (2.308)$$

RGATEMOD = 3 (IIR model with two nodes): In this case, the gate electrode resistance R_{geltd} is in series with the intrinsic-input resistance R_{ii} through two internal gate nodes, so that the overlap capacitance current will not pass through the intrinsic-input resistance.

2.24.2 Substrate Resistance Network

General Description: For CMOS RF circuit simulation, it is essential to consider the high frequency coupling through the substrate. BSIM6 offers a flexible built-in substrate resistance network. This network is constructed such that little simulation efficiency penalty will result. Note that the substrate resistance parameters should be extracted for the total device, not on a per-finger basis.

Model Selector and Topology The model selector **RBODYMOD** can be used to turn on or turn off the resistance network.

RBODYMOD = 0 (Off):

No substrate resistance network is generated at all.

RBODYMOD = 1 (On):

All five resistances $RBPS$, $RBPD$, $RBPB$, $RBSB$, and $RBDB$ in the substrate network as shown schematically below are present simultaneously.

A minimum conductance, $GBMIN$, is introduced in parallel with each resistance and therefore to prevent infinite resistance values, which would otherwise cause poor convergence. $GBMIN$ is merged into each resistance to simplify the representation of the model topology. Note that the intrinsic model substrate reference point in this case is the internal body node **bNodePrime**, into which the impact ionization current I_{ii} and the GIDL current I_{GIDL} flow.

RBODYMOD = 2 (On : Scalable Substrate Network):

The schematic is similar to **RBODYMOD = 1** but all the five resistors in the substrate network are now scalable with a possibility of choosing either five resistors, three resistors or one resistor as the substrate network.

The resistors of the substrate network are scalable with respect to channel length (L), channel width (W) and number of fingers (NF). The scalable model allows to account for both horizontal and vertical contacts.

The scalable resistors $RBPS$ and $RBPD$ are evaluated through

$$RBPS = RBPS0 \cdot \left(\frac{L}{10^{-6}} \right)^{RBPSL} \cdot \left(\frac{W}{10^{-6}} \right)^{RBPSW} \cdot NF^{RBPSNF} \quad (2.309)$$

$$RBPD = RBPD0 \cdot \left(\frac{L}{10^{-6}} \right)^{RBPDL} \cdot \left(\frac{W}{10^{-6}} \right)^{RBPDW} \cdot NF^{RBPDNF} \quad (2.310)$$

The resistor $RBPB$ consists of two parallel resistor paths, one to the horizontal contacts and other to the vertical contacts. These two resistances are scalable and $RBPB$ is given

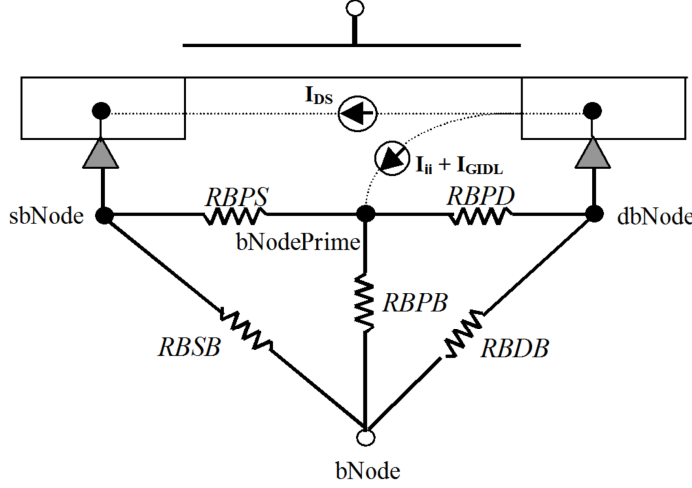


Figure 4: Topology with the substrate resistance network turned on.

by a parallel combination of these two resistances.

$$RBPBX = RBPBX_0 \cdot \left(\frac{L}{10^{-6}} \right)^{RBPBX_L} \cdot \left(\frac{W}{10^{-6}} \right)^{RBPBX_W} \cdot NF^{RBPDX} \quad (2.311)$$

$$RBPBY = RBPBY_0 \cdot \left(\frac{L}{10^{-6}} \right)^{RBPBY_L} \cdot \left(\frac{W}{10^{-6}} \right)^{RBPBY_W} \cdot NF^{RBPDX} \quad (2.312)$$

$$RBPB = \frac{RBPBX \cdot RBPBY}{RBPBX + RBPBY} \quad (2.313)$$

The resistors RBSB and RBDB share the same scaling parameters but have different scaling prefactors. These resistors are modeled in the same way as RBPB. The equations

for RBSB are shown below. The calculation for RBDB follows RBSB.

$$RBSBX = RBSBX0 \cdot \left(\frac{L}{10^{-6}} \right)^{RBSBXL} \cdot \left(\frac{W}{10^{-6}} \right)^{RBSBXW} \cdot NF^{RBSDNF} \quad (2.314)$$

$$RBSBY = RBSBY0 \cdot \left(\frac{L}{10^{-6}} \right)^{RBSBYL} \cdot \left(\frac{W}{10^{-6}} \right)^{RBSBYW} \cdot NF^{RBSDNF} \quad (2.315)$$

$$RBSB = \frac{RBSBX \cdot RBSBY}{RBSBX + RBSBY} \quad (2.316)$$

Similarly, the equations for RBDB is as follows

$$RBDBX = RBDBX0 \cdot \left(\frac{L}{10^{-6}} \right)^{RBDBXL} \cdot \left(\frac{L}{10^{-6}} \right)^{RBDBXW} \cdot (NF)^{RBDBXNF} \quad (2.317)$$

$$RBDBY = RBDBY0 \cdot \left(\frac{L}{10^{-6}} \right)^{RBDBYL} \cdot \left(\frac{L}{10^{-6}} \right)^{RBDBYW} \cdot (NF)^{RBDBYNF} \quad (2.318)$$

$$RBDB = \frac{RBDBX \times RBDBY}{RBDBX + RBDBY} \quad (2.319)$$

The implementation of **RBODYMOD** = 2 allows the user to chose between the 5-R network (with all five resistors), 3-R network (with RBPS, RBPD and RBPB) and 1-R network (with only RBPB).

If the user does not provide both the scaling parameters RBSBX0 and RBSBY0 for RBSB or both the scaling parameters RBDBX0 and RBDBY0 for RBDB, then the conductances for both RBSB and RBDB are set to GDMIN. This converts the 5-R schematic to 3-R schematic where the substrate network consists of the resistors RBPS, RBPD and RBPB. RBPS, RBPD and RBPB are then calculated using (2.309), (2.310), and (2.313).

If the user chooses not to provide either of RBPS0 or RBPD0, then the 5-R schematic is converted to 1-R network with only one resistor RBPB. The conductances for RBSB and RBDB are set to GDMIN. The resistances RBPS and RBPD are set to 1e-3 Ohm. The resistor RBPB is then calculated using (2.313).

In all other situations, 5-R network is used with the resistor values calculated from the equations aforementioned.

2.25 Noise Modeling

The following noise sources in MOSFETs are modeled in BSIM6 for SPICE noise analysis: flicker noise (also known as 1/f noise), channel thermal noise and induced gate noise and their correlation, thermal noise due to physical resistances such as the source/ drain, gate electrode, and substrate resistances, and shot noise due to the gate dielectric tunneling current.

Noise models in BSIM 6.0.0	Origin
Flicker noise model	BSIM4 Unified Model (FNOIMOD=0)
Thermal noise(TNOIMOD=0)	BSIM4 (TNOIMOD=0)
Thermal noise (TNOIMOD=1)	BSIM4 (TNOIMOD=2)
Gate current shot noise	BSIM4 gate current noise
Noise associated with parasitic resistances	BSIM4 parasitic resistance noise

2.25.1 Flicker Noise Models

FNOIMOD = 0 (Flicker Noise Model): BSIM-BULK's flicker noise model for FNOIMOD=0 is same as FNOIMOD=1 in BSIM4. The unified physical flicker noise model is smooth over all bias regions.

The physical mechanism for the flicker noise is trapping/detrapping-related charge fluctuation in oxide traps, which results in fluctuations of both mobile carrier numbers and mobilities in the channel. The unified flicker noise model captures this physical process. In the inversion region, the noise density is expressed as [12]

$$\begin{aligned}
T2 &= NOIA \cdot \log \left(\frac{N_0 + N^*}{N_l + N^*} \right) \\
T3 &= NOIB \cdot (N_0 - N_l) \\
T4 &= \frac{NOIC}{2} (N_0^2 - N_l^2) \\
T0C &= NOIA + NOIB \cdot N_l + NOIC \cdot N_l^2 \\
S_{id,inv}(f) &= \frac{kTq^2\mu_{eff}I_{ds}}{C_{oxe}L_{effNOI}^2f^{EF} \cdot 10^{10}} \left(T2 + T3 + T4 \right) \\
&\quad + \frac{kTI_{ds}^2\Delta L_{clm}}{W_{eff}L_{effNOI}^2f^{EF} \cdot 10^{10}} \left(\frac{T0C}{(N_l + N^*)^2} \right)
\end{aligned} \tag{2.320}$$

where $L_{effNOI} = L_{eff} - 2 \cdot LINTNOI$, μ_{eff} is the effective mobility at the given bias condition, and L_{eff} and W_{eff} are the effective channel length and width, respectively. The parameter N_0 is the charge density at the source side given by

$$N_0 = \frac{2n_q C_{ox} V_t q_s}{q} \quad (2.321)$$

The parameter N_l is the charge density at the drain end given by

$$N_l = \frac{2n_q C_{ox} V_t q_{deff}}{q} \quad (2.322)$$

and N^* is given by

$$N^* = \frac{V_t (C_{ox} + C_d + CIT)}{q} \quad (2.323)$$

where CIT is a model parameter from DC IV and C_d is the depletion capacitance.

ΔL_{clm} is the channel length reduction due to channel length modulation and given by

$$\begin{aligned} \Delta L_{clm} &= l_{itl} \cdot \log \left(\frac{\frac{V_{ds} - V_{dseff}}{l_{itl}} + EM}{E_{sat}} \right) \\ E_{sat} &= \frac{2V_{SAT}}{\mu_{eff}} \end{aligned} \quad (2.324)$$

In the subthreshold region, the noise density is written as

$$S_{id,subVt}(f) = \frac{NOIA_{eff} \cdot k \cdot T \cdot I_{ds}^2}{W_{eff} L_{eff} f^{EF} N^{*2} \cdot 10^{10}} \quad (2.325)$$

$$NOIA_{eff} = \text{Max} \left[1, \left(\frac{\frac{NOIA_3}{NOIA}}{1 + \left(\frac{q_{ia}}{QSREF} \right)^{MPOWER}} \right) \right] \cdot NOIA$$

The Max[.] function is implemented using $\text{Max}(x, y) = \frac{1}{2} \left(x + y + \sqrt{(x - y)^2 + 0.25 \times SPFN^2} \right)$

The total flicker noise density is

$$S_{id}(f) = \frac{S_{id,inv} \cdot S_{id,subVt}}{S_{id,inv} + S_{id,subVt}} \quad (2.326)$$

FNOIMOD = 1 (Flicker Noise Model for Halo Transistors): For the noise modeling, it is now assumed that the transistor is composed of two transistors, channel transistor of length $L - LH$ and halo transistor of length LH connected in series and carries same current (IDS) as in single transistor configuration. The individual contribution of the halo and channel transistors to overall noise is obtained using small signal analysis and principle of superposition [13] [14].

Total drain current noise PSD becomes,

$$S_{ID} = S_{ID,1} + S_{ID,2} \quad (2.327)$$

$$\begin{aligned} &= S_{ID,h} \left[\frac{g_{m,ch} + g_{d,ch}}{g_{m,ch} + g_{d,ch} + g_{d,h}} \right]^2 + \\ &S_{ID,ch} \left[\frac{g_{d,h}}{g_{m,ch} + g_{d,ch} + g_{d,h}} \right]^2 \end{aligned} \quad (2.328)$$

$$= S_{ID,h} \cdot CF_h + S_{ID,ch} \cdot CF_{ch} \quad (2.329)$$

We refer to the multiplying factors to $S_{ID,h}$ and $S_{ID,ch}$ in (2.328) as contribution factors (CF). Where,

$$g_{d,ch} = 2n_q \mu C_{ox} \frac{W}{L - L_h} V_t q_{d,ch} \quad (2.330)$$

$$g_{d,h} = 2n_q \mu C_{ox} \frac{W}{L_h} V_t q_{d,h} \quad (2.331)$$

$$g_{m,ch} = 2\mu C_{ox} \frac{W}{L - L_h} V_t (q_{s,ch} - q_{d,ch}) \quad (2.332)$$

To calculate $q_{d,h}$ and $q_{s,ch}$, the fact that the same current flows in one transistor and two transistor noise equivalent configuration is used,

$$i_h = \frac{I_{DS}}{-2n_q \mu C_{ox} \frac{W}{L_h} V_t^2} = (q_{s,h}^2 + q_{s,h}) - (q_{d,h}^2 + q_{d,h}) \quad (2.333)$$

$$i_{ch} = \frac{I_{DS}}{-2n_q \mu C_{ox} \frac{W}{L-L_h} V_t^2} = (q_{s,ch}^2 + q_{s,ch}) - (q_{d,ch}^2 + q_{d,ch}) \quad (2.334)$$

where i_h and i_{ch} are the normalized drain current of halo and channel transistor respec-

tively. Since I_{DS} is known from DC modeling, the above equations are solved for,

$$q_{d,h} = -\frac{1}{2} + \frac{1}{2}\sqrt{1 + 4(q_{s,h}^2 + q_{s,h} - i_h)} \quad (2.335)$$

$$q_{s,ch} = -\frac{1}{2} + \frac{1}{2}\sqrt{1 + 4(q_{d,ch}^2 + q_{d,ch} + i_{ch})} \quad (2.336)$$

Here we have used the unified model presented in for halo and channel transistors separately, where S_{ID} is expressed as

$$S_{ID,h} = \frac{kTI_{DS}^2}{\gamma fWL_h^2} \int_0^{L_h} \frac{N_{t,h}^*(E_{F_n})}{N_h^2} dx \quad (2.337)$$

$$S_{ID,ch} = \frac{kTI_{DS}^2}{\gamma fW(L - L_h)^2} \int_{L_h}^L \frac{N_{t,ch}^*(E_{F_n})}{N_{ch}^2} dx \quad (2.338)$$

where apparent trap density $N_{t,ch(h)}^*(E_{F_n}) = A_{ch(h)} + B_{ch(h)}N_{ch(h)} + C_{ch(h)}N_{ch(h)}^2$, A , B , C are the noise parameters, γ is the tunneling parameter, k is the Boltzmann constant and T is the temperature.

Flicker Noise Tuning Flexibility:

$$S_{ID,new} = \frac{S_{ID,old}}{1 + NOIA1 \cdot (qs - qdeff)(NOIAX)} \quad (2.339)$$

Flicker Noise due to drain and source resistance: Flicker noise due to source resistance (S_{id,R_s}) is given by

$$S_{id,R_s} = \frac{KFNS * W * (\frac{I_d}{W})^{AFNS}}{f^{BFNS}} \quad (2.340)$$

Flicker noise due to drain resistance (S_{id,R_d}) is given by

$$S_{id,R_d} = \frac{KFND * W * (\frac{I_d}{W})^{AFND}}{f^{BFND}} \quad (2.341)$$

AFNS, BFNS, KFNS, AFND, BFND and KFND are the model parameters.

Flicker Noise due to EDGEFET (EDGEFET=1): The Edge FET Model noise is added to the main flicker noise S_{ID} [15], when the parameter EDGEFET is 1

$$noia_{edge} = NOIA * NEDGE; \quad (2.342)$$

$$noib_{edge} = NOIB * NEDGE; \quad (2.343)$$

$$noic_{edge} = NOIC * NEDGE; \quad (2.344)$$

$$N_0 = \frac{2n_q C_{ox} V_t q_{s,edge}}{q} \quad (2.345)$$

The parameter N_l is the charge density at the drain end given by

$$N_l = \frac{2n_q C_{ox} V_t q_{def,edge}}{q} \quad (2.346)$$

$$\begin{aligned} S_{id,inv,edge}(f) &= \frac{kT q^2 \mu_{eff} I ds_{edge}}{C_{oxe} L_{eff NOI}^2 f^{EF} \cdot 10^{10}} \left(noia_{edge} \cdot \log \left(\frac{N_0 + N^*}{N_1 + N^*} \right) \right. \\ &\quad \left. noib_{edge} \cdot (N_0 - N_l) + \frac{noic_{edge}}{2} (N_0^2 - N_l^2) \right) \\ &\quad \frac{kT I ds_{edge}^2 \Delta L_{clm}}{W_{edge} L_{eff NOI_{edge}}^2 f^{EF} \cdot 10^{10}} \left(\frac{noia_{edge} + noib_{edge} \cdot N_l + noic_{edge} \cdot N_l^2}{(N_l + N^*)^2} \right) \end{aligned} \quad (2.347)$$

$$S_{id,subVt,edge}(f) = \frac{noia_{edge} \cdot k \cdot T \cdot I ds_{edge}^2}{W_{edge} L_{eff NOI_{edge}}^2 f^{EF} N^{*2} \cdot 10^{10}} \quad (2.348)$$

$$S_{id,edge}(f) = \frac{S_{id,inv,edge} \cdot S_{id,subVt,edge}}{S_{id,inv,edge} + S_{id,subVt,edge}} \quad (2.349)$$

2.25.2 Channel Thermal Noise

There are two channel thermal noise models in BSIM6. One is a charge-based model (default model) similar to that used in BSIM3v3.2 and BSIM4.7.0 (TNOIMOD=0). The other is the holistic model similar to BSIM4.7.0 (TNOIMOD=2). These two models can be selected through the model selector TNOIMOD.

TNOIMOD = 0 (Charge based Model): The noise current is given by

$$Q_{inv} = |Q_{s,intrinsic} + Q_{d,intrinsic}| \times NFIN_{total} \quad (2.350)$$

$$\overline{i_d^2} = \begin{cases} NTNOI \cdot \frac{4kT\Delta f}{L_{eff}^2} & \text{if RDSMOD} = 0 \\ NTNOI \cdot \frac{R_{ds} + \frac{4kT\Delta f}{L_{eff}^2}}{\mu_{eff}Q_{inv}} & \text{if RDSMOD} = 1 \end{cases} \quad (2.351)$$

where $R_{ds}(V)$ is the bias-dependent LDD source/drain resistance, and the parameter NTNOI is introduced for more accurate fitting of short-channel devices. Q_{inv} is the total inversion charge in the channel.

TNOIMOD = 1 (Correlated Noise Model): In this thermal noise model (similar to TNOIMOD = 2 in BSIM4.7.0), all the short-channel effects and velocity saturation effect incorporated in the IV model are automatically included, hence the name "holistic thermal noise model". In this thermal noise model both the gate and the drain noise are implemented as current noise sources. The drain current noise flows from drain to source; whereas the induced gate current noise flows from the gate to the source. The correlation between the two noise sources is independently controllable and can be tuned using the parameter RNOIC, although the use of default value 0.395 is recommended when measured data is not available. As illustrated in Fig. 5, TNOIMOD=1 shows good physical behavior in both the weak and strong inversion regions. The white noise gamma factor $\gamma_{WN} = \frac{S_{Id}}{4kTg_{d0}}$ shows a value of 1 at low V_{ds} , as expected. At high V_{ds} , it correctly goes to 2/3 for strong inversion and 1/2 in sub-threshold [16]. The relevant formulations of TNOIMOD=2 are given below. For more details, see Ph.D. thesis of

Darsen Lu and BSIM4 manual.

$$\beta_{tnoi} = RNOIA \cdot \left[1.0 + TNOIA \cdot L_{eff} \cdot \left(\frac{q_{ia}}{E_{sat,noi} L_{eff}} \right)^2 \right] \quad (2.352)$$

$$\theta_{tnoi} = RNOIB \cdot \left[1.0 + TNOIB \cdot L_{eff} \cdot \left(\frac{q_{ia}}{E_{sat,noi} L_{eff}} \right)^2 \right] \quad (2.353)$$

$$c_{tnoi} = RNOIC \cdot \left[1.0 + TNOIC \cdot L_{eff} \cdot \left(\frac{q_{ia}}{E_{sat,noi} L_{eff}} \right)^2 \right] \quad (2.354)$$

$$(2.355)$$

$$S_{id} = 4KT \cdot \mu C_{ox} \frac{W_{eff}}{L_{vsat}} V_t D_{ptwg} M_{oc} \left[\frac{q_s + q_{deff}}{2} \cdot \left(1 + \frac{\beta_{lowId}^2}{TNOIK2 + q_{ia}} \cdot \frac{V_{dseff}}{V_{dsat}} \right) \right. \\ \left. + (3 \cdot \beta_{tnoi}^2) \cdot \frac{(q_s - q_{deff})^2}{12 \left(\frac{1+q_s+q_{deff}}{2} \right)} \right] \quad (2.356)$$

$$mig = \frac{1}{12 \cdot NF \cdot W_{eff} \mu_{eff} \cdot D_{ptwg} M_{oc} C_{ox} \cdot V_t \frac{L_{vsat}^3}{L_{eff}^2}} \cdot \left[\frac{\frac{q_s + q_{deff}}{2}}{\left(\frac{1+q_s+q_{deff}}{2} \right)^2} \right. \\ \left. - \frac{\left(6 \left(\frac{q_s + q_{deff}}{2} \right) + \frac{1}{2} \right) (q_s - q_{deff})^2}{60 \left(\frac{1+q_s+q_{deff}}{2} \right)^4} + \frac{(q_s - q_{deff})^4}{144 \left(\frac{1+q_s+q_{deff}}{2} \right)^5} \right] \cdot \left(\frac{15}{4} \cdot \theta_{tnoi}^2 \right) \quad (2.357)$$

$$S_{ig} = \frac{4KT \cdot [\omega \cdot C_{ox} \cdot W \cdot NF \cdot L]^2 \cdot mig}{1 + (\omega \cdot C_{0x} \cdot L \cdot W \cdot NF \cdot mig)^2} \quad (2.358)$$

$$S_{ig,id} = -j\omega \cdot 4KT \cdot \mu C_{ox} D_{ptwg} M_{oc} V_t \left(\frac{L_{vsat}}{L_{eff}} \right) \cdot \left[\frac{(q_s - q_{deff})}{12 \left(\frac{1+q_s+q_{deff}}{2} \right)} - \frac{(q_s - q_{deff})^3}{144 \left(\frac{1+q_s+q_{deff}}{2} \right)^3} \right] \cdot \frac{c_{tnoi}}{0.395} \quad (2.359)$$

$$c = \frac{S_{ig,id}}{\sqrt{S_{ig}} \cdot \sqrt{S_{id}}} \quad (2.360)$$

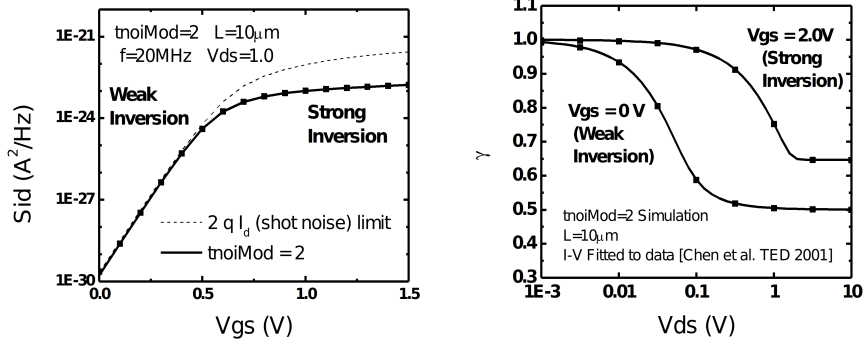


Figure 5: TNOIMOD=1 shows good physical behavior at high and low V_{ds} from sub-threshold to strong inversion regions.

2.25.3 Gate Current Shot Noise

$$\overline{i_{gs}^2} = 2q(I_{gcs} + I_{gs}) \quad (2.361)$$

$$\overline{i_{gd}^2} = 2q(I_{gcd} + I_{gd}) \quad (2.362)$$

$$\overline{i_{gb}^2} = 2qI_{gbinv} \quad (2.363)$$

2.25.4 Resistor Noise

The noise associated with each parasitic resistors in BSIM6 are calculated

If $RDSMOD = 1$ then

$$\frac{\overline{i_{RS}^2}}{\Delta f} = 4kT \cdot \frac{1}{R_{source}} \quad (2.364)$$

$$\frac{\overline{i_{RD}^2}}{\Delta f} = 4kT \cdot \frac{1}{R_{drain}} \quad (2.365)$$

If $RGATEMOD = 1$ then

$$\frac{\overline{i_{RG}^2}}{\Delta f} = 4kT \cdot \frac{1}{R_{geltd}} \quad (2.366)$$

If $RBODYHVMOD = 1$ then

$$\frac{\overline{i_{RDB}^2}}{\Delta f} = 4kT \cdot \frac{1}{R_{DB}} \quad (2.367)$$

If $RDSMOD = 1$ & $HVMOD = 1$ then

$$\frac{\overline{i_{DRIFT,D}^2}}{\Delta f} = 4kT \cdot \frac{1}{R_{DRIFT,D}} \quad (2.368)$$

$$\frac{\overline{i_{DRIFT,S}^2}}{\Delta f} = 4kT \cdot \frac{1}{R_{DRIFT,S}} \quad (2.369)$$

2.26 Self Heating Model

Effect of self heating is modeled by employing a thermal network consisting of thermal resistance (R_{th}) and capacitance (C_{th}) as shown in Fig.6. The voltage at thermal node T gives the rise in temperature, which is added to the ambient temperature and all the temperature sensitive variables in the model are updated accordingly [17].

$$R_{th} = \frac{RTH0}{(WTH0 + Weff) \cdot NF}$$

$$C_{th} = CTH0 * (WTH0 + Weff) \cdot NF$$

3 Asymmetric MOS Junction Diode Models

3.1 Junction Diode IV Model

In BSIM6, there is only one diode model (DIOMOD=2 from BSIM4), which includes resistance and breakdown. BSIM6 models the diode breakdown with current limiting in both forward IJTHSFWD or IJTHDFWD and reverse operations XJBVS, XJBVD, BVS, and BVD.

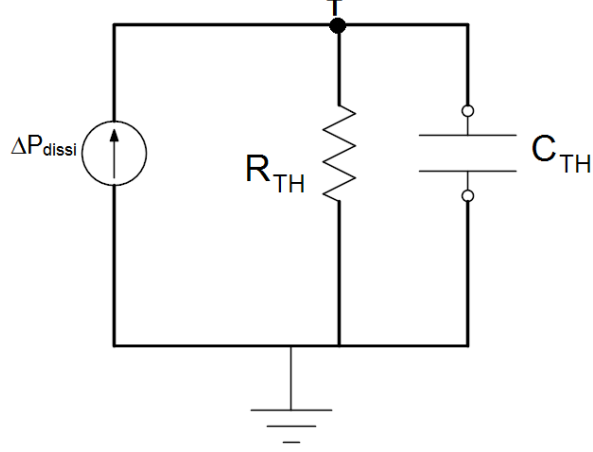


Figure 6: Thermal Network for Self Heating Model.

Source/Body Junction Diode The equations for the source-side diode are as follows:

$$I_{bs} = I_{sbs} \left[\exp\left(\frac{V_{bs}}{NJS \cdot V_t}\right) - 1 \right] \cdot f_{breakdown} + V_{bs} \cdot G_{min} \quad (3.1)$$

where I_{sbs} is the total saturation current consisting of the components through the gate-edge (Jsswgs) and isolation-edge sidewalls (Jssws) and the bottom junction (Jss),

$$I_{sbs} = A_{seff} J_{ss}(T) + P_{seff} J_{ssws}(T) + W_{effcj} \cdot NF \cdot J_{sswgs}(T) \quad (3.2)$$

where the calculation of the junction area and perimeter is discussed in section Layout-Dependent Parasitics Models, and the temperature-dependent current density model is given in Section Temperature Dependence of Junction Diode IV. The exponential term in equation given below is linearized at both the limiting current IJTHSFWD in the forward-bias mode and the limiting current IJTHSREV in the reverse-bias mode. In (3.1), $f_{breakdown}$ is given by

$$f_{breakdown} = 1 + XJBVS \cdot \exp\left(-\frac{(BVS + V_{bs})}{NJS \cdot V_t}\right) \quad (3.3)$$

Drain/Body Junction Diode The equations for the drain-side diode are as follows:

$$I_{bd} = I_{sbd} \left[\exp \left(\frac{V_{bd}}{NJD \cdot V_t} \right) - 1 \right] \cdot f_{breakdown} + V_{bd} \cdot G_{min} \quad (3.4)$$

where I_{sbs} is the total saturation current consisting of the components through the gate-edge (Jsswgs) and isolation-edge sidewalls (Jssws) and the bottom junction (Jss),

$$I_{sbd} = A_{deff} J_{sd}(T) + P_{deff} J_{sswd}(T) + W_{effcj} \cdot NF \cdot J_{sswgd}(T) \quad (3.5)$$

where the calculation of the junction area and perimeter is discussed in Section Layout-Dependent Parasitics Models, and the temperature-dependent current density model is given in Section Temperature Dependence of Junction Diode IV. The exponential term in (3.6) is linearized at both the limiting current IJTHDFWD in the forward-bias mode and the limiting current IJTHDREV in the reverse-bias mode. In (3.1), $f_{breakdown}$ is given by

$$f_{breakdown} = 1 + XJBVD \cdot \exp \left(- \frac{\cdot(BVD + V_{bd})}{NJD \cdot V_t} \right) \quad (3.6)$$

Total Junction Source/Drain Diode Including Tunneling Total diode current including the carrier recombination and trap-assisted tunneling current in the space-charge region is modeled by:

$$\begin{aligned} I_{bs_totle} &= I_{bs} \\ &- W_{effcj} \cdot NF \cdot J_{tsswgs}(T) \cdot \left[\exp \left(\frac{-V_{bs}}{NJTSSWG(T) \cdot Vtm0} \cdot \frac{VTSSWGS}{VTSSWGS - V_{bs}} \right) \right] \\ &- P_{s,deff} J_{tssws}(T) \left[\exp \left(\frac{-V_{bs}}{NJTSSW(T) \cdot Vtm0} \cdot \frac{VTSSWS}{VTSSWS - V_{bs}} \right) - 1 \right] \\ &- A_{s,deff} J_{tss}(T) \left[\exp \left(\frac{-V_{bs}}{NJTSS(T) \cdot Vtm0} \cdot \frac{VTSS}{VTSS - V_{bs}} \right) - 1 \right] + g_{min} \cdot V_{bs} \end{aligned} \quad (3.7)$$

$$\begin{aligned} I_{bd_totle} &= I_{bd} \\ &- W_{effcj} \cdot NF \cdot J_{tsswgd}(T) \cdot \left[\exp \left(\frac{-V_{bd}}{NJTSSWGD(T) \cdot Vtm0} \cdot \frac{VTSSWGD}{VTSSWGD - V_{bd}} \right) \right] \\ &- P_{d,deff} J_{tsswd}(T) \left[\exp \left(\frac{-V_{bd}}{NJTSSWD(T) \cdot Vtm0} \cdot \frac{VTSSWD}{VTSSWD - V_{bd}} \right) - 1 \right] \\ &- A_{d,deff} J_{tsd}(T) \left[\exp \left(\frac{-V_{bd}}{NJTSD(T) \cdot Vtm0} \cdot \frac{VTSD}{VTSD - V_{bd}} \right) - 1 \right] + g_{min} \cdot V_{bd} \end{aligned} \quad (3.8)$$

3.2 Junction Diode CV Model

Source and drain junction capacitances consist of three components: the bottom junction capacitance, sidewall junction capacitance along the isolation edge, and sidewall junction capacitance along the gate edge. An analogous set of equations are used for both sides but each side has a separate set of model parameters.

Source/Body Junction Diode The source-side junction capacitance can be calculated by

$$C_{bs} = A_{seff} C_{jbs} + P_{seff} C_{jbssw} + W_{effcj} \cdot NF \cdot C_{jbsswg} \quad (3.9)$$

where C_{jbs} is the unit-area bottom S/B junciton capacitance, C_{jbssw} is the unit-length S/B junction sidewall capacitance along the isolation edge, and C_{jbsswg} is the unit-length S/B junction sidewall capacitance along the gate edge. The effective area and perimeters in (3.9) are given in Section Layout-Dependent Parasitics Models.

C_{jbs} is calculated by

$$C_{jbs} = \begin{cases} CJS(T) \cdot \left(1 - \frac{V_{bs}}{PBS(T)}\right)^{-MJS} & \text{if } \frac{V_{bs}}{PBS(T)} \leq x_0 \\ CJS(T) \cdot \frac{1}{(1-x_0)^{MJS}} \cdot \left[1 + MJS \left(1 + \frac{\frac{V_{bs}}{PBS} - 1}{1-x_0}\right)\right] & \text{otherwise} \end{cases} \quad (3.10)$$

where the value of x_0 is taken as 0.9.

C_{jbssw} is calculated by

$$C_{jbssw} = \begin{cases} CJSWS(T) \cdot \left(1 - \frac{V_{bs}}{PBSWS(T)}\right)^{-MJSWS} & \text{if } \frac{V_{bs}}{PBSWS(T)} \leq x_0 \\ CJSWS(T) \cdot \frac{1}{(1-x_0)^{MJSWS}} \cdot \left[1 + MJSWS \left(1 + \frac{\frac{V_{bs}}{PBSWS(T)} - 1}{1-x_0}\right)\right] & \text{otherwise} \end{cases} \quad (3.11)$$

where the value of x_0 is taken as 0.9.

Cjbsswg is calculated by

$$C_{jbsswg} = \begin{cases} CJSWGS(T) \cdot \left(1 - \frac{V_{bs}}{PBSWGS(T)}\right)^{-MJSWGS} & \text{if } \frac{V_{bs}}{PBSWGS(T)} \leq x_0 \\ CJSWGS(T) \cdot \frac{1}{(1-x_0)^{MJSWGS}} \cdot \left[1 + MJSWGS \left(1 + \frac{\frac{V_{bs}}{PBSWGS(T)} - 1}{1-x_0}\right)\right] & \text{otherwise} \end{cases} \quad (3.12)$$

where the value of x_0 is taken as 0.9.

Drain/Body Junction Diode The drain-side junction capacitance can be calculated by

$$C_{bd} = A_{def} C_{jbd} + P_{def} C_{jbds} + W_{effc} \cdot NF \cdot C_{jbds} \quad (3.13)$$

where C_{jbd} is the unit-area bottom D/B junciton capacitance, C_{jbds} is the unit-length D/B junction sidewall capacitance along the isolation edge, and C_{jbds}^{wg} is the unit-length D/B junction sidewall capacitance along the gate edge. The effective area and perimeters in (3.13) are given in Section Layout-Dependent Parasitics Models.

Cjbd is calculated by

$$C_{jbd} = \begin{cases} CJD(T) \cdot \left(1 - \frac{V_{bs}}{PBD(T)}\right)^{-MJD} & \text{if } \frac{V_{bs}}{PBD(T)} \leq x_0 \\ CJD(T) \cdot \frac{1}{(1-x_0)^{MJD}} \cdot \left[1 + MJD \left(1 + \frac{\frac{V_{bs}}{PBD(T)} - 1}{1-x_0}\right)\right] & \text{otherwise} \end{cases} \quad (3.14)$$

where the value of x_0 is taken as 0.9.

Cjbds is calculated by

$$C_{jbds} = \begin{cases} CJSWD(T) \cdot \left(1 - \frac{V_{bs}}{PBSWD(T)}\right)^{-MJSWS} & \text{if } \frac{V_{bs}}{PBSWD(T)} \leq x_0 \\ CJSWD(T) \cdot \frac{1}{(1-x_0)^{MJSWD}} \cdot \left[1 + MJSWD \left(1 + \frac{\frac{V_{bs}}{PBSWD(T)} - 1}{1-x_0}\right)\right] & \text{otherwise} \end{cases} \quad (3.15)$$

where the value of x_0 is taken as 0.9.

Cjbdswg is calculated by

$$C_{jbdswg} = \begin{cases} CJSWGD(T) \cdot \left(1 - \frac{V_{bs}}{PBSWGD(T)}\right)^{-MJSWGD} & \text{if } \frac{V_{bs}}{PBSWGD(T)} \leq x_0 \\ CJSWGD(T) \cdot \frac{1}{(1-x_0)^{MJSWGD}} \cdot \left[1 + MJSWGD \left(1 + \frac{\frac{V_{bs}}{PBSWGD(T)} - 1}{1-x_0}\right)\right] & \text{otherwise} \end{cases} \quad (3.16)$$

where the value of x_0 is taken as 0.9.

4 Layout dependent Parasitics Models

4.1 Layout-Dependent Parasitics Models

BSIM6 provides a comprehensive and versatile geometry/layout-dependent parasitics model taken from BSIM4. It supports modeling of series (such as isolated, shared, or merged source/ drain) and multi-finger device layout, or a combination of these two configurations. This model has impact on every BSIM6 sub-models except the substrate resistance network model. Note that the narrow-width effect in the per-finger device with multi-finger configuration is accounted for by this model. A complete list of model parameters and selectors can be found at the end.

4.1.1 Geometry Definition

Figure 7 schematically shows the geometry definition for various source/drain connections and source/drain/gate contacts. The layout parameters shown in this figure will be used to calculate resistances and source/drain perimeters and areas.

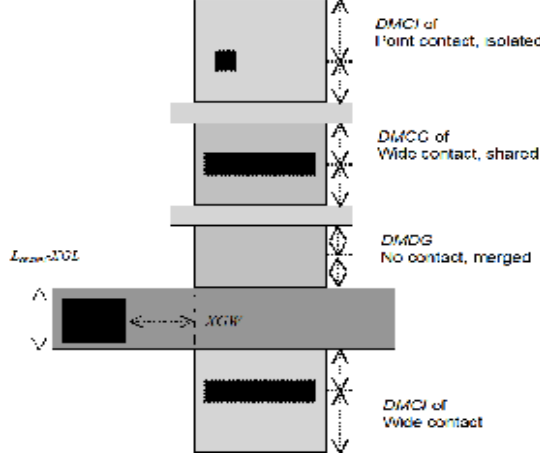


Figure 7: Definition for layout parameters.

4.1.2 Model Formulation and Options

Effective Junction Perimeter and Area: In the following, only the source-side case is illustrated. The same approach is used for the drain side. The effective junction perimeter on the source side is calculated by

If (PS is given)

if (**perMod**=0)

$$P_{seff} = PS$$

else

Else

P_{seff} computed from NF, DWJ, **geoMod**, DMCG, DMCI, DMDG, DMC GT, RSH, and MIN.

The effective junction area on the source side is calculated by

If (AS is given)

$$A_{seff} = AS$$

Else

A_{seff} computed from NF, DWJ, **geoMod**, DMCG, DMCI, DMDG, DMC GT, RSH, and MIN.

In the above, P_{seff} and A_{seff} will be used to calculate junction diode IV and CV. P_{seff} does not include the gate-edge perimeter.

Source/Drain Diffusion Resistance: The source diffusion resistance is calculated by

If(number of sources NRS is given)

ELSE if(rgeoMod=0)

Source diffusion resistance R_{sdiff} is not generated.

Else

R_{sdiff} computed from NF, DWJ, **geoMod**, DMCG, DMCI, DMDG, DMCGT, RSH, and MIN.

where the number of source squares NRS is an instance parameter. Similarly, the drain diffusion resistance is calculated by

If(number of sources NRD is given)

ELSE if(rgeoMod=0)

Drain diffusion resistance R_{ddiff} is not generated.

Else

R_{ddiff} computed from NF, DWJ, **geoMod**, DMCG, DMCI, DMDG, DMCGT, RSH, and MIN.

Gate Electrode Resistance: The gate electrode resistance with multi-finger configuration is modeled by

$$R_{geltd} = \frac{RSHG \cdot \left(XGW + \frac{W_{effci}}{3NGCON} \right)}{NGCON \cdot \left(L_{drawn} - XGL \right) \cdot NF} \quad (4.1)$$

Option for Source/Drain Connections: Table 1 lists the options for source/drain connections through the model selector **geoMod**. For multi-finger devices, all inside S/D diffusions are assumed shared.

Option for Source/Drain Contacts: Table 2 lists the options for source/drain contacts through the model selector **rgeoMod**.

geomod	End Source	End drain	Note
0	isolated	isolated	NF=Odd
1	isolated	shared	NF=Odd, Even
2	shared	shared	NF=Odd, Even
3	shared	isolated	NF=Odd, Even
4	isolated	merged	NF=Odd
5	shared	merged	NF=Odd, Even
6	merged	isolated	NF=Odd
7	merged	shared	NF=Odd, Even
8	merged	merged	NF=Odd
9	sha/iso	shared	NF=Even
10	shared	sha/iso	NF=Even

Table 1: geoMod options.

rgeoMod	End-source contact	End-drain contact
0	No R_{sdiff}	No R_{ddiff}
1	wide	wide
2	wide	point
3	point	wide
4	point	point
5	wide	merged
6	point	merged
7	merged	wide
8	merged	point

Table 2: rgeoMod options.

5 Temperature dependence Models

5.1 Temperature Dependence Model

Accurate modeling of the temperature effects on MOSFET characteristics is important to predict circuit behavior over a range of operating temperatures (T). The operating temperature might be different from the nominal temperature (TNOM) at which the BSIM6 model parameters are extracted. This chapter presents the BSIM6 temperature dependence models for threshold voltage, mobility, saturation velocity, source/drain resistance, and junction diode IV and CV.

5.1.1 Length Scaling of Temperature parameters

$$UTE = UTE \cdot \left(1 + UTEL \frac{1}{L_{eff}}\right) \quad (5.1)$$

$$UA1 = UA1 \cdot \left(1 + UA1L \frac{1}{L_{eff}}\right) \quad (5.2)$$

$$UD1 = UD1 \cdot \left(1 + UD1L \frac{1}{L_{eff}}\right) \quad (5.3)$$

$$AT = AT \cdot \left(1 + ATL \frac{1}{L_{eff}}\right) \quad (5.4)$$

$$PTWGT = PTWGT \cdot \left(1 + PTWGTL \frac{1}{L_{eff}}\right) \quad (5.5)$$

$$(5.6)$$

5.1.2 Temperature Dependence of Threshold Voltage

The temperature dependence of V_{th} is modeled by

$$\begin{aligned} V_{th}(T) &= V_{th}(TNOM) + \left(KT1_i + KT2_i \cdot V_{bref} \right) \cdot \left(\left(\frac{T}{TNOM} \right)^{KT1EXP} - 1 \right) \\ V_{fb}(T) &= V_{fb}(TNOM) - KT1 \cdot \left(\frac{T}{TNOM} - 1 \right) \end{aligned} \quad (5.7)$$

$$VFBSDOFF(T) = VFBSDOFF(TNOM) \cdot [1 + TVFBSDOFF \cdot (T - TNOM)]$$

$$NFACTOR(T) = NFACTOR(TNOM) + TFACTOR \cdot \left(\frac{T}{TNOM} - 1 \right) \quad (5.8)$$

$$ETA0(T) = ETA0(TNOM) + TETA0 \left(\frac{T}{TNOM} - 1 \right) \quad (5.9)$$

5.1.3 Temperature Dependence of Mobility

$$U0(T) = U0(TNOM) \cdot (T/TNOM)^{UTE} \quad (5.10)$$

$$UA(T) = UA(TNOM) [1 + UA1 \cdot (T - TNOM)] \quad (5.11)$$

$$UC(T) = UC(TNOM) [1 + UC1 \cdot (T - TNOM)] \quad (5.12)$$

$$UD(T) = UD(TNOM) \cdot (T/TNOM)^{UD1} \quad (5.13)$$

$$UCS(T) = UCS(TNOM) \cdot (T/TNOM)^{UCSTE} \quad (5.14)$$

$$EU(T) = EU(TNOM) \cdot (1 + EU1 \cdot (\frac{T}{TNOM} - 1)) \quad (5.15)$$

$$(5.16)$$

5.1.4 Temperature Dependence of Saturation Velocity

$$VSAT(T) = VSAT(TNOM) \cdot (T/TNOM)^{-AT} \quad (5.17)$$

5.1.5 Temperature Dependence of LDD Resistance

$$rdstemp = (T/TNOM)^{PRT} \quad (5.18)$$

$$rdstemphv = (T/TNOM)^{PRTHV} \quad (5.19)$$

$$(5.20)$$

RDSMOD = 0 (internal source/drain LDD resistance)

$$RDSW(T) = RDSW(TNOM) \cdot rdstemp \quad (5.21)$$

$$RDSWMIN(T) = RDSWMIN(TNOM) \cdot rdstemp \quad (5.22)$$

RDSMOD = 1 (external source/drain LDD resistance)

$$RDW(T) = RDW(TNOM) \cdot rdstemp \quad (5.23)$$

$$RDWMIN(T) = RDWMIN(TNOM) \cdot rdstemp \quad (5.24)$$

$$RSW(T) = RSW(TNOM) \cdot rdstemp \quad (5.25)$$

$$RSWMIN(T) = RSWMIN(TNOM) \cdot rdstemp \quad (5.26)$$

5.1.6 Temperature Dependence of Junction Diode IV

- **Source-side diode** The source-side diode is turned off if both A_{seff} and P_{seff} are zero. Otherwise, the source-side saturation current is given by

$$I_{sbs} = A_{seff} J_{ss}(T) + P_{seff} J_{ssws}(T) + W_{effcj} \cdot NF \cdot J_{sswgs}(T) \quad (5.27)$$

where

$$\begin{aligned}
J_{ss}(T) &= JSS(TNOM) \cdot \exp\left(\frac{\frac{E_g(TNOM)}{v_t(TNOM)} - \frac{E_g(T)}{v_t(T)} + XTIS \cdot \ln\left(\frac{T}{TNOM}\right)}{NJS}\right) \\
J_{ssws}(T) &= JSSWS(TNOM) \cdot \exp\left(\frac{\frac{E_g(TNOM)}{v_t(TNOM)} - \frac{E_g(T)}{v_t(T)} + XTIS \cdot \ln\left(\frac{T}{TNOM}\right)}{NJS}\right) \\
J_{sswgs}(T) &= JSSWGS(TNOM) \cdot \exp\left(\frac{\frac{E_g(TNOM)}{k_b \cdot TNOM} - \frac{E_g(T)}{k_b \cdot T} + XTIS \cdot \ln\left(\frac{T}{TNOM}\right)}{NJS}\right)
\end{aligned} \tag{5.28}$$

where E_g is given in Temperature Dependences of E_g and n_i .

- **Drain-side diode** The drain-side diode is turned off if both A_{seff} and P_{seff} are zero. Otherwise, the drain-side saturation current is given by

$$I_{sbd} = A_{deff} J_{sd}(T) + P_{deff} J_{sswd}(T) + W_{effcj} \cdot NF \cdot J_{sswgd}(T) \tag{5.29}$$

where

$$\begin{aligned}
J_{sd}(T) &= JSD(TNOM) \cdot \exp\left(\frac{\frac{E_g(TNOM)}{k_b \cdot TNOM} - \frac{E_g(T)}{k_b \cdot T} + XTID \cdot \ln\left(\frac{T}{TNOM}\right)}{NJD}\right) \\
J_{sswd}(T) &= JSSWD(TNOM) \cdot \exp\left(\frac{\frac{E_g(TNOM)}{k_b \cdot TNOM} - \frac{E_g(T)}{k_b \cdot T} + XTID \cdot \ln\left(\frac{T}{TNOM}\right)}{NJD}\right) \\
J_{sswgd}(T) &= JSSWGD(TNOM) \cdot \exp\left(\frac{\frac{E_g(TNOM)}{k_b \cdot TNOM} - \frac{E_g(T)}{k_b \cdot T} + XTID \cdot \ln\left(\frac{T}{TNOM}\right)}{NJD}\right)
\end{aligned} \tag{5.30}$$

5.1.7 Temperature Dependence of Junction Diode CV

- Source-side diode: The temperature dependences of zero-bias unit-length/area junction capacitances on the source side are modeled by

$$CJS(T) = CJS(TNOM) + TCJ \cdot (T - TNOM) \quad (5.31)$$

$$CJSWS(T) = CJSWS(TNOM) + TCJSW \cdot (T - TNOM) \quad (5.32)$$

$$CJSWGS(T) = CJSWGS(TNOM) + TCJSWG \cdot (T - TNOM) \quad (5.33)$$

The temperature dependences of the built-in potentials on the source side are modeled by

$$PBS(T) = PBS(TNOM) - TPB \cdot (T - TNOM) \quad (5.34)$$

$$PBSWS(T) = PBSWS(TNOM) - TPBSW \cdot (T - TNOM) \quad (5.35)$$

$$PBSWGS(T) = PBSWGS(TNOM) - TPBSWG \cdot (T - TNOM) \quad (5.36)$$

- Drain-side diode: The temperature dependences of zero-bias unit-length/area junction capacitances on the drain side are modeled by

$$CJS(T) = CJS(TNOM)[1 + TCJ \cdot (T - TNOM)] \quad (5.37)$$

$$CJSWS(T) = CJSWS(TNOM) + TCJSW \cdot (T - TNOM) \quad (5.38)$$

$$CJSWGS(T) = CJSWGS(TNOM)[1 + TCJSWG \cdot (T - TNOM)] \quad (5.39)$$

The temperature dependences of the built-in potentials on the drain side are modeled by

$$PBD(T) = PBD(TNOM) - TPB \cdot (T - TNOM) \quad (5.40)$$

$$PBSWD(T) = PBSWD(TNOM) - TPBSW \cdot (T - TNOM) \quad (5.41)$$

$$PBSWGD(T) = PBSWGD(TNOM) - TPBSWG \cdot (T - TNOM) \quad (5.42)$$

- trap-assisted tunneling (TAT) and recombination current

$$\begin{aligned}
J_{tsswgs}(T) &= J_{tsswgs}(TNOM) \cdot \left(\sqrt{\frac{JTWEFF}{W_{effcj}}} + 1 \right) \\
&\cdot \exp \left[\frac{-E_g(TNOM)}{k_b T} \cdot X_{tsswgs} \cdot \left(1 - \frac{T}{TNOM} \right) \right] \quad (5.43)
\end{aligned}$$

$$J_{tssws}(T) = J_{tssws}(TNOM) \cdot \exp \left[\frac{-E_g(TNOM)}{k_b T} \cdot X_{tssws} \cdot \left(1 - \frac{T}{TNOM} \right) \right]$$

$$J_{tss}(T) = J_{tss}(TNOM) \cdot \exp \left[\frac{-E_g(TNOM)}{k_b T} \cdot X_{tss} \cdot \left(1 - \frac{T}{TNOM} \right) \right]$$

$$\begin{aligned}
J_{tsswgd}(T) &= J_{tsswgd}(TNOM) \cdot \left(\sqrt{\frac{JTWEFF}{W_{effcj}}} + 1 \right) \\
&\cdot \exp \left[\frac{-E_g(TNOM)}{k_b T} \cdot X_{tsswgd} \cdot \left(1 - \frac{T}{TNOM} \right) \right] \quad (5.44)
\end{aligned}$$

$$J_{tsd}(T) = J_{tsd}(TNOM) \cdot \exp \left[\frac{-E_g(TNOM)}{k_b T} \cdot X_{tsd} \cdot \left(1 - \frac{T}{TNOM} \right) \right]$$

$$NJTSSWG(T) = NJTSSWG(TNOM) \cdot \left[1 + TNJTSSWG \left(\frac{T}{TNOM} - 1 \right) \right]$$

$$NJTSSW(T) = NJTSSW(TNOM) \cdot \left[1 + TNJTSSW \left(\frac{T}{TNOM} - 1 \right) \right]$$

$$NJTS(T) = NJTS(TNOM) \cdot \left[1 + TNJTS \left(\frac{T}{TNOM} - 1 \right) \right]$$

$$NJTSSWGD(T) = NJTSSWGD(TNOM) \cdot \left[1 + TNJTSSWGD \left(\frac{T}{TNOM} - 1 \right) \right]$$

$$NJTSSWD(T) = NJTSSWD(TNOM) \cdot \left[1 + TNJTSSWD \left(\frac{T}{TNOM} - 1 \right) \right]$$

$$NJTSSWD(T) = NJTSSWD(TNOM) \cdot \left[1 + TNJTSSWD \left(\frac{T}{TNOM} - 1 \right) \right]$$

$$NJTSD(T) = NJTSD(TNOM) \cdot \left[1 + TNJTS \left(\frac{T}{TNOM} - 1 \right) \right]$$

(5.45)

5.1.8 Temperature Dependences of E_g and n_i

- Energy-band gap of channel (E_g): The temperature dependence of E_g is modeled by

$$Eg0 = BG0SUB - \frac{TBGASUB \times T_{nom}^2}{T_{nom} + TBGBSUB} \quad (5.46)$$

$$E_g = BG0SUB - \frac{TBGASUB \times T^2}{T + TBGBSUB} \quad (5.47)$$

- Intrinsic carrier concentration of non-silicon channel (n_i)

$$n_i = NI0SUB \times \left(\frac{T}{T_{nom}} \right)^{(3/2)} \times \exp \left(\frac{Eg}{2^{kT_{nom}/q}} - \frac{Eg}{2^{kT/q}} \right) \quad (5.48)$$

6 Stress effect Model Development

6.1 Stress Effect Model

CMOS feature size aggressively scaling makes shallow trench isolation(STI) very popular active area isolation process in advanced technologies. Recent years, strain channel materials have been employed to achieve high device performance. The mechanical stress effect induced by these process causes MOSFET performance function of the active area size(OD: oxide definition) and the location of the device in the active area. And the necessity of new models to describe the layout dependence of MOS parameters due to stress effect becomes very urgent in advance CMOS technologies. Influence of stress on mobility has been well known since the 0.13um technology. The stress influence on saturation velocity is also experimentally demonstrated. Stress-induced enhancement or suppression of dopant diffusion during the processing is reported. Since the doping profile may be changed due to different STI sizes and stress, the threshold voltage shift and changes of other second-order effects, such as DIBL and body effect, were shown in process integration. BSIM4 considers the influence of stress on mobility, velocity saturation, threshold voltage, body effect, and DIBL effect.

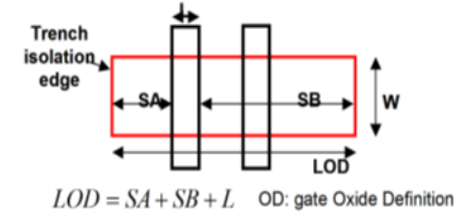


Figure 8: the typical layout of a MOSFET

6.1.1 Stress Effect Model Development

Experimental analysis show that there exist at least two different mechanisms within the influence of stress effect on device characteristics. The first one is mobility-related and is induced by the band structure modification. The second one is V_{th}-related as a result of doping profile variation. Both of them follow the same 1/LOD trend but reveal different L and W scaling. We have derived a phenomenological model based on these findings by modifying some parameters in the BSIM model. Note that the following equations have no impact on the iteration time because there are no voltage-controlled components in them.

Mobility-related Equations: This model introduces the first mechanism by adjusting the U₀ and V_{sat} according to different W, L and OD shapes. Define mobility relative change due to stress effect as :

$$\rho_{\mu_{eff}} = \Delta\mu_{eff}/\mu_{effo} = (\mu_{eff} - \mu_{effo})/\mu_{effo} = \frac{\mu_{eff}}{\mu_{effo}} - 1 \quad (6.1)$$

So,

$$\frac{\mu_{eff}}{\mu_{effo}} = 1 + \rho_{\mu_{eff}} \quad (6.2)$$

Figure 8 shows the typical layout of a MOSFET on active layout surrounded by STI isolation. SA, SB are the distances between isolation edge to Poly from one and the other side, respectively. 2D simulation shows that stress distribution can be expressed by a simple function of SA and SB. Assuming that mobility relative change is proportional to stress distribution. It can be described as function of SA, SB(LOD effect), L, W, and

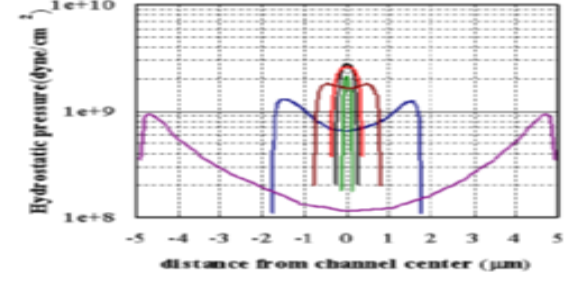


Figure 9: Stress distribution within MOSFET channel using 2D simulation

T dependence:

$$\rho_{\mu_{eff}} = \frac{KU0}{Kstress_u0} \cdot (Inv_sa + Inv_sb) \quad (6.3)$$

where:

$$Inv_sa = \frac{1}{SA + 0.5 \cdot L_{drawn}} \quad (6.4)$$

$$Inv_sb = \frac{1}{SB + 0.5 \cdot L_{drawn}} \quad (6.5)$$

$$\begin{aligned} Kstress_u0 = & \left(1 + \frac{LKU0}{(L_{drawn} + XL)^{LLDKU0}} \right. \\ & + \frac{WKU0}{(W_{drawn} + XW + WLOD)^{WLDKU0}} \\ & + \frac{PKU0}{(L_{drawn} + XL)^{LLDKU0} \cdot (W_{drawn} + XW + WLOD)^{WLDKU0}} \Big) \\ & \times \left(1 + TKU0 \cdot \left(\frac{\text{Temperature}}{TNOM} - 1 \right) \right) \end{aligned} \quad (6.6)$$

So that:

$$\mu_{eff} = \frac{1 + \rho_{\mu_{eff}}(SA, SB)}{1 + \rho_{\mu_{eff}}(SA_{ref}, SB_{ref})} \mu_{eff0} \quad (6.7)$$

$$\nu_{sattemp} = \frac{1 + KV_{SAT} \cdot \rho_{\mu_{eff}}(SA, SB)}{1 + KV_{SAT} \cdot \rho_{\mu_{eff}}(SA_{ref}, SB_{ref})} \nu_{sattemp0} \quad (6.8)$$

and SA_{ref} , SB_{ref} are reference distances between OD edge to poly from one and the other side.

Vth-related Equations: Vth0 (threshold voltage without stress effect), K2 and ETA0 are modified to cover the doping profile change in the devices with different LOD. They use the same 1/LOD formulas as shown in earlier sections, but different equations for W and L scaling:

$$\begin{aligned} VTH0 &= VTH0_{original} + \frac{KVTH0}{Kstress_vth0} \cdot (Inv_sa + Inv_sb - Inv_sa_{ref} - Inv_sb_{ref}) \\ K2 &= K2_{original} + \frac{STK2}{Kstress_vth0^{LODK2}} \cdot (Inv_sa + Inv_sb - Inv_sa_{ref} - Inv_sb_{ref}) \\ ETA0 &= ETA0_{original} + \frac{STETA0}{Kstress_vth0^{LODETA0}} \cdot (Inv_sa + Inv_sb - Inv_sa_{ref} - Inv_sb_{ref}) \end{aligned} \quad (6.9)$$

where:

$$Inv_sa_{ref} = \frac{1}{SA_{ref} + 0.5 \cdot L_{drawn}} \quad (6.10)$$

$$Inv_sb_{ref} = \frac{1}{SB_{ref} + 0.5 \cdot L_{drawn}} \quad (6.11)$$

$$\begin{aligned} Kstress_vth0 &= \left(1 + \frac{LKVTH0}{(L_{drawn} + XL)^{LLODKVTH}} \right. \\ &\quad + \frac{WKVTH0}{(W_{drawn} + XW + WL) ^{WLKVTH}} \\ &\quad \left. + \frac{PKVTH0}{(L_{drawn} + XL)^{LLODKVTH} \cdot (W_{drawn} + XW + WL)^{WLKVTH}} \right) \end{aligned} \quad (6.12)$$

Multiple Finger Device: For multiple finger device, the total LOD effect is the average of LOD effect to every finger. That is (see Figure 10) for the layout for multiple

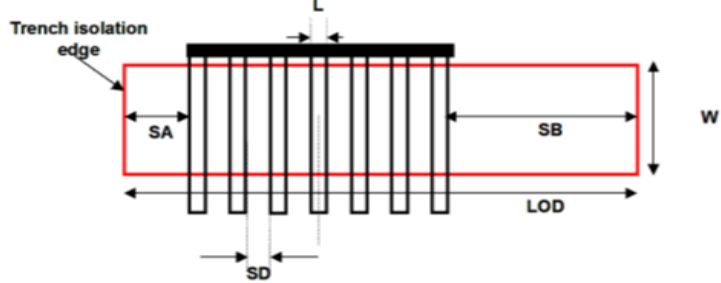


Figure 10: Layout of multiple finger MOSFET

finger device):

$$Inv_{sa} = \frac{1}{NF} \sum_{i=0}^{NF-1} \frac{1}{SA + 0.5 \cdot L_{drawn} + i \cdot (SD + L_{drawn})} \quad (6.13)$$

$$Inv_{sb} = \frac{1}{NF} \sum_{i=0}^{NF-1} \frac{1}{SB + 0.5 \cdot L_{drawn} + i \cdot (SD + L_{drawn})} \quad (6.14)$$

$$(6.15)$$

6.1.2 Effective SA and SB for Irregular LOD

General MOSFET has an irregular shape of active area shown in Figure 11 To fully describe the shape of OD region will require additional instance parameters. However, this will result in too many parameters in the net lists and would massively increase the read-in time and degrade the readability of parameters. One way to overcome this difficulty is the concept of effective SA and SB similar to [18]. Stress effect model as described earlier allows an accurate and efficient layout extraction of effective SA and

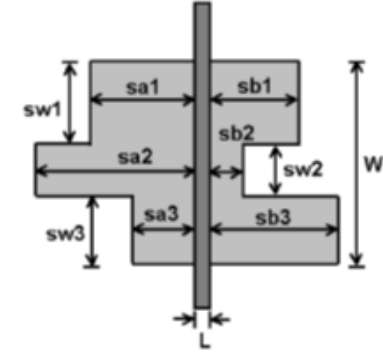


Figure 11: A typical layout of MOS devices with more instance parameters (sw_i , sai and sbi) in addition to the traditional L and W

SB while keeping fully compatibility of the LOD model. They are expressed as:

$$\frac{1}{SA_{eff} + 0.5 \cdot L_{drawn}} = \sum_{i=1}^n \frac{sw_i}{W_{drawn}} \cdot \frac{1}{sa_i + 0.5 \cdot L_{drawn}} \quad (6.16)$$

$$\frac{1}{SB_{eff} + 0.5 \cdot L_{drawn}} = \sum_{i=1}^n \frac{sw_i}{W_{drawn}} \cdot \frac{1}{sb_i + 0.5 \cdot L_{drawn}} \quad (6.17)$$

$$(6.18)$$

Stress Model for EDGEFET: Same stress model is implemented for the EDGEFET. New parameters are **SAEDGE**, **SBEDGE**, **KVTH0EDGE**, **STK2EDGE**, **STETA0EDGE**.

7 Well Proximity Effect Model

7.1 Well Proximity Effect Model

Retrograde well profiles have several key advantages for highly scaled bulk complementary metal oxide semiconductor(CMOS) technology. With the advent of high-energy implanters and reduced thermal cycle processing, it has become possible to provide a

relatively heavily doped deep nwell and pwell without affecting the critical device-related doping at the surface. The deep well implants provide a low resistance path and suppress parasitic bipolar gain for latchup protection, and can also improve soft error rate and noise isolation. A deep buried layer is also key to forming triple-well structures for isolated-well NMOSFETs. However, deep buried layers can affect devices located near the mask edge. Some of the ions scattered out of the edge of the photoresist are implanted in the silicon surface near the mask edge, altering the threshold voltage of those devices [19]. It is observed a threshold voltage shifts of up to 100 mV in a deep boron retrograde pwell, a deep phosphorus retrograde nwell, and also a triple-well implementation with a deep phosphorus isolation layer below the pwell over a lateral distance on the order of a micrometer [19]. This effect is called well proximity effect. BSIM6 considers the influence of well proximity effect on threshold voltage, mobility, and body effect. This well proximity effect model is developed by the Compact Model Council [20]. Experimental analysis [19] shows that well proximity effect is strong function of distance of FET from mask edge, and electrical quantities influenced by it follow the same geometrical trend. A phenomenological model based on these findings has been developed by modifying some parameters in the BSIM model. Note that the following equations have no impact on the iteration time because there are no voltage controlled components in them. Well proximity affects threshold voltage, mobility and the body effect of the device. The effect of the well proximity can be described through the following equations :

If SCA, SCB, SCC are given then WPE is given by (7.1), otherwise it is given by (7.2)

$$\begin{aligned}
 Vth0 &= Vth0_{org} + KVTH0WE \cdot (SCA + WEB \cdot SCB + WEC \cdot SCC) \\
 K2 &= K2_{org} + K2WE \cdot (SCA + WEB \cdot SCB + WEC \cdot SCC) \\
 \mu_{eff} &= \mu_{eff,org} \cdot (1 + KU0WE \cdot (SCA + WEB \cdot SCB + WEC \cdot SCC)) \quad (7.1)
 \end{aligned}$$

$$\begin{aligned}
W_{drn} &= W/NF \\
T1 &= SC + W_{drn} \\
T2 &= 1.0/SCREF \\
T3 &= \exp(-10.0 \cdot SC \cdot T2) \\
T4 &= \exp(-10.0 \cdot T1 \cdot T2) \\
T5 &= \exp(-20.0 \cdot SC \cdot T2) \\
T6 &= \exp(-20.0 \cdot T1 \cdot T2) \\
LOCAL_{SCA} &= \frac{SCREF \cdot SCREF}{SC \cdot T1} \\
LOCAL_{SCB} &= \frac{(0.1 \cdot SC + 0.01 \cdot SCREF) \cdot T3 - (0.1 \cdot T1 + 0.01 \cdot SCREF) \cdot T4}{W_{drn}} \\
LOCAL_{SCC} &= \frac{(0.05 \cdot SC + 0.0025 \cdot SCREF) \cdot T5 - (0.05 \cdot T1 + 0.0025 \cdot SCREF) \cdot T6}{W_{drn}} \\
Vth0 &= Vth0_{org} + KVTH0WE \cdot (LOCAL_{SCA} + WEB \cdot LOCAL_{SCB} + WEC \cdot LOCAL_{SCC}) \\
K2 &= K2_{org} + K2WE \cdot (LOCAL_{SCA} + WEB \cdot LOCAL_{SCB} + WEC \cdot LOCAL_{SCC}) \\
\mu_{eff} &= \mu_{eff,org} \cdot (1 + KU0WE \cdot (LOCAL_{SCA} + WEB \cdot LOCAL_{SCB} + WEB \cdot LOCAL_{SCC})) \\
&\quad (7.2)
\end{aligned}$$

where SCA, SCB, SCC are instance parameters that represent the integral of the first/second/third distribution function for scattered well dopant. The guidelines for calculating the instance parameters SCA, SCB, SCC have been developed by the Compact Model Council which can be found at the CMC website [20].

Well proximity Model for EDGEFET: Same well proximity model is implemented for the EDGE-FET. New parameters are KVTH0EDGEWE, LKVTH0EDGEWE, WKVTH0EDGEWE, PKVTH0EDGEWE, K2EDGEWE, LK2EDGEWE, WK2EDGEWE, PK2EDGEWE.

8 High Voltage Model

8.1 High Voltage Model

High voltage (HV) devices are important for power semiconductor industry. MOS based HV devices are more popular than bipolar counterpart due to their high input

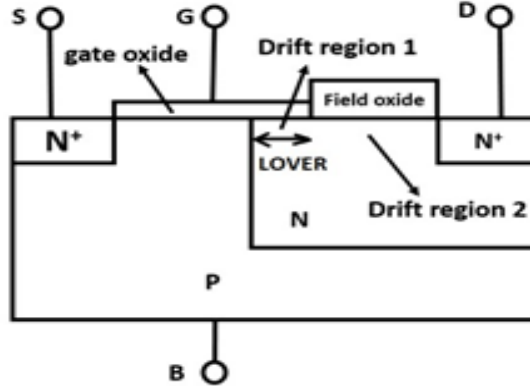


Figure 12: Illustration of High Voltage MOS structure.

impedance and fast turn-off. Here we present a simple enhancement to our next generation BSIM-BULK model for extending its applicability in the medium/high voltage domain

8.2 Drift Resistance Model Equations

Figure 12 shows the basic structure of a high voltage device. HV devices generally have thicker gate oxide to withstand high gate voltage and have drift region at the drain end for protection against high drain voltage. There are several forms of HV devices, for example LDMOS, VDMOS etc., and note that Figure 12 is merely an illustration. The approach to model HV devices is shown in Figure 13. The intrinsic region is very much similar to the conventional MOS transistor. The drift region is modeled using voltage dependent resistance model, which can be written in simplified form as follows: Drift resistance equation at the drain side:

$$R_{drift,satD} = R_o \left[1 + \left(\frac{\delta^{1/MDRIFT} * \text{abs}(V(di1, di))}{V_{drift-sat,D}} \right)^{MDRIFT} \right]^{(1/MDRIFT)} \quad (8.1)$$

$$R_o = rdstemp hv * RDLCW * W_{eff}^{WR} * (1.0 - PDRWB * V_{sb_noswap.}) \quad (8.2)$$

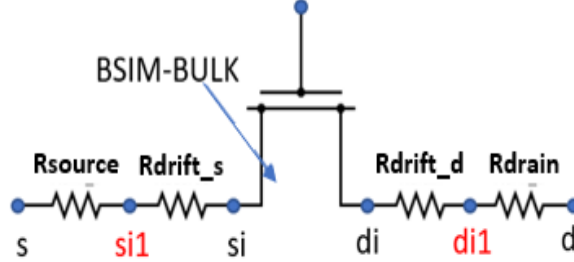


Figure 13: Modeling HV devices: BSIM-BULK model is employed for the channel part. Voltage dependent resistance is used to capture drift region electrostatics. Flag for the new resistance model- set HVMOD=1 and RDMSMOD=1 .

$$V_{drift,sat,D} = I_{drift,sat,D} * R_o \quad (8.3)$$

$$\delta = \frac{abs(V(di1, di))^{(4-MDRIFT)}}{abs(V(di1, di))^{(4-MDRIFT)} + HVFACTOR * V_{drift,satD}^{(4-MDRIFT)}} \quad (8.4)$$

Modeling of body-bias and gate bias dependency of drift current:

$$T1 = qs - PTWGHV1 \quad (8.5)$$

$$T2 = 10 * PSATXHV * T1 / (10 * PSATXHV + T1) \quad (8.6)$$

$$VDRIFT_{eff} = VDRIFT * (1 + PTWGHV * T2) \quad (8.7)$$

$$\gamma = 1 - DRB1 * (sqrt(1 + V_{sb,noswap}/V_{bi,drift})) - DRB2 * V_{sb,noswap} \quad (8.8)$$

Model to enhance the fitting flexibility at high V_{gs} and high V_{ds}

$$T0 = 1 + GADRIFT * (abs(V(di1, di)) - RDVDS) \quad (8.9)$$

$$I_{drift,satD} = NDRIFTD \cdot W \cdot NF \cdot VDRIFT_{eff} * T0 * \gamma \cdot \left[1 + CMD1 \cdot (V_{bcm})^{CMD2} \right] \quad (8.10)$$

where $V_{bcm} = \sqrt{V(bi, b)^2 + 10^{-6}}$

Drift resistance equation at the source side:

$$I_{drift,satS} = NDRIFTS \cdot W \cdot NF \cdot VDRIFT_{eff} \cdot \left[1 + CMS1 \cdot (V_{bcm})^{CMS2} \right] \quad (8.11)$$

$$R_{drift,satS} = R_o \left[1 + \left(\frac{\delta^{1/MDRIFT} * abs(V(si, si1))}{V_{drift,sat,S}} \right)^{MDRIFT} \right]^{(1/MDRIFT)} \quad (8.12)$$

$$R_o = rdstemp hv * RSLCW * W_{eff}^{WR} * (1.0 - PDRWB * V_{sb_noswap}) \quad (8.13)$$

$$V_{drift,sat,S} = I_{drift,sat,S} * R_o \quad (8.14)$$

$$\delta = \frac{abs(V(si, si1))^{(4-MDRIFT)}}{abs(V(si, si1))^{(4-MDRIFT)} + HVFACTOR * V_{drift,sat,S}^{(4-MDRIFT)}} \quad (8.15)$$

Parameters:

RDLCW: Resistance of the Drain at Low Current

NDRIFTD: Drift region charge density

VDRIFT: Carrier velocity in the drift region

MDRIFT: Parameter for Id,lin to Id,sat transition in Id-Vd

RSLCW and NDRIFTS: corresponding source side parameters

DRB1 and DRB2: Body bias parameters

PSATXHV, PTWGHV and PTWGHV1: Tuning parameters for VDRIFT

GADRIFT and RDVDS: Model parameters to enhance fitting flexibility at high V_{gs} and high V_{ds}

HVMOD=1 and RDSMOD=1: Flag to ON the HV model

RBODYHVMOD: Flag for HV substrate network - set RBODYHVMOD = 1

8.3 Decoupling Drain-side Drift Resistance

Drain-side drift resistance (`Rdrift_d` in Figure 13) used in I-V and C-V calculations has been decoupled. The parameter `RDLCW` will be used in the current calculations and the parameter `RDLCWCV` will be used instead of `RDLCW` in the capacitance calculations. The default value of `RDLCWCV` is same as that of the parameter `RDLCW`. Therefore, if one does not use the `RDLCWCV` parameter, `RDLCW` parameter will be used in both current and capacitance calculations.

Decoupling of the drain-side drift resistance is implemented in the model by modifying the potential at the internal drain node `di` (Node `di` can be seen in Figure 13) used in the capacitance calculations. Let $V_{di,CV}$ refer to the potential at node `di` used in capacitance calculations and $V_{di,IV}$ refer to the potential at node `di` used in the current calculations. Then $V_{di,CV}$ is defined in the model as shown below.

$$V_{di,CV} = V_{di,IV} + devsign \left(1.0 - \frac{RDLCWCV}{RDLCW} \right) V(di1, di) \quad (8.16)$$

Decoupling drain-side drift resistance allows better C-V fitting without affecting the I-V fitting. Parameter `RDLCWCV` is used after achieving I-V fitting to a satisfactory level, to improve the C-V fitting without impacting the I-V fitting.

8.4 Substrate Resistance Network for HVMOS

`Ddb` is body diode between `dbulk` and `di` (Details are given in section 2.24.2). When `Ddb` is forward biased, series resistance is significantly over-estimated. To solve this issue, DB diode is split into two parts with a partition factor `X`, as shown in Figure 14. This implementation can be turn on or turn off by model selector parameter `RBODY-HVMOD`.

8.5 Parameter Extraction for DC: Guideline

Guideline to extract parameters of the HVMOS is discussed below. These are preliminary steps based on our experience, and may not be comprehensive. However, they may give good starting point. For a conventional HV device without drift region at the source, `RSLCW=0` should be used.

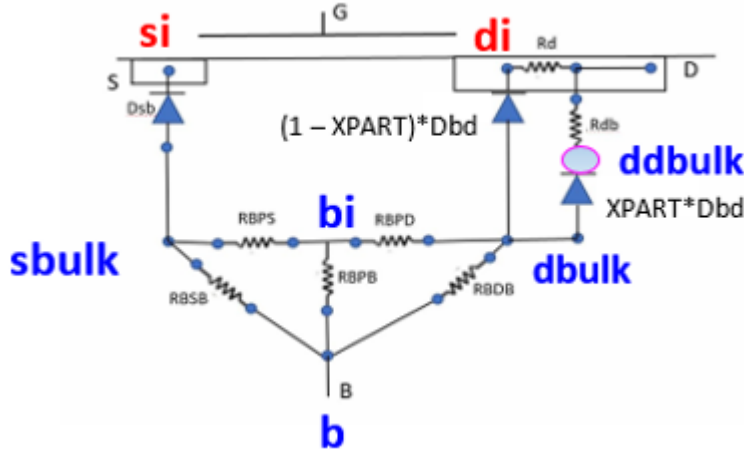


Figure 14: Substrate resistance network topology when RBODYHVMOD=1 .

8.5.1 Id-Vg Sub-threshold region

Set VDRIFT to large value such that Rdrift,D does not have velocity saturation effect. In this region, HV device characteristics are mainly governed by the MOS parameters. Extract VFB, NFACTOR, NDEP.

8.5.2 Id-Vg Above threshold region, low drain bias

Let VDRIFT to remain at the large value.

Extract MOS resistance and drift resistance parameters: U0, UA, EU, ETAMOB, RDW, PRWG etc. (for the MOS) and RDLCW for the drift region.

Note: RDW and PRWG are important MOS parameters for $I_{d,lin} - Vg$ fitting.

8.5.3 Id-Vd Characteristics

Step 1- Let VDRIFT to remain at the large value.

Step 2- Extract M0, K0, VSAT, PTWG, PSATX and other MOS parameters to match Id,sat level (indicated in Figure 15(a)). Since VDRIFT is large, the plot will look like Figure 15(a) after extraction.

Step 3- Start reducing VDRIFT to tune lin-sat transition. Extract MDRIFT for smoothing this region. Now the plot will look like Figure 15(b).

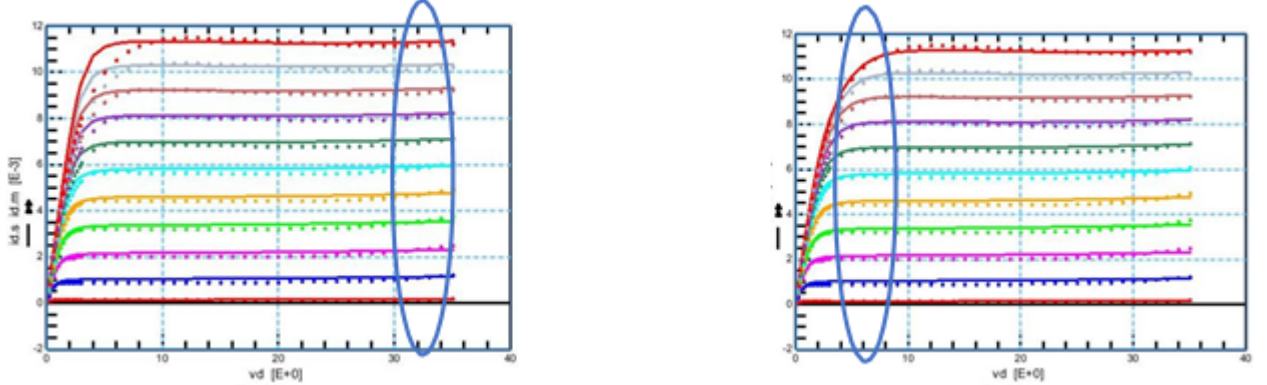


Figure 15: Id-Vd extraction (a) Step 2: Target Id_{sat} (b) Step 3: extract VDRIFT and MDRIFT.

8.5.4 Capacitance Parameters and their impact

The length of the drift region overlap with the gate (represented by LOVER in Figure 12) is a key variable in capacitance modeling. It is assumed that LOVER is already known beforehand. The capacitance model is activated by setting HVCAP=1. Note that the drift region specific capacitance model is added only at the drain side as of now. For the model equation, please refer to the section (2.15) of the manual. The capacitance related parameters are listed below:

HVCAP: Flag to turn on high voltage capacitance model.

VFBOV: Flat band voltage of the drift region.

LOVER: Length of overlap between the drift region and gate in inversion.

LOVERACC: Length of overlap between the drift region and gate in accumulation.

NDR: Doping of the drift region.

SLHV: Parameter for tuning C_{gg} slope in accumulation. Also a flsg, set=1 to enable the model.

SLHV1: Parameter for tuning C_{gg} slope in accumulation.

Following figures plot the overlap capacitance only i.e. the main transistor capacitance is turned off. Total capacitance is the sum of overlap capacitance and the main channel capacitance. We validated this model with the TCAD as well as exp. data. Please refer [21] for more details.

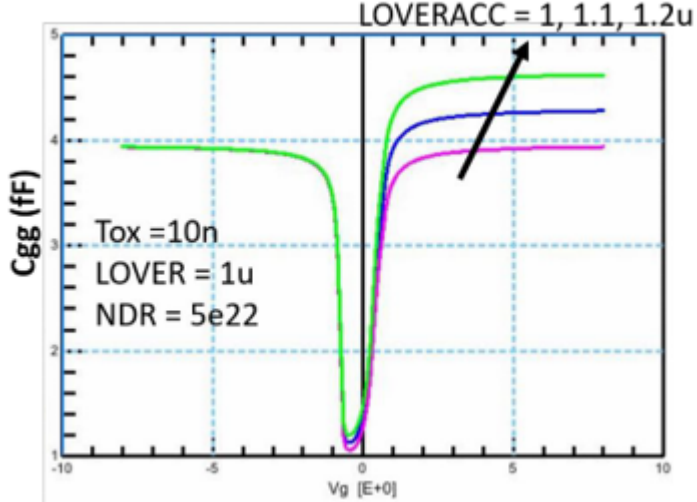


Figure 16: Impact of the parameter LOVERACC.

9 C-V Model

Inversion Charge : Total inversion charge (excluding velocity saturation, CLM and poly depletion) can be expressed explicitly in terms of normalized charge densities at source and drain sides as follows,

$$Q_I = W \cdot \int_0^L Q_i \, dx \quad (9.1)$$

$$= -WL \cdot C_{ox} \cdot V_t \int_0^1 2.n_q.q \, d\xi \quad (9.2)$$

$$-\frac{Q_I}{WL \cdot C_{ox} V_t} = q_I = 2.n_q \cdot \int_0^1 q \, d\xi \quad (9.3)$$

Here $\xi = \frac{x}{L}$. Inversion charge density is normalized to $-2.n_q.C_{ox}.V_t$ and voltages to V_t . From (2.228),

$$I_{ds} = -2 \cdot n_q \cdot \mu_{eff} \cdot \frac{W_{eff}}{L_{eff}} \cdot C_{ox} \cdot nV_t^2 \cdot (2q + 1) \frac{dq}{d\xi} \quad (9.4)$$

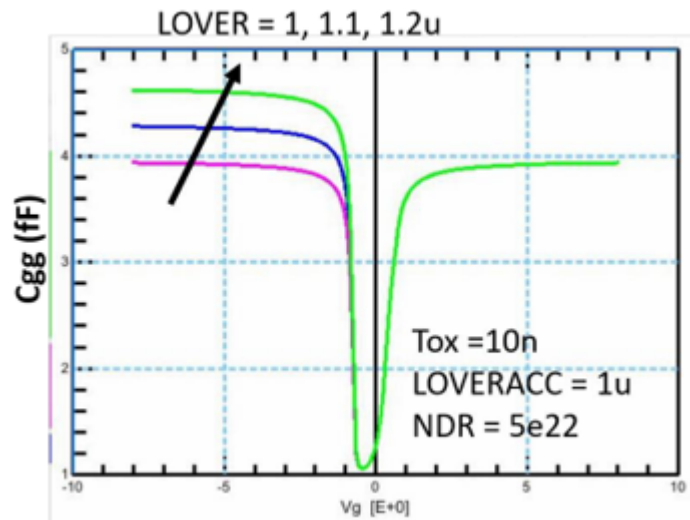


Figure 17: Impact of the parameter $LOVER$.

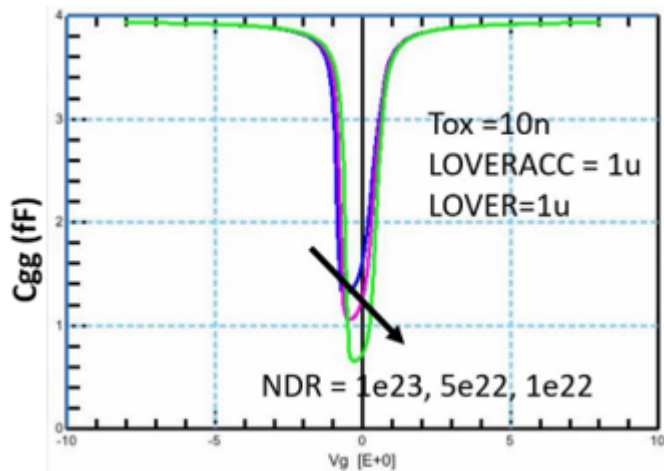


Figure 18: Impact of the parameter NDR .

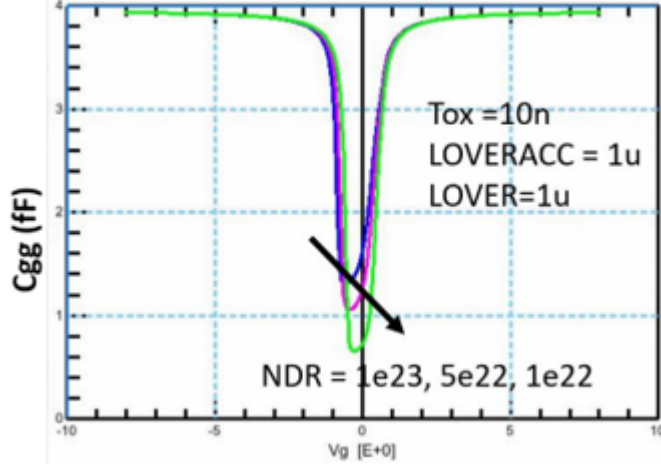


Figure 19: Impact of the parameter SLHV and SLHV1.

Normalizing current with $2 \cdot n_q \cdot \mu_{eff} \cdot \frac{W_{eff}}{L_{eff}} \cdot C_{ox} \cdot nV_t^2$,

$$i = -(2q + 1) \frac{dq}{d\xi} \quad (9.5)$$

which gives $d\xi = -\frac{(2q+1)}{i} dq = -\frac{(2q+1)}{(q_s-q_d)(1+q_s+q_d)}$. Substituting in (9.3)

$$q_I = -\frac{2n_q}{(q_s - q_d)(1 + q_s + q_d)} \int_{q_s}^{q_d} q(2q + 1) dq \quad (9.6)$$

$$= -\frac{2n_q}{(q_s - q_d)(1 + q_s + q_d)} \left[\frac{2}{3}(q_d^3 - q_s^3) + \frac{1}{2}(q_d^2 - q_s^2) \right] \quad (9.7)$$

on rearranging,

$$q_I = n_q \cdot \left[q_s + q_d + \frac{1}{3} \cdot \frac{(q_s - q_d)^2}{1 + q_s + q_d} \right] \quad (9.8)$$

Bulk Charge: Bulk charge density is given as

$$Q_b = -C_{ox} \cdot (V_G - V_{FB} - \psi_S) - Q_i \quad (9.9)$$

$$(9.10)$$

using charge linearization

$$Q_b = -C_{ox} \cdot (V_G - V_{FB} - \psi_p) - Q_i \left(1 - \frac{1}{n_q} \right) \quad (9.11)$$

Total bulk charge,

$$Q_B = W \cdot \int_0^L Q_b \, dx \quad (9.12)$$

$$= -WL \cdot C_{ox} \cdot \left[V_G - V_{FB} - \psi_p + \left(1 - \frac{1}{n_q} \right) \cdot \int_0^1 \frac{Q_i}{C_{ox}} \, d\xi \right] \quad (9.13)$$

Normalizing the bulk charge to $-W.L.C_{ox}.V_t$,

$$q_B = v_g - v_{fb} - \psi_p - 2(n_q - 1) \cdot \int_0^1 q \, d\xi \quad (9.14)$$

We know that $i_{ds} = -(2q + 1) \frac{dq}{d\xi}$ with i_{ds} given by (2.237). Thus $d\xi = -\frac{-(2q+1)}{i_{ds}} dq$,

$$q_B = v_g - v_{fb} - \psi_p + \frac{2(n_q - 1)}{i_{ds}} \cdot \int_{q_s}^{q_d} q(2q + 1) \, dq \quad (9.15)$$

$$= v_g - v_{fb} - \psi_p + \frac{2(n_q - 1)}{(q_s - q_d)(1 + q_s + q_d)} \int_{q_s}^{q_d} \left[\frac{2q^3}{3} + \frac{q^2}{2} \right] \quad (9.16)$$

$$= v_g - v_{fb} - \psi_p + \frac{2(n_q - 1)}{(q_s - q_d)(1 + q_s + q_d)} \left[\frac{2}{3} \cdot (q_d - q_s)(q_d^2 + q_s^2 + q_s \cdot q_d) + \frac{1}{2} \cdot (q_d - q_s)(q_d + q_s) \right] \quad (9.17)$$

which on rearrangement becomes,

$$q_B = v_g - v_{fb} - \psi_p - (n_q - 1) \left[q_s + q_d + \frac{1}{3} \cdot \frac{(q_s - q_d)^2}{1 + q_s + q_d} \right] \quad (9.18)$$

Flexibility of Tuning Cgg in Accumulation

'PO_psip((vgfbCV + DELVFBACC * inv_Vt), gam, 0, phib_n, psipACC)

$$q_B = v_g - v_{fb} - psipACC - (n_q - 1) \left[q_s + q_d + \frac{1}{3} \cdot \frac{(q_s - q_d)^2}{1 + q_s + q_d} \right] \quad (9.19)$$

And old ψ_p will be used for calculating qs and qdeff

Bulk charge with poly depletion effect :

$$q_B = A + B + \frac{1}{3} \cdot \frac{\Delta q^2}{C^3} \cdot \left[\frac{4}{5} \cdot \left(C^2 + P.Q \right) \cdot \frac{1}{1 + q_s + q_d} + \frac{2}{\gamma_g^2} \right] - n_q \cdot \left[q_s + q_d + \frac{1}{3} \cdot \frac{(q_s - q_d)^2}{1 + q_s + q_d} \right] \quad (9.20)$$

where

$$P = \sqrt{\frac{1}{4} + \frac{v_g - v_{fb} - \psi_p + 2.q_s}{\gamma_g^2}} \quad (9.21)$$

$$Q = \sqrt{\frac{1}{4} + \frac{v_g - v_{fb} - \psi_p + 2.q_d}{\gamma_g^2}} \quad (9.22)$$

$$A = \frac{v_g - v_{fb} - \psi_p + 2.q_s}{1 + 2 \cdot \sqrt{\frac{1}{4} + \frac{v_g - v_{fb} - \psi_p + 2.q_s}{\gamma_g^2}}} \quad (9.23)$$

$$B = \frac{v_g - v_{fb} - \psi_p + 2.q_d}{1 + 2 \cdot \sqrt{\frac{1}{4} + \frac{v_g - v_{fb} - \psi_p + 2.q_d}{\gamma_g^2}}} \quad (9.24)$$

$$C = \sqrt{\frac{1}{4} + \frac{v_g - v_{fb} - \psi_p + 2.q_s}{\gamma_g^2}} + \sqrt{\frac{1}{4} + \frac{v_g - v_{fb} - \psi_p + 2.q_d}{\gamma_g^2}} \quad (9.25)$$

Bulk charge with poly depletion effect, CLM and Velocity Saturation effects :

$$d_{qgeff} = (v_g - v_{fb} - \psi_p + 2.q_d) \left[\frac{2 \sqrt{\frac{1}{4} + \frac{v_g - v_{fb} - \psi_p + 2.q_d}{\gamma_g^2}} - 1}{2 \sqrt{\frac{1}{4} + \frac{v_g - v_{fb} - \psi_p + 2.q_d}{\gamma_g^2}} + 1} \right] \quad (9.26)$$

$$q_{beff} = \left[(v_g - v_{fb} - \psi_p) - 2(n_q - 1)q_d + d_{qgeff} \right] \quad (9.27)$$

$$q_B = \frac{1}{MDL} \left[A + B + \frac{1}{3} \cdot \frac{\Delta q^2}{C^3} \cdot \left(\frac{4}{8} \cdot (C^2 + P.Q) \cdot \frac{1}{1 + q_s + q_d} + \frac{2}{\gamma_g^2} \right) - n_q \cdot \left(q_s + q_d + \frac{1}{3} \cdot \frac{(q_s - q_d)^2}{1 + q_s + q_d} \right) \right] + (MDL - 1)q_{beff} \quad (9.28)$$

where

$$P = \sqrt{\frac{1}{4} + \frac{v_g - v_{fb} - \psi_p + 2.q_s}{\gamma_g^2}} \quad (9.29)$$

$$Q = \sqrt{\frac{1}{4} + \frac{v_g - v_{fb} - \psi_p + 2.q_d}{\gamma_g^2}} \quad (9.30)$$

$$A = \frac{v_g - v_{fb} - \psi_p + 2.q_s}{1 + 2 \cdot \sqrt{\frac{1}{4} + \frac{v_g - v_{fb} - \psi_p + 2.q_s}{\gamma_g^2}}} \quad (9.31)$$

$$B = \frac{v_g - v_{fb} - \psi_p + 2.q_d}{1 + 2 \cdot \sqrt{\frac{1}{4} + \frac{v_g - v_{fb} - \psi_p + 2.q_s}{\gamma_g^2}}} \quad (9.32)$$

$$C = \sqrt{\frac{1}{4} + \frac{v_g - v_{fb} - \psi_p + 2.q_s}{\gamma_g^2}} + \sqrt{\frac{1}{4} + \frac{v_g - v_{fb} - \psi_p + 2.q_d}{\gamma_g^2}} \quad (9.33)$$

Source and Drain Charges

$$Q_s = \frac{n_q}{3} \left[2 \cdot q_s + q_{deff} + \frac{1}{2} \cdot \left(1 + \frac{4}{5} \cdot q_s + \frac{6}{5} \cdot q_{deff} \right) \left(\frac{q_s - q_{deff}}{1 + q_s + q_{deff}} \right)^2 \right] \quad (9.34)$$

$$Q_d = \frac{n_q}{3} \left[q_s + 2 \cdot q_{deff} + \frac{1}{2} \cdot \left(1 + \frac{6}{5} \cdot q_s + \frac{4}{5} \cdot q_{deff} \right) \left(\frac{q_s - q_{deff}}{1 + q_s + q_{deff}} \right)^2 \right] \quad (9.35)$$

Source and Drain Charges with CLM and Velocity Saturation Model

$$Q_i = \frac{n_q}{MDL} \left[(q_s + q_{deff}) + \frac{1}{3} (q_s - q_{deff})^2 \frac{DV SAT}{MDL \cdot (1 + q_s + q_{deff})} + 2n_q(MDL - 1)q_{deff} \right] \quad (9.36)$$

$$Q_d = \frac{n_q}{3 \cdot MDL^2} \left[q_s + 2 \cdot q_{deff} + \frac{1}{2} \cdot \left(\frac{1}{5} \cdot (q_s - q_{deff}) + \frac{MDL}{DV SAT} \cdot (1 + q_s + q_{deff}) \right) \left(\frac{q_s - q_{deff}}{1 + q_s + q_{deff}} \right)^2 \left(\frac{DV SAT}{MDL} \right)^2 \right] + n_q \left[MDL - \frac{1}{MDL} \right] \quad (9.37)$$

$$Q_s = Q_i - Q_d \quad (9.38)$$

Flexibility of tuning Cgg in strong inversion for $V_{ds} \neq 0$ (AbulkCV implementation)

$$T1 = \frac{Leff}{Leff + sqrt(XJ_i * Xdep)} \quad (9.39)$$

$$AbulkCV = 1 + \frac{A0CV * T1 - AGSCV * q_s * V_T * T1}{1 + KETACV * V_{bsx}} \quad (9.40)$$

$$VdssatCV = VdssatCV / AbulkCV \quad (9.41)$$

If A0CV and AGSCV=0, then ABULKCV=ABULK, to maintain backward compatibility

$$T7 = pow(Vds / VdssatCV, 1 / Delta_t) \quad (9.42)$$

$$T8 = pow(1 + T7, -Delta_t) \quad (9.43)$$

$$Vdseff = Vds * T8 \quad (9.44)$$

$$Vdeff = (Vdseff + Vs) * inv_Vt \quad (9.45)$$

Calculate qdeff using new Vdeff and then recalculate Qi

$$Q_i = \frac{n_q}{MDL} \left[(q_s + q_{deff}) + \frac{1}{3}(q_s - q_{deff})^2 \frac{AbulkCV * DVSAT}{MDL \cdot (1 + q_s + q_{deff})} + 2n_q(MDL - 1)q_{deff} \right] \quad (9.46)$$

Quantum Mechanical Effect

$$X_{DC}^{inv} = \frac{ADOS \cdot (1.9 \cdot 10^{-9})}{1 + \left[\frac{Q_i + ETAQM \cdot Q_B}{QM0} \right]^{0.7 * BDOS}} \quad (9.47)$$

$$C_{ox}^{inv} = \frac{3.9 \cdot \epsilon_0}{TOXP \cdot \frac{3.9}{EPSROX} + \frac{X_{DC}^{inv}}{\epsilon_{ratio}}} \quad (9.48)$$

Intrinsic Charge expressions:

$$WLCOXVt_{inv} = NF \cdot Wact \cdot Lact \cdot C_{ox}^{inv} \cdot nVt \quad (9.49)$$

$$QBi = -NF \cdot Wact \cdot Lact \cdot \left(\frac{\epsilon_0 \cdot EPSROX}{TOXP} \right) \cdot nVt \cdot Qb \quad (9.50)$$

$$QSi = -WLCOXVt_{inv} \cdot Qs \quad (9.51)$$

$$QDi = -WLCOXVt_{inv} \cdot Qd \quad (9.52)$$

$$QGi = QSi + QDi + QBi \quad (9.53)$$

Note: QM contribution to capacitance is usually between 10-15%, and we recommend not using extreme values of QM parameters to achieve it.

Bias-dependent overlap capacitance model

An accurate overlap capacitance model is essential. This is especially true for the drain side where the effect of the capacitance is amplified by the transistor gain. The overlap capacitance changes with gate to source and gate to drain biases. In LDD MOSFETs a substantial portion of the LDD region can be depleted, both in the vertical and lateral directions. This can lead to a large reduction of the overlap capacitance. This LDD region can be in accumulation or depletion. We use a single equation for both regions by using such smoothing parameters as $V_{gs,overlap}$ and $V_{gd,overlap}$ for the source and drain side, respectively. Unlike the case with the intrinsic capacitance, the overlap capacitances are reciprocal. In other words, $C_{gs,overlap} = C_{sg,overlap}$ and $C_{gd,overlap} = C_{dg,overlap}$.

The bias-dependent overlap capacitance model in BSIM6 is adopted from BSIM4. The overlap charge is given by:

$$V_{gs,overlap} = \frac{1}{2} \left[V_{gs} - V_{fbsd} + \delta_1 - \sqrt{(V_{gs} - V_{fbsd} + \delta_1)^2 + 4\delta_1} \right] \quad (9.54)$$

$$T6 = \frac{V_{gs,overlap}}{[1 + (\frac{-V_{gs,overlap}}{CKAPPAS1})]^{1/CKAPPAS2}} \quad (9.55)$$

$$\begin{aligned} \frac{Q_{gs,ov}}{NF \cdot W_{effCV}} &= CGSO \cdot V_{gs} + \\ &CGSL \cdot \left[V_{gs} - V_{fbsd} - V_{gs,overlap} - \frac{CKAPPAS}{2} \left(\sqrt{1 - \frac{4 * T6}{CKAPPAS}} - 1 \right) \right] \end{aligned} \quad (9.56)$$

$$V_{gd,overlap} = \frac{1}{2} \left[V_{gd} - V_{fbsd} + \delta_1 - \sqrt{(V_{gd} - V_{fbsd} + \delta_1)^2 + 4\delta_1} \right] \quad (9.57)$$

$$T6 = \frac{V_{gd,overlap}}{\left[1 + \left(\frac{-V_{gd,overlap}}{CKAPPAD1} \right) \right]^{1/CKAPPAD2}} \quad (9.58)$$

$$\begin{aligned} \frac{Q_{gd,ov}}{NF \cdot W_{effCV}} &= CGDO \cdot V_{gd} + \\ CGDL \cdot \left[V_{gd} - V_{fbsd} - V_{gd,overlap} - \frac{CKAPPAD}{2} \left(\sqrt{1 - \frac{4 * T6}{CKAPPAD}} - 1 \right) \right] \end{aligned} \quad (9.59)$$

$$\delta_1 = 0.02V \quad (9.60)$$

Outer Fringing Capacitance

The fringing capacitance consists of a bias-independent outer fringing capacitance and a bias-dependent inner fringing capacitance. Only the bias-independent outer fringing capacitance is modeled. If CF is not given then outer fringe capacitance is calculated as

$$CF = \frac{2 \cdot EPSROX \cdot \epsilon_0}{\pi} \cdot \ln[CFRCOEFF \cdot (1 + \frac{0.4e - 6}{TOX})] \quad (9.61)$$

10 Parameter Extraction Procedure

The objective of this section is to provide guidelines for the extraction of the main model parameters. The procedure is structured in such a way that parameters linked to specific psychical phenomena are extracted from analyses where these effects are prominent. Although parameter extraction is not always a straight-forward procedure, the aim is to minimize the effort invested and the number of the essential loops performed.

If all the steps of the described procedure are followed then a global model card is obtained which means that the model can be used across the entire width/length plane of the technology. If a local fitting is targeted, then only the parameters of Section 10.1 need to be extracted for each DUT. However, in that case binning is necessary if the model card is to be used for the entire geometry range of the technology. Irrespectively of the choice between global and local fitting, different model cards should be extracted for nmos and pmos devices or for different technologies.

Before proceeding to the extraction of any parameter, it is very important that **TNOM** is set to the value of the temperature at which the measurements were carried out. Also, it is recommended that if they are available, the values of the process parameters are provided. The most common process parameters are shown in Table 3.

Parameter Name	Physical Description
EPSROX	Relative Gate Dielectric Constant
EPSRSUB	Relative Dielectric Constant of the Channel
TOXE	Electrical Gate Equivalent Oxide Thickness
TOXP or DTOX	Physical Gate Equivalent Oxide Thickness
NDEP	Channel Doping Concentration
NGATE	Gate Doping Concentration
NSD	S/D Doping Concentration
XJ	S/D Junction Depth
XW/XL	Channel W/L Offset due to Mask/Etch Effect

Table 3: Process parameters which are recommended to be provided before parameter extraction.

10.1 Extraction of Geometry Independent Parameters

The first part of the model parameter extraction procedure is to extract the parameters that are related to the main physical phenomena, which define transistor's behavior, and are also geometry independent. For that, a wide and long channel device should be chosen. At this point, **WWIDE** and **LLONG** parameters must be assigned to the values of the width and length of this large chosen DUT. This ensures that once the behavior of the long/wide channel device is fitted, it cannot be further affected by the values scaling parameters that will be extracted in the next steps.

10.1.1 Gate Capacitance C_{GG} vs. V_G Analysis @ $V_S = 0\text{ V}$, $V_D = 0\text{ V}$ & $V_B = 0\text{ V}$

At this step process parameters and parameters related to quantum mechanical effect are extracted. Even if values have been already assigned to process parameters, a fine tuning should be made in order to fit accurately the electrical behavior of the device. From C_{GG} vs. V_G analysis the following process parameters can be extracted: **NDEP**, **TOXE**, **VFB** and **NGATE**. Each of these parameters affects a different region or in a different way the C_{GG} capacitance, so they should be extracted accordingly. More specifically:

- **VFB** is defining the flat-band voltage of the device and it can be extracted by studying the region from depletion till the onset of strong-inversion.
- **NDEP** is affecting C_{GG} in the depletion region. If possible, **NDEP**, which defines the doping level, is better to be extracted from C_{GB} vs. V_G analysis (S and D terminals are grounded).
- **TOXE** is affecting the deep accumulation and strong-inversion regions.
- **NGATE** is related to the poly-silicon depletion effect, so it affects the slope of C_{GG} in the strong-inversion region.

Furthermore, the value of C_{OX} is affected by the Quantum Mechanical effect. So, the parameters: **ADOS**, **BDOS**, **QM0** and **ETAQM** are also extracted from C_{GG} vs. V_G analysis, when focusing at the slope of C_{GG} at the onset of the strong-inversion region.

10.1.2 Drain Current I_D vs. V_G Analysis @ $V_D = [V_{D,lin}, V_{D,sat}]$, $V_S = 0 V$ & $V_B = 0 V$

In this step, the V_G dependence of the drain current - I_D , is extracted. Different parameters are extracted in two different regions of operation, namely *linear mode* (i.e. $V_D \ll V_G - V_{TH}$) and *saturation* (i.e. $V_D \gg V_G - V_{TH}$). It is very important that during extraction in this step, both I_D and the transconductance - g_m (even g'_m and g''_m) are extracted at once.

Linear Mode

- Focusing in *weak-inversion* region (I_D vs. V_G characteristic when y-axis is in logarithmic scale), **NFACTOR**, which is related to the sub-threshold slope of the I_D , can be extracted. Furthermore, a fine tuning of the **NDEP** and **VFB** parameters is performed. In case the values of **NDEP** and **VFB** obtained during the fitting of I_D vs. V_G characteristic differ much from those obtained during the fitting of C_{GG} vs. V_G characteristic (Section 10.1.1), parameters **NDEPCV** and **VFCBV** can be used for dynamic operation (CV) and **NDEP** and **VFB** for static operation (IV). In general, using different values for **NDEP** and **NDEPCV** for IV and CV operation is not recommended unless necessary.
- From *strong-inversion* region, the mobility **U0**, the parameter for the effective field **ETAMOB**, the parameters related to the effect of mobility reduction due to vertical field **UA** and **EU** and the parameters for the coulomb scattering effect **UD** and **UCS**, are extracted. Furthermore, the parameters for S/D series resistances are also extracted under the same bias conditions. If **RDSMOD = 0** (internal S/D series resistances), **RDSW** is extracted. Otherwise, **RSW** and **RDW** are extracted.

Saturation

- From *weak-inversion* region (I_D vs. V_G characteristic when y-axis is in logarithmic scale), **CDS_{CD}** parameterer, which is linked to the dependence of the sub-threshold slope on drain bias, is extracted.
- Focusing in *strong-inversion* region, the parameters that are connected to the velocity saturation effect, namely **VSAT**, **PSAT**, **PTWG** and **PSATX**, can be extracted. **PSATX** does need to be changed.

Finally, from *accumulation* to *depletion* region, in both *linear mode* and *saturation*, the parameters related to GIDL effect are extracted. First, the selector **GIDLMOD** should be set to 1 to activate GIDL/GILS currents and then the parameters **AGIDL**, **BGIDL**, **CGIDL** and **EGIDL** are extracted. Ideally GIDL and GILS currents should be equal, so it is sufficient to extract **AGIDL**, **BGIDL**, **CGIDL** and **EGIDL** parameters. But in case GIDL and GILS currents differ, then parameters **AGISL**, **BGISL**, **CGISL** and **EGISL** can also be used.

10.1.3 Gate Current I_G vs. V_G Analysis @ various V_D , $V_S = 0\text{ V}$ & $V_B = 0\text{ V}$

From I_G vs. V_G analysis, parameters related to the gate current can be extracted. First, the tunneling components should be activated by setting to 1 the selectors **IGC-MOD** and **IGBMOD**. Different parameters are extracted in different regions of operation and more specifically:

Accumulation to weak-inversion Region

- **AIGBACC**, **BIGBACC**, **CIGBACC** and **NIGBACC**, which are linked to the gate-to-substrate current component determined by ECB.
- **AIGS**, **BIGS** and **CIGS**, which are linked to the tunneling current between the gate and the source diffusion region and **AIGD**, **BIGD** and **CIGD**, which are linked to the tunneling current between the gate and the drain diffusion region.
- **DLCIG** and **DLCIGD**, which are linked to the S/D overlap length for I_{GS} and I_{GD} respectively.

Weak to strong-inversion Region

- **AIGBINV**, **BIGBINV**, **CIGBINV**, **EIGBINV** and **NIGBINV**, which are linked to the gate-to-substrate current component determined by EVB.
- **AIGC**, **BIGC**, **CIGC**, **NIGC** and **PIGCD**, which are linked to the gate-to-channel current. **PIGCD** is expressing the V_D dependence of gate-to-channel current.

10.1.4 Drain Current I_D vs. V_D Analysis @ various V_G , $V_S = 0 V$ & $V_B = 0 V$

In this step, both I_D vs. V_D and output conductance - g_{ds} (even g'_{ds}) vs. V_D characteristics are studied at once. Different effects impact both the characteristics, so the parameters related to those effects are extracted. In detail,

- **DELTA**, which is a smoothing factor for the transition between V_{DS} and $V_{DS,sat}$.
- **PDITS** and **PDITSD**, linked to DITS effect.
- **PCLM**, **PCLMG** and **FPROUT** linked to the CLM effect.
- **PDIBLC**, linked to the impact of DIBL effect on R_{out} .
- **PVAG**, linked to the V_G dependence on Early voltage.

10.1.5 Gate Capacitance C_{GG} vs. V_G Analysis @ $V_{DS} \neq 0 V$ & $V_B = 0 V$

Velocity saturation (VS) and channel length modulation (CLM) effects not only affect the static behavior of the transistor but the dynamic as well. The extraction of **VSAT** and **PCLM** from I_D vs. V_G and I_D vs. V_D characteristics should be sufficient in order to capture these effects for CV operation. To verify that, C_{GG} vs. V_G characteristic for different $V_{DS} \neq 0 V$, from linear mode to saturation must be studied. If different values for **VSAT** and **PCLM** are necessary for accurate fitting of the CV behavior at different V_D biases, then **VSATCV** and **PCLMCV** can be used.

10.1.6 Drain Current I_D vs. V_G Analysis @ $V_D = [V_{D,lin}, V_{D,sat}]$ & various V_B

In this step almost the same procedure as in Section 10.1.2 will be repeated in order to extract the parameters that are linked to the body effect. Similar to Section 10.1.2, it is also very important that during the extraction in this step both I_D and g_m are studied at once.

Linear Mode

- Focusing in *weak-inversion* region, **CDSCB**, which is linked to the V_B (or V_S) dependence of the sub-threshold slope, is extracted. Also **K2**, which is linked to the V_{TH} shift due to vertical non-uniform doping, is extracted in the same region.

- In *strong-inversion* region, **UC**, which is linked to the V_B (or V_S) dependence of mobility, is extracted. The parameter for V_B (or V_S) dependence of S/D series resistances, **PRWB**, is also extracted under the same bias conditions.

Saturation

- In *strong-inversion* region, the parameter that is connected to V_B (or V_S) dependence of the velocity saturation effect, i.e. **PSATB**, is extracted.

In order to validate that the values of the parameters, which are linked to V_B (or V_S) dependencies, are correctly extracted, it is useful to check I_D vs. V_D and g_{ds} vs. V_D characteristics @ various V_G & $V_B \neq 0$ V (or $V_S \neq 0$ V) and, if needed, to fine tune the values of the parameters.

10.1.7 Fitting Verification

When all the extraction steps of this part have been performed, the fitting of the model should be checked for all the analyses carried out up to this point. Parameters can be fine tuned for better fitting in all regions.

10.2 Extraction of Short Channel Effects & Length Scaling Parameters

Once the behavior of the wide/long channel device has been accurately modeled, the next step is the extraction of the parameters that are either related to short channel effects or express the different length dependencies. So at this part, devices across the entire length range of the technology, from the shortest to the longest one, are studied simultaneously. In order to avoid the impact of narrow channel effects or of the width dependencies these devices should have the same **wide** channel. The extraction that is carried out follows the same flow as in Section 10.1, but now a set of devices with constant **wide** channel but different channel lengths is used.

10.2.1 Gate Capacitance C_{GG} vs. V_G Analysis @ $V_S = 0$ V, $V_D = 0$ V & $V_B = 0$ V

In this step, parameters related to overlap and fringing capacitances as well as those that are linked to the length dependence of doping concentration and flat-band voltage are extracted. More specifically:

- **NDEPL1**, **NDEPLEXP1**, **NDEPL2** and **NDEPLEXP2**, which are the length scaling parameters for the doping concentration, are extracted from C_{GG} in the depletion region. If possible, it is recommended that those parameters are extracted from C_{GB} vs. V_G analysis (S and D terminals are grounded).
- Extraction of parameters related to overlap and fringing capacitances is carried out by studying the entire range of V_G bias of C_{GG} vs. V_G characteristic. These parameters are: **CGSO**, **CGDO**, **CGBO**, **CGSL**, **CGDL**, **CKAPPAS**, **CKAPPAD** and **CF**. If possible, it is recommended that **CGSO**, **CGDO**, **CGBO** and **CF** are extracted from C_{GD} vs. V_G at low V_B (when S and D terminals are connected together and B terminal is grounded), while **CGSL**, **CGDL**, **CKAPPAS** and **CKAPPAD** are extracted from C_{GD} vs. V_G at high V_B (when S, D and B terminals are connected together).
- **DLC**, which is the channel-length offset parameter for the CV model, is extracted in the strong-inversion region of C_{GG} .
- **VFB** and **VFBLEXP**, which express the length dependence of flat-band voltage at IV, are extracted from depletion region till the onset of strong-inversion. In order to be able to use **VFB** and **VFBLEXP** parameters, **VFB** must be $\neq 0$.
- **VFBCVL** and **VFBCVLEXP**, which express the length dependence of flat-band voltage at CV, are extracted from depletion region till the onset of strong-inversion. In order to be able to use **VFBCVL** and **VFBCVLEXP** parameters, **VFBCV** must be $\neq 0$.

10.2.2 Drain Current I_D vs. V_G Analysis @ $V_D = [V_{D,lin}, V_{D,sat}]$, $V_S = 0$ V & $V_B = 0$ V

In this step, parameters related to short channel effects or to length dependencies of I_D vs. V_G , are extracted. Similar to the procedure described in Section 10.1.2, the

parameters are divided in two groups, those which are extracted in *linear mode* (i.e. $V_D \ll V_G - V_{TH}$) and those which are extracted in *saturation* (i.e. $V_D \gg V_G - V_{TH}$). It is very important that during the extraction both I_D and g_m of all the devices are studied at once.

Linear Mode

- Focusing in *weak-inversion* region (I_D vs. V_G characteristic when y-axis is in logarithmic scale), **NFACTORL** and **NFACTORLEXP**, which are related to the length dependence of the sub-threshold slope of I_D vs. V_G , can be extracted. Furthermore, **LINT**, which is the channel length offset parameter, is used to fit both the sub-threshold slope and the V_{TH} . For fitting the V_{TH} of the devices also **DVTP0** and **UD** can prove to be useful. **UD** should be used only for fine tuning because it mainly affects the region above threshold. It is recommended that the parameters **NDEPL1**, **NDEPLEXP1**, **NDEPL1** and **NDEPLEXP1** keep the values extracted from the C_{GG} vs. V_G analysis (Section 10.2.1). But, if the fitting of the V_{TH} across the entire length range cannot be achieved without changing the values of **NDEPL1**, **NDEPLEXP1**, **NDEPL1** and **NDEPLEXP1**, then these parameters are used for static operation (IV) and **NDEPCVL1**, **NDEPCVLEXP1**, **NDEPCVL1** and **NDEPCVLEXP1** parameters are used for dynamic operation (CV).
- In *strong-inversion* region, the parameters related to the length dependence of: i) the mobility; **U0L** and **U0LEXP**, ii) the effect of mobility reduction due to vertical field; **UAL**, **UALEXP**, **EUL** and **EULEXP** and iii) the coulomb scattering effect; **UDL** and **UDLEXP**, are extracted. Furthermore, parameters for the length dependence of S/D series resistances, namely **RDSWL** and **RDSWL-EXP** (when **RDSMOD = 0**) or **RSWL**, **RSWLEXP**, **RDWL** and **RDWL-EXP** (when **RDSMOD = 1**), are also extracted under the same bias conditions.

Saturation

- In *weak-inversion* region (I_D vs. V_G characteristic when y-axis is in logarithmic scale), **CDSCDL** and **CDSCDLEXP** parameters, which are linked to the length dependence of the sub-threshold slope dependence on drain bias, are extracted. Moreover, parameters for DIBL effect, which control V_{TH} when $V_{DS} \neq 0$, namely **ETA0** and **DSUB**, are also extracted in the same region.

- Focusing in *strong-inversion* region, the length scaling parameters linked to the velocity saturation effect, i.e **VSATL**, **VSATEXP**, **PSATL**, **PSATEXP**, **PTWGL** and **PTWGLEXP**, can be extracted.

Finally, from *accumulation* to *depletion* region, in both *linear mode* and *saturation*, the parameters **AGIDLL**/**AGISLL**, which are related the length dependence of GIDL effect (GIDL/GISL currents), are extracted.

10.2.3 I_G vs. V_G Analysis @ various V_D , $V_S = 0\text{ V}$ & $V_B = 0\text{ V}$

From I_G vs. V_G analysis, parameters related to the length dependence of gate current are extracted. These parameters are: **AIGCL**, **AIGSL**, **AIGDL** and **PIGCDL**.

10.2.4 I_D vs. V_D Analysis @ various V_G , $V_S = 0\text{ V}$ & $V_B = 0\text{ V}$

In this step, both I_D vs. V_D and g_{ds} vs. V_D characteristics should be studied at once. Similar to the procedure described in Section 10.2.4 the parameters that are extracted are:

- **DELTAL** and **DELTALEXP**, which are related to the length dependence of the smoothing factor for the transition between V_{DS} and $V_{DS,sat}$.
- **PDITSL**, linked to the length dependence of DITS effect.
- **PCLML**, **PCLMLEXP**, **FPROUTL** and **FPROUTLEXP** linked to the length dependence of CLM effect.
- **PDIBLCL** and **PDIBLCLEXP**, linked to the length dependence of the impact of DIBL effect on R_{out} .

It is very important to be mentioned here, that if the slope of g_{ds} vs. V_D characteristic at low levels of inversion is steeper than the measurements, then **ETA0** should be decreased and **DVTP1** can be used to achieve an accurate fit for the V_{TH} in *saturation*.

10.2.5 C_{GG} vs. V_G Analysis @ $V_{DS} \neq 0 V$ & $V_B = 0 V$

The extraction of the length scaling parameters of **VSAT** and **PCLM** from I_D vs. V_G and I_D vs. V_D characteristics (Steps 10.2.2 and 10.2.4) should be sufficient in order to capture VS and CLM effects for CV operation. To verify that, C_{GG} vs. V_G characteristic of all devices, for different $V_{DS} \neq 0 V$, from linear mode to saturation, must be studied. If different values for **VSATL**, **VSATLEXP**, **PCLML** and **PCLMLEXP** are necessary for accurate fitting of the CV behavior across L, then **VSATCVL**, **VSATCVLEXP**, **PCLMCVL** and **PCLMCVLEXP** can be used.

10.2.6 I_D vs. V_G Analysis @ $V_D = [V_{D,lin}, V_{D,sat}]$ & various V_B (or various V_S)

In this step almost the same procedure as in Section 10.1.6 will be repeated in order to extract the length scaling parameters that are linked to the body effect. Similar to Section 10.1.6, it is also very important that during the extraction in this step both I_D and g_m of all devices are studied at once.

Linear Mode

- Focusing in *weak-inversion* region, **K2L** and **K2LEXP**, which are linked to the length dependence V_{TH} shift due to vertical non-uniform doping, are extracted.
- In *strong-inversion* region, **UCL** and **UCLEXP**, which are linked to the length dependence of mobility reduction with V_B (or V_S) bias, are extracted. The parameters for the length dependence of S/D series resistances with V_B (or V_S) bias, namely **PRWBL** and **PRWBLEXP**, are also extracted under the same bias conditions.

Saturation

- In *weak-inversion* region (I_D vs. V_G characteristic when y-axis is in logarithmic scale), the parameters related to length dependence of DIBL effect dependence on V_B (or V_S) bias, namely **ETAB** and **ETABEXP**, are extracted.

In order to validate that the values of the length scaling parameters, which are linked to V_B (or V_S) dependencies, are correctly extracted, it is useful to check I_D vs. V_D and g_{ds} vs. V_D characteristics @ various V_G & $V_B \neq 0 V$ (or $V_S \neq 0 V$) and, if needed, to fine tune the values of the parameters.

10.2.7 Fitting Verification

When all the steps for the extraction of short channel effects and length scaling parameters have been performed, the fitting of the model should be checked for all the analyses carried out in Section 10.2 and parameters can be fine tuned for better fitting.

10.3 Extraction of Narrow Channel Effects & Width Scaling Parameters

The next step in the parameter extraction procedure is the extraction of the parameters that are either related to narrow channel effects or express the different width dependencies. So at this part, devices across the entire width range of the technology, from the narrowest to the widest one, are studied simultaneously. In order to avoid the impact of short channel effects or of the length dependencies these devices should have the same **long** channel. The extraction that is carried out follows the same flow as in Section 10.2, but now a set of devices with constant **long** channel but different channel widths is used.

10.3.1 Gate Capacitance C_{GG} vs. V_G Analysis @ $V_S = 0$ V, $V_D = 0$ V & $V_B = 0$ V

In this step, parameters related to the width dependencies of the CV behavior of the device, e.g. width dependence of the doping concentration and flat-band voltage, are extracted. More specifically:

- **NDEPW** and **NDEPWEXP**, which are the width scaling parameters for the doping concentration, are extracted from C_{GG} in the depletion region. If possible, it is recommended that those parameters are extracted from C_{GB} vs. V_G analysis (S and D terminals are grounded).
- **DWC**, which is the channel-width offset parameter for the CV model, is extracted in the strong-inversion region of C_{GG} .
- **VFBCVW** and **VFBCVWEXP**, which express the width dependence of flat-band voltage at CV, are extracted along the entire V_G bias range of C_{GG} characteristic. In order to be able to use **VFBCVW** and **VFBCVWEXP** parameters, **VFBCV** must be $\neq 0$.

10.3.2 Drain Current I_D vs. V_G Analysis @ $V_D = [V_{D,lin}, V_{D,sat}]$, $V_S = 0 V$ & $V_B = 0 V$

In this step, parameters related to width dependencies of I_D vs. V_G , are extracted. Similar to the procedure described in Section 10.1.2, the parameters are divided in two groups, those which are extracted in *linear mode* (i.e. $V_D \ll V_G - V_{TH}$) and those which are extracted in *saturation* (i.e. $V_D \gg V_G - V_{TH}$). It is very important that during the extraction both I_D and g_m of all the devices are studied at once.

Linear Mode

- Focusing in *weak-inversion* region (I_D vs. V_G characteristic when y-axis is in logarithmic scale), **NFACTORW** and **NFACTORWEXP**, which are related to the width dependence of the sub-threshold slope of I_D vs. V_G , can be extracted. Furthermore, **WINT**, which is the channel width offset parameter, is used to fit both the sub-threshold slope and the V_{TH} across W. It is recommended that the parameters **NDEPW** and **NDEPWEXP** keep the values extracted from the C_{GG} vs. V_G analysis (Section 10.3.1). But, if the fitting of the V_{TH} across the entire width range cannot be achieved without changing the values of **NDEPW** and **NDEPWEXP**, then these parameters are used for static operation (IV) and **NDEPCVW** and **NDEPCVWEXP** parameters are used for dynamic operation (CV).
- In *strong-inversion* region, the parameters related to the width dependence of mobility reduction due to vertical field effect, namely **UAW**, **UAWEXP**, **EUW** and **EUWEXP**, are extracted.

Saturation

- Focusing in *strong-inversion* region, the width scaling parameters linked to the velocity saturation effect, i.e. **VSATW** and **VSATWEXP**, can be extracted.

Finally, from *accumulation* to *depletion* region, in both *linear mode* and *saturation*, the parameters **AGIDLW/AGISLW**, which are related the width dependence of GIDL effect (GIDL/GISL currents), are extracted.

In order to validate that the values of the width scaling parameters are correctly extracted, it is useful to check I_D vs. V_D and g_{ds} vs. V_D characteristics @ various V_G , $V_S = 0 V$ & $V_B = 0 V$ (or $V_S \neq 0 V$) and, if needed, to fine tune the values of the parameters.

10.3.3 Gate Current I_G vs. V_G Analysis @ various V_D , $V_S = 0 V$ & $V_B = 0 V$

From I_G vs. V_G analysis, parameters related to the width dependence of gate current are extracted. These parameters are: **AIGCW**, **AIGSW** and **AIGDW**.

10.3.4 Gate Capacitance C_{GG} vs. V_G Analysis @ $V_{DS} \neq 0 V$ & $V_B = 0 V$

The extraction of the width scaling parameters of **VSATW** and **VSATWEXP** from I_D vs. V_G and I_D vs. V_D characteristics (Step 10.3.2) should be sufficient in order to capture VS for CV operation. To verify that, C_{GG} vs. V_G characteristic of all devices, for different $V_{DS} \neq 0 V$, from linear mode to saturation, must be studied. If different values for **VSATW** and **VSATWEXP** are necessary for accurate fitting of the CV behavior across W, then **VSATCVW** and **VSATCVWEXP** can be used.

10.3.5 Drain Current I_D vs. V_G Analysis @ $V_D = [V_{D,lin}, V_{D,sat}]$ & various V_B (or various V_S)

In this step, from *weak-inversion* region of *linear mode*, **K2W** and **K2WEXP**, which are linked to the width dependence V_{TH} shift due to vertical non-uniform doping, can be extracted. For validation purposes, it is useful to check: i) I_D vs. V_G and g_m vs. V_G characteristics in *weak* and *strong-inversion* and for both *linear mode* and *saturation*, and ii) I_D vs. V_D and g_{ds} vs. V_D characteristics @ various V_G & $V_B \neq 0 V$ (or $V_S \neq 0 V$) and, if needed, extract **K2W** and **K2WEXP** to fit both (i) and (ii).

10.3.6 Fitting Verification

When all the extraction steps for the width scaling have been performed, the fitting of the model should be checked for all the analyses carried out in Section 10.3 and parameters can be further tuned for better fitting.

10.4 Extraction of Parameters for Narrow/Short Channel Devices

The final part in the parameter extraction procedure from a geometrical point of view, is the extraction of the parameters for narrow/short channel devices. These devices have the minimum dimensions so it is more difficult to capture their behavior. Since the narrow/short channel device parameters can affect the already performed fitting across length and width, it is recommended that two different sets of devices are studied simultaneously, i.e. one set with a constant **short** channel but different channel widths (from narrowest to widest) and one set with a constant **narrow** channel but different channel lengths (from the shortest to the longest one).

10.4.1 Gate Capacitance C_{GG} vs. V_G Analysis @ $V_S = 0$ V, $V_D = 0$ V & $V_B = 0$ V

In this step, geometry dependent parameters for modeling the CV behavior of the narrow/short channel devices, are extracted. More specifically:

- **NDEPWL** and **NDEPWLEXP**, which are used to fit the doping concentration of small channel devices, are extracted from C_{GG} in the depletion region. If possible, it is recommended that those parameters are extracted from C_{GB} vs. V_G analysis (S and D terminals are grounded).
- **LWLC** and **WWLC**, which are coefficients of length/width dependencies for CV model, are extracted in the strong-inversion region of C_{GG} .
- **VFBCVWL** and **VFBCVWLEXP**, which are used to fit the flat-band voltage at CV, are extracted from depletion till the onset of strong-inversion region of C_{GG} characteristic. In order to be able to use **VFBCVWL** and **VFBCVWLEXP** parameters, **VFBCV** must be $\neq 0$.

10.4.2 Drain Current I_D vs. V_G Analysis @ $V_D = [V_{D,lin}, V_{D,sat}]$, $V_S = 0$ V & $V_B = 0$ V

In this step, geometry dependent parameters for modeling I_D of the narrow/short channel devices, are extracted. Similar to the procedure described in Section 10.1.2, the

parameters are divided in two groups, those which are extracted in *linear mode* (i.e. $V_D \ll V_G - V_{TH}$) and those which are extracted in *saturation* (i.e. $V_D \gg V_G - V_{TH}$). It is very important that during the extraction both I_D and g_m of all the devices are studied at once.

Linear Mode

- Focusing in *weak-inversion* region (I_D vs. V_G characteristic when y-axis is in logarithmic scale), **NFACTORWL** and **NFACTORWLEXP**, which are used to fit the sub-threshold slope of I_D vs. V_G for small channel devices, can be extracted. It is recommended that the parameters **NDEPWL** and **NDEPWLEXP** keep the values extracted from the C_{GG} vs. V_G analysis (Section 10.4.1). But, if the fitting of the V_{TH} for both sets of devices cannot be achieved without changing the values of **NDEPWL** and **NDEPWLEXP**, then these parameters are used for static operation (IV) and **NDEPCVWL** and **NDEPCVWLEXP** parameters are used for dynamic operation (CV).
- In *strong-inversion* region, the parameters which are used to model the effect of mobility reduction due to vertical field in small channel devices, namely **UAWL**, **UAWLEXP**, **EUWL** and **EUWLEXP**, are extracted.

Saturation

- Focusing in *strong-inversion* region, the parameters which are used to model to the velocity saturation effect in small channel devices, i.e. **VSATWL** and **VSATWLEXP**, can be extracted.

In order to validate that the values of the parameters, modeling the behavior of narrow/short channel devices, are correctly extracted, it is useful to check I_D vs. V_D and g_{ds} vs. V_D characteristics @ various V_G , $V_S = 0\text{ V}$ & $V_B = 0\text{ V}$ and, if needed, to fine tune the values of the parameters.

10.4.3 C_{GG} vs. V_G Analysis @ $V_{DS} \neq 0\text{ V}$ & $V_B = 0\text{ V}$

The extraction of the parameters, which are used to model to the velocity saturation effect in small channel devices, **VSATWL** and **VSATWEXP**, from I_D vs. V_G and I_D vs. V_D characteristics (Step 10.4.2) should be sufficient in order to capture VS for

CV operation. To verify that, C_{GG} vs. V_G characteristic of all devices, for different $V_{DS} \neq 0 V$, from linear mode to saturation, must be studied. If different values for **VSATWL** and **VSATWLEXP** are necessary for accurate fitting of the CV behavior for both sets of devices, then **VSATCVWL** and **VSATCVWLEXP** can be used.

10.4.4 Drain Current I_D vs. V_G Analysis @ $V_D = [V_{D,lin}, V_{D,sat}]$ & various V_B (or various V_S)

In this step, from *weak-inversion* region of *linear mode*, **K2WL** and **K2WLEXP**, which are linked to the V_{TH} shift due to vertical non-uniform doping in small channel devices, can be extracted. For validation purposes, it is useful to check: i) I_D vs. V_G and g_m vs. V_G characteristics in *weak* and *strong-inversion* and for both *linear mode* and *saturation*, and ii) I_D vs. V_D and g_{ds} vs. V_D characteristics @ various V_G & $V_B \neq 0 V$ (or $V_S \neq 0 V$) and, if needed, extract **K2WL** and **K2WLEXP** to fit both (i) and (ii).

10.4.5 Fitting Verification

When all the steps for narrow/short channel devices have been performed, the fitting of the model should be checked for all the analyses carried out in Section 10.4 and parameters can be fine tuned for better fitting.

10.5 Extraction of Impact Ionisation parameters

10.5.1 Extraction in Intrinsic region

- When V_{DS} is low and V_{GS} is above threshold, the parameters **ALPHA0**, **BETA0** are extracted in the intrinsic region (first peak of impact ionization).
- When V_{DS} is high and V_{GS} is above threshold, the parameters **ALPHA0**, **BETA0**, **BETA1**, **BETA2**, **BETA3** are extracted in the intrinsic region (first peak of impact ionization).
- Parameters linked with body effect in intrinsic region, **ALPHA1** and **ALPHA2**, are then extracted.

10.5.2 Extraction in Drift region

- When V_{DS} is moderate to high, and V_{GS} is high, the parameters **ALPHADR**, **BETADR**, **DRII1**, **DRII2**, and **DRII3** are extracted in the drift region (second peak of impact ionization).
- Parameters linked with body effect in drift region, **ALPHADR1** and **ALPHADR2**, are then extracted.

10.6 Extraction of Conductivity Modulation parameters for HV FETs

- When V_{DS} and V_{GS} are both high, conductivity modulation effect occurs in the device. Use **RBODYMOD** = 2 (without specifying **RBPS0** or **RBD0**) and extract the parameter **CMD1** for charge carrier concentration increment and internal voltage change.
- The parameters **CMD2** and **DRII4** can be used for additional fine-tuning of increase in charge carrier concentration and internal voltage change, respectively.
- The resistance **RBPB** can be tuned to change the voltage drop V_{bcm} .

10.7 Extraction of Temperature Dependence Parameters

Up to this point of the parameter extraction procedure, the temperature dependence of the parameters has been ignored since all the parameters were extracted at **TNOM**. In this part, the parameters that are related to the impact of temperature on the behavior of devices are extracted, and for that, data across the temperature range of the technology are necessary. The behavior of devices is studied with the same geometrical sequence as the previous steps, while the temperature dependence parameters are extracted in the same regions of operation as the parameters of the corresponding physical effects.

10.7.1 Wide & Long Channel Devices

The first step, in the extraction of temperature dependence parameters, is to extract the behavior of a long and wide channel device @ different **T** and for different analy-

ses. It is recommended that the same device as the one in Section 10.1 is used. In detail:

I_D vs. V_G analysis @ $V_D = V_{D,lin}$, $V_S = 0 V$ & $V_B = 0 V$

- From *weak-inversion* region (I_D vs. V_G characteristic when y-axis is in logarithmic scale), the parameters **TBGASUB** and **TBGBSUB**, which control the temperature dependence of E_g , are extracted. Also, **TNFACTOR** is extracted in order to fit the sub-threshold slope of I_D in different T, while **KT1** and **KT1EXP** are extracted for fitting the V_{TH} across T.
- From *strong-inversion* region, the mobility temperature exponent, **UTE** and the temperature coefficients: i) for mobility reduction due to vertical field effect, namely **UA1** and **UD1**, ii) for coulomb scattering effect, **UCSTE** and iii) for S/D series resistances, **PRT**, are extracted.

I_D vs. V_G analysis @ $V_D = V_{D,sat}$, $V_S = 0 V$ & $V_B = 0 V$

- From *strong-inversion* region, the parameters that are used to model to the temperature dependence of velocity saturation effect, i.e. **AT** and **PTWGT**, are extracted.

It is very important that in the above analyses both I_D and g_m of all the devices are studied at once. Furthermore, from *accumulation* to *depletion* region, in both *linear mode* and *saturation* of I_D vs. V_G analysis, the parameter **TGIDL**, which controls the temperature dependence of GIDL effect, is extracted.

I_D vs. V_D Analysis @ various V_G , $V_S = 0 V$ & $V_B = 0 V$

From I_D vs. V_D analysis in different temperatures, **TDELTA**, which is related to the temperature dependence of the smoothing factor for the transition between V_{DS} and $V_{DS,sat}$, is extracted.

I_D vs. V_G Analysis @ $V_D = V_{D,lin}$ & various V_B (or various V_S)

- From weak-inversion region (I_D vs. V_G characteristic when y-axis is in logarithmic scale) **KT2**, which is linked to the temperature dependence of V_{TH} shift due to vertical non-uniform doping with V_B (or V_S) bias, is extracted.

- From *strong-inversion* region, the temperature coefficient for mobility reduction with V_B (or V_S) bias, namely **UC1**, is extracted.

For validation purposes, it is useful to check: i) I_D vs. V_G and g_m vs. V_G characteristics in *weak* and *strong-inversion* and for both *linear mode* and *saturation*, and ii) I_D vs. V_D and g_{ds} vs. V_D characteristics @ various V_G & $V_B \neq 0$ V (or $V_S \neq 0$ V) and, if needed, extract **KT2** and **UC1** to fit both (i) and (ii).

10.7.2 Length Scaling of Wide Channel Devices

The following step in the extraction of temperature dependence parameters, is to study the temperatures dependences across L. For this, data @ **different T** of a set of devices with constant **wide** channel but different channel lengths are used.

I_D vs. V_G analysis @ $V_D = V_{D,lin}$, $V_S = 0$ V & $V_B = 0$ V

- From *weak-inversion* region (I_D vs. V_G characteristic when y-axis is in logarithmic scale), the parameter **KT1L** is extracted for fitting the V_{TH} across L, at different T.
- From *strong-inversion* region, the length scaling parameters for: i) mobility temperature exponent, **UTEL** and for the temperature coefficients or mobility reduction due to vertical field effect, namely **UA1L** and **UD1L**, are extracted.

I_D vs. V_G analysis @ $V_D = V_{D,sat}$, $V_S = 0$ V & $V_B = 0$ V

- From *weak-inversion* region (I_D vs. V_G characteristic when y-axis is in logarithmic scale), the parameter **TETA0**, which is related to the temperature dependence of DIBL effect and thus is controlling the V_{TH} in saturation, is extracted.
- From *strong-inversion* region, the parameters that are used to model the temperature dependence of velocity saturation effect across L, i.e. **ATL** and **PTWGTL**, are extracted.

It is very important that in the above analyses both I_D and g_m of all the devices are studied at once. For validating that the values of length scaling parameters for temperature dependence parameters are extracted correctly, it is useful to check also I_D vs. V_D and g_{ds} vs. V_D characteristics and, if needed, to fine tune their value by repeating Step 10.7.2.

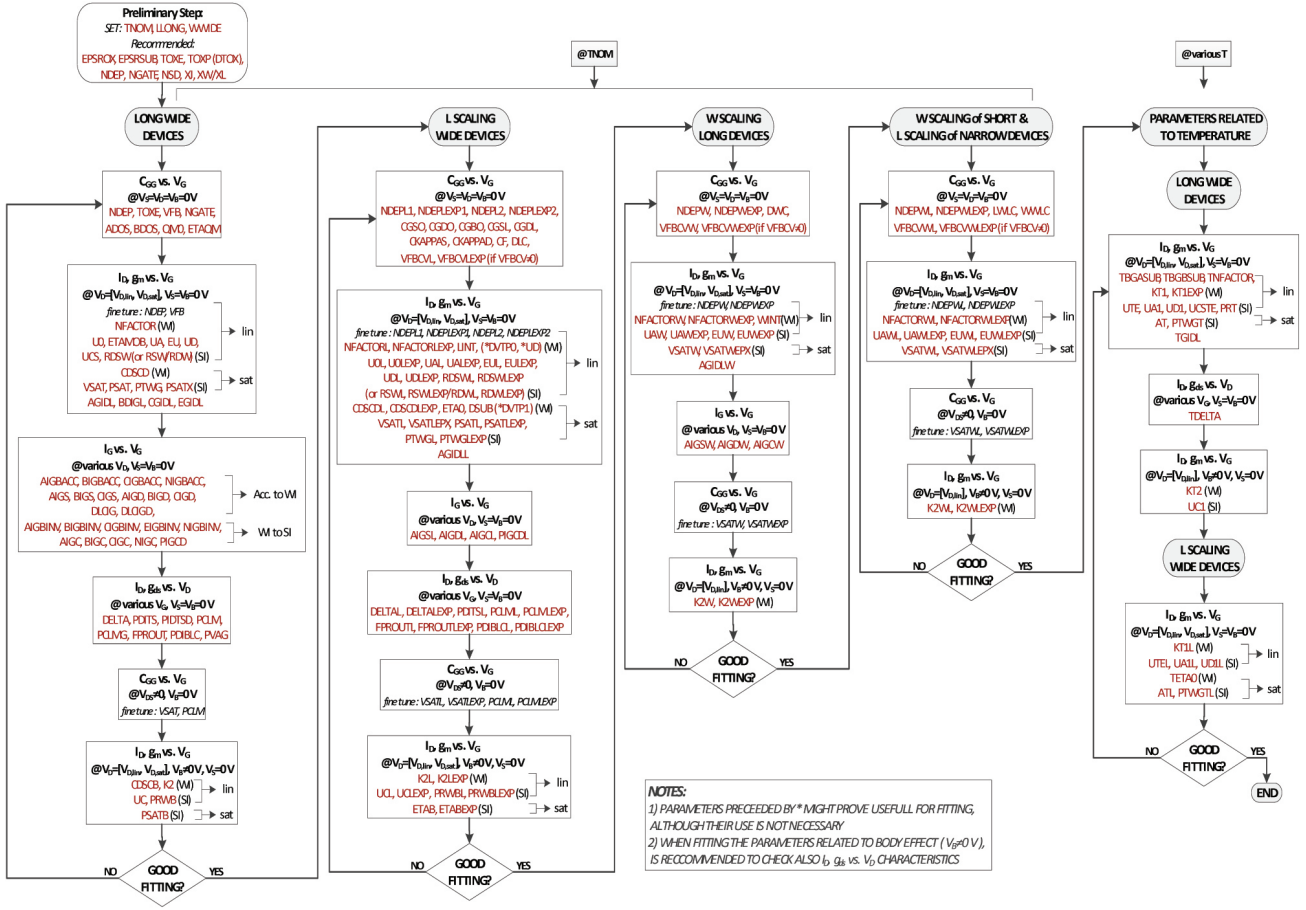


Figure 20: Parameters Extraction Procedure.

11 Instance Parameters

Name	Unit	Default	Min	Max	Description
L	m	10u	-	-	Designed Gate Length
W	m	10u	-	-	Designed Gate Width (per finger)
NF	-	1	1	-	Number of fingers
NRS	-	1	-	-	Number of source diffusion squares
NRD	-	1	-	-	Number of drain diffusion squares
VFBSDOFF	V	0	-	-	Source-Drain flat band offset
MINZ	-	0	0	1	Minimize either no. of drain or source ends
RGATEMOD	-	0	0	2	Gate resistance model selector
RBODYMOD	-	0	0	2	Substrate resistance network model selector
GEOMOD	-	0	0	10	Geometry-dependent parasitic model selector-specifying how the end S/D diffusion are connected
RGEOMOD	-	0	0	8	Bias independent parasitic resistance model selector
RBPB	Ohm	50	1mV	-	Resistance between bNodePrime and bNode
RBPD	Ohm	50	1mV	-	Resistance between bNodePrime and dbNode
RBPS	Ohm	50	1mV	-	Resistance between bNodePrime and sbNode
RBDB	Ohm	50	1mV	-	Resistance between dbNode and bNode
RBSB	Ohm	50	1mV	-	Resistance between sbNode and bNode
RDB	Ohm	50	1mV	-	Resistance between ddbulk node and d node when RBODYHVMOD=1
SA	m	0	0	-	Distance between OD edge from Poly from one side
SB	m	0	0	-	Distance between OD edge from Poly from other side
SD	m	0	0	-	Distance between neighboring fingers
SCA	-	0	0	-	Integral of the first distribution function for scattered well dopant
SCB	-	0	0	-	Integral of second distribution function for scattered well dopant

SCC	-	0	0	-	Integral of third distribution function for scattered well dopant
SC	m	0	0	-	Distance to a single well edge
AS	m^2	0	0	-	Source to Substrate Junction Area
AD	m^2	0	0	-	Drain to Substrate Junction Area
PS	m	0	0	-	Source to Substrate Junction Perimeter
PD	m	0	0	-	Drain to Substrate Junction Perimeter

12 Model Controllers and Process Parameters

Note: binnable parameters are marked as: ^(b)

Name	Unit	Default	Min	Max	Description and Scaling Parameters
TYPE	-	1	-1	1	NMOS=1, PMOS=-1
CVMOD	-	0	0	1	IV-CV: Consistent:0, Different:1
GEOMOD	-	0	0	10	For description, please refer Table 1
RGEOMOD	-	0	0	8	Bias independent parasitic resistance model selector, refer Table 2
RGATEMOD	-	0	0	2	Gate resistance Model selector
ASYMMOD	-	0	0	1	Asymmetry model will be ON or OFF
MOBSCALE	-	0	0	1	Two different models for mobility.
RBODYMOD	-	0	0	2	Substrate resistance network model selector
RBODYHVMOD	-	0	0	1	HV substrate resistance network model selector
RDSMOD	-	0	0	2	0: Bias dependent internal, independent external, 1: External RDS, 2: Internal RDS
COVMOD	-	0	0	1	Bias-independent overlap capacitance:0, Bias-dependent overlap capacitance:1
GIDLMOD	-	0	0	1	Turn off GIDL model:0, Turn-on GIDL model:1
SHMOD	-	0	0	1	Turn off Self Heating model:0, Turn-on :1

PERMOD	-	1	0	1	Whether PS/PD (when given) includes the gate-edge perimeter 1: (including the gate-edge perimeter) 0: (not including the gate-edge perimeter)
GADRIFT	-	0	0	1	Turn off high Vg and High Vd tunning for HV devices:0, Turn-on :1
TNOIMOD	-	0	0	1	Thermal noise model selector
FNOIMOD	-	0	0	1	Flicker noise model selector
BINUNIT	-	1	0	1	Binning unit selector
XL	m	0	-	-	L offset for channel length due to mask/etch effect
XW	m	0	-	-	W offset for channel length due to mask/etch effect
LINT ^(b)	m	0	-	-	Length reduction parameter (dopant diffusion effect)
WINT ^(b)	m	0	-	-	Width reduction parameter (dopant diffusion effect)
DLC ^(b)	m	0	-	-	Length reduction parameter for CV (dopant diffusion effect)
DWC ^(b)	m	0	-	-	Width reduction parameter for CV (dopant diffusion effect)
TOXE	m	3.0n	-	-	SiO_2 equivalent gate dielectric thickness
TOXP	m	TOXE	-	-	Physical dielectric thickness
DTOX	m	0.0	-	-	Difference between effective dielectric thickness and physical thickness
NDEP ^(b)	m^{-3}	1e24	-	-	channel (body) doping concentration. Global Scaling Parameters - NDEPL1, NDEPLEXP1, NDEPL2, NDEPLEXP2, NDEPW, NDEPWEXP, NDEPWL, NDEPWLEXP
NSD ^(b)	m^{-3}	1e26	2e25	1e27	S/D doping concentration
EASUB	eV	4.05	-	-	Electron affinity of substrate
NGATE ^(b)	m^{-3}	5e25	-	-	parameter for Poly Gate doping. Set NGATE = 0 for metal gates

VFB ^(b)	<i>V</i>	-0.5	-	-	Flat band Voltage
EPSROX	-	3.9	1	-	relative dielectric constant of the gate insulator
EPSRSUB	-	11.9	1	-	relative dielectric constant of the channel material
NI0SUB	m^{-3}	1.1e16	-	-	intrinsic carrier concentration of channel at 300.15K
XJ ^(b)	<i>m</i>	1.5e-7	-	-	S/D junction depth
DMCG	<i>m</i>	0	0	-	Distance of Mid-Contact to Gate edge
DMCI	<i>m</i>	DMCG	0	-	Distance of Mid-Contact to Isolation
DMDG	<i>m</i>	0	0	-	Distance of Mid-Diffusion to Gate edge
DMCGT	<i>m</i>	0	0	-	Distance of Mid-Contact to Gate edge in Test

13 Basic Model Parameters

Note: binnable parameters are marked as: ^(b)

Name	Unit	Default	Min	Max	Description
LLONG	m	$10\mu m$	-	-	Length of extracted long channel device
WWIDE	m	$10\mu m$	-	-	Width of extracted long channel device
ASYMP	-	0.6	-	-	Tuning parameter for Asymmetry mode
CIT ^(b)	F/m^2	0	-	-	Interface trap capacitance
NFACTOR ^(b)		0	-	-	Subthreshold Swing factor. Global Scaling Parameters - NFACTORL, NFACTORLEXP, NFACTORW, NFACTORWEXP, NFACTORWL
CDSCD ^(b)	$F/m^2/V$	1e-9	-	-	Drain-bias sensitivity of Subthreshold Swing. Global Scaling Parameters - CDSCDL, CDSCDLEXP
CDSCB ^(b)	$F/m^2/V$	1e-9	-	-	Drain-bias sensitivity of Subthreshold Swing. Global Scaling Parameters - CDSCBL, CDSCBLEXP
CDSCBR ^(b)	$F/m^2/V$	CDSCD	0.0	-	Reverse-mode drain-bias sensitivity. Global Scaling Parameter - CDSCDLR
CDSCDR ^(b)	$F/m^2/V$	1e-9	-	-	Drain-bias sensitivity of Subthreshold Swing. Global Scaling Parameters - CDSCDR, LCDSCDR
DVTP0 ^(b)	m	1e-10	-	-	Coefficient of drain-induced V_{th} shift for long channel devices with pocket implant
DVTP1 ^(b)	$1/V$	0	-	-	Coefficient of drain-induced V_{th} shift for long channel devices with pocket implant
DVTP2 ^(b)	$m * V$	0	-	-	Coefficient of drain-induced V_{th} shift for long channel devices with pocket implant

DVTP3 ^(b)	-	0	-	-	Coefficient of drain-induced V_{th} shift for long channel devices with pocket implant
DVTP4 ^(b)	$1/V$	0	-	-	Coefficient of drain-induced V_{th} shift for long channel devices with pocket implant
DVTP5 ^(b)	V	0	-	-	Coefficient of drain-induced V_{th} shift for long channel devices with pocket implant
PHIN ^(b)	V	0.045	-	-	Vertical nonuniform doping effect on surface potential
K2 ^(b)	V	0	-	-	V_{th} shift due to nonuniform vertical doping. Global Scaling Parameters - K2L, K2LEXP, K2W, K2WEXP
K1 ^(b)	$V^{0.5}$	0	-	-	V_{th} shift due to nonuniform vertical doping. Global Scaling Parameters - K1L, K1LEXP, K1W, K1WL, K1WEXP, K1WLEXP
ETA0 ^(b)	-	0.08	-	-	DIBL coefficient
ETA0R ^(b)	-	0.08	-	-	DIBL coefficient
DSUB ^(b)	-	0.375	> 0	-	DIBL exponent coefficient
ETAB ^(b)	$1/V$	-0.07	-	-	Body bias sensitivity to DIBL effect. Global Scaling Parameters - ETABEXP
U0 ^(b)	$m^2/V/s$	67e-3	-	-	Low field mobility. Global Scaling Parameters - U0L, U0LEXP
ETAMOB	-	1.0	-	-	effective field parameter
UA ^(b)	$(m/V)^{EU}$	0.001	> 0.0	-	Phonon / surface roughness scattering parameter. Global Scaling Parameters - UAL, UALEXP, UAW, UAWEXP, UAWL
EU ^(b)	-	1.5	> 0.0	-	Phonon / surface roughness scattering parameter. Global Scaling Parameters - EUL, EULEXP, EUW, EUWEXP, EUWL

UD ^(b)	-	0.001	> 0.0	-	Columbic scattering parameter. Global Scaling Parameters - UDL, UDLEXP
UCS ^(b)	-	2.0	1	2	Columbic scattering parameter.
UC ^(b)	$(m/V)^{EU}/V$	0.0	-	-	Body-bias sensitivity on mobility. Global Scaling Parameters - UCL, UCLEXP
VSAT ^(b)	m/s	1e6	-	-	Saturation velocity. Global Scaling Parameters - VSATL, VSALEXP, VSATW, VSATWEXP
VSATR ^(b)	m/s	1e6	-	-	Saturation velocity. Global Scaling Parameters - VSATR, LVSATR, WVSATR, PVSATR
DELTA ^(b)	-	0.125	> 0	0.5	Smoothing factor for Vds to Vdsat. Global Scaling Parameters - DELTAL, DELTALEXP
AVDSX	-	0.16	> 0	-	Smoothing factor for Vdsx calculation.
PSAT ^(b)	-	1.0	0.25	1.0	Velocity saturation exponent. Global Scaling Parameters - PSATL, PSATL-EXP
PTWG ^(b)	-	0	-	-	Correction factor for velocity saturation in forward mode. Global Scaling Parameters - PTWGL, PTWGLEXP
PTWGR ^(b)	-	PTWG	-	-	Correction factor for velocity saturation in reverse mode. Global Scaling Parameters - PTWGLR, PTWGLEXP
A1 ^(b)	V^{-2}	0.0	-	-	Non-saturation effect parameter in strong inversion region.
A2 ^(b)	V^{-1}	0.0	-	-	Non-saturation effect parameter in moderate inversion region.
PSATX	-	1	0.25	4	Fine tuning of PTWG effect
PSATB ^(b)	$1/V$	0	-	-	Velocity saturation exponent for non-zero V_{bs}

PCLM ^(b)	-	0.00	-	-	Channel Length Modulation (CLM) parameter. Global Scaling Parameters - PCLML, PCLMLEXP
PCLMG	V	0	-	-	Gate bias dependent parameter for channel Length Modulation (CLM)
PSCBE1 ^(b)	V/m	4.24e8	-	-	Substrate current body-effect coefficient
PSCBE2 ^(b)	m/V	1.0e-8	-	-	Substrate current body-effect coefficient
PDITS ^(b)	$1/V$	0	-	-	Drain-induced Vth shift
PDITSL	$1/m$	0	-	-	L dependence of Drain-induced Vth shift
PDITSD ^(b)	$1/V$	0	-	-	VDS dependence of Drain-induced Vth shift
RSWMIN ^(b)	Ωum^{WR}	0.0	0.0	-	source extension resistance per unit width at high V_{gs}
RSW ^(b)	Ωum^{WR}	10	0.0	-	Zero bias source extension resistance per unit width. Global Scaling Parameters - RSWL, RSWLEXP
RDWMIN ^(b)	Ωum^{WR}	0.0	0.0	-	Drain extension resistance per unit width at high V_{gs}
RDW ^(b)	Ωum^{WR}	10	0.0	-	Zero bias drain extension resistance per unit width. Global Scaling Parameters - RDWL, RDWLEXP
RDSWMIN ^(b)	Ωum^{WR}	0.0	0.0	-	LDD resistance per unit width at high V_{gs} for RDSTMOD = 0
RDSW ^(b)	Ωum^{WR}	10	0.0	-	Zero bias LDD resistance per unit width for RDSTMOD=0. Global Scaling Parameters - RDSWL, RDSWLEXP
PRWG ^(b)	V^{-1}	1	0	-	gate bias dependence of S/D extension resistance
PRWB ^(b)	V^{-1}	0	0	-	body bias dependence of S/D extension resistance. Global Scaling Parameters - PRWBL, PRWBLEXP

WR ^(b)	-	1.0	-	-	W dependence parameter of S/D extension resistance
RSH	Ω	0	0	-	Sheet resistance
PDIBLC ^(b)	-	2e-4	0	-	DIBL effect on Rout. Global Scaling Parameters - PDIBLCL, PDIBLCLEXP
PDIBLCB ^(b)	$1/V$	0	0	-	Body-bias sensitivity on DIBL
PVAG ^(b)	-	1	-	-	V_{gs} dependence on early voltage
FPROUT ^(b)	$V/m^{0.5}$	0	0	-	g_{ds} degradation factor due to pocket implant. Global Scaling Parameters - FPROUTL, FPROUTLEXP
ABULK	-	1	1	2	For flexibility of tuning Cgg in strong inversion
A0	-	0	-	-	Gate bias dependent parameter for ABULK
AGS	-	0	-	-	Gate bias dependent parameter for ABULK
KETA	-	0	-	-	Body bias dependent parameter for ABULK
AGS1	-	1	-	-	Parameter for Non linearity of Source charge
AGIDL ^(b)	V/m	0	-	-	Pre-exponential coefficient for GIDL. Global Scaling Parameters - AGIDLL, AGIDLW
BGIDL ^(b)	V/m	2.3e-9	-	-	exponential coefficient for GIDL
CGIDL ^(b)	V/m	0.5	-	-	exponential coefficient for GIDL
EGIDL ^(b)	V	0.8	-	-	band bending parameter for GIDL
AGISL ^(b)	V/m	0	-	-	Pre-exponential coefficient for GISL (AGISL < 0 means GISL parameters will same as GIDL parameters). Global Scaling Parameters - AGISLL, AGISLW
BGISL ^(b)	V/m	2.3e-9	-	-	exponential coefficient for GISL

CGISL ^(b)	V/m	0.5	-	-	exponential coefficient for GISL
EGISL ^(b)	V	0.8	-	-	band bending parameter for GISL
ALPHA0 ^(b)	m/V	0.0	-	-	First parameter of impact ionization current. Global Scaling Parameters - ALPHA0L, ALPHA0LEXP
ALPHA0R ^(b)	m/V	ALPHA0	-	-	First parameter of reverse mode impact ionization current in intrinsic region. Global Scaling Parameters - LAL-PHA0R, WALPHA0R, PALPHA0R
BETA0 ^(b)	$1/V$	0.0	-	-	V_{ds} dependent parameter of impact ionization current
BETA0R ^(b)	$1/V$	BETA0	-	-	V_{ds} dependent parameter of reverse mode impact ionization current in intrinsic region
AIGC ^(b)	$(Fs^2/g)^{0.5}/m$	1.36e-2 (NMOS) and 9.8e-3 (PMOS)	-	-	Parameter for I_{gcs} and I_{gcd} . Global Scaling Parameters - AIGCL, AIGCW
BIGC ^(b)	$(Fs^2/g)^{0.5}/m/V$	1.71e-3 (NMOS) and 7.59e-4 (PMOS)	-	-	Parameter for I_{gcs} and I_{gcd}
CIGC ^(b)	$1/V$	0.075 (NMOS) and 0.03 (PMOS)	-	-	Parameter for I_{gcs} and I_{gcd}
AIGS ^(b)	$(Fs^2/g)^{0.5}/m$	1.36e-2 (NMOS) and 9.8e-3 (PMOS)	-	-	Parameter for I_{gs} . Global Scaling Parameters - AIGSL, AIGSW

BIGS ^(b)	$(Fs^2/g)^{0.5}/m/V$	1.71e-3 (NMOS) and 7.59e-4 (PMOS)	-	-	Parameter for I_{gs}
CIGS ^(b)	$1/V$	0.075 (NMOS) and 0.03 (PMOS)	-	-	Parameter for I_{gs}
DLCIG ^(b)	m	LINT	-	-	Source/Drain overlap length for I_{gs}
AIGD ^(b)	$(Fs^2/g)^{0.5}m$	1.36e-2 (NMOS) and 9.8e-3 (PMOS)	-	-	Parameter for I_{gd} . Global Scaling Parameters - AIGDL, AIGDW
BIGD ^(b)	$(Fs^2/g)^{0.5}m/V$	1.71e-3 (NMOS) and 7.59e-4 (PMOS)	-	-	Parameter for I_{gd}
CIGD ^(b)	$1/V$	0.075 (NMOS) and 0.03 (PMOS)	-	-	Parameter for I_{gd}
DLCIGD ^(b)	m	DLCIG	-	-	Source/Drain overlap length for I_{gd}
POXEDGE ^(b)	-	1.0	-	-	Factor for the gate oxide thickness in source/drain overlap regions
PIGCD ^(b)	-	1.0	-	-	V_{ds} dependence of I_{gcs} and I_{gcd} . Global Scaling Parameters - PIGCDL, PIGCDLEXP
NTOX ^(b)	-	1.0	-	-	Exponent for the gate oxide ratio
TOXREF	m	3.0e-9	-	-	Nominal gate oxide thickness for gate dielectric tunneling current model only
VFBSDOFF ^(b)	V	0.0	-	-	Flatband Voltage Offset Parameter

NDEPCV ^(b)	m^{-3}	NDEP	-	-	channel (body) doping concentration for CV. Global Scaling Parameters - NDEPCVL1, NDEPCVLEXP1, NDEPCVL2, NDEPCVLEXP2, NDEPCVW, NDEPCVWEXP, NDEPCVWL, NDEPCVWLEXP
VFBCV ^(b)	V	VFB	-	-	channel (body) doping concentration for CV. Global Scaling Parameters - VFBCVL, VFBCVLEXP, VFBCVW, VFBCVWEXP, VFBCVWL, VFBCVWLEXP
VSATCV ^(b)	m/s	VSAT	-	-	Saturation velocity for CV. Global Scaling Parameters - VSATCVL, VSACVL-EXP, VSATCVW, VSATCVWEXP
PCLMCV ^(b)	-	PCLM	-	-	Channel Length Modulation (CLM) parameter for CV. Global Scaling Parameters - PCLMCVL, PCLMCVLEXP
A0CV	-	A0	-	-	For flexibility of tuning Cgg in strong inversion
AGSCV	-	AGS	-	-	For flexibility of tuning Cgg in strong inversion
KETACV	-	KETACV	-	-	For flexibility of tuning Cgg in strong inversion
DELVFBACC	V	0	-	-	VFB shift in the accumulation region, valid for CVMOD=1 only
CF ^(b)	F/m	0	0.0	-	Outer fringe cap
CFRCOEFF ^(b)	F/m	1	1	-	Outer fringe cap coefficient
CGSO	F/m	calculated	0.0	-	Non LDD region source-gate overlap capacitance per unit channel width
CGDO	F/m	calculated	0.0	-	Non LDD region drain-gate overlap capacitance per unit channel width
CGSL ^(b)	F/m	0	0.0	-	Overlap capacitance between gate and lightly-doped source region

CGDL ^(b)	F/m	0	0.0	-	Overlap capacitance between gate and lightly-doped drain region
CKAPPAS ^(b)	V	0.6	0.02	-	Coefficient of bias-dependent overlap capacitance for the source side
CKAPPAS1	-	1e6	-	-	Coefficient of bias-dependent overlap capacitance for the source side
CKAPPAS2	-	1	-	-	Coefficient of bias-dependent overlap capacitance for the source side
CKAPPAD ^(b)	V	0.6	0.02	-	Coefficient of bias-dependent overlap capacitance for the drain side
CKAPPAD1	-	1e6	-	-	Coefficient of bias-dependent overlap capacitance for the drain side
CKAPPAD2	-	1	-	-	Coefficient of bias-dependent overlap capacitance for the drain side
CGBO	F/m	0	0.0	-	Gate-substrate overlap capacitance per unit channel length
ADOS	-	0	0	-	Quantum mechanical effect prefactor cum switch in inversion
BDOS	-	1.0	0	-	Charge centroid parameter - slope of CV curve under QME in inversion
K0 ^(b)	-	0	0	-	Non-saturation effect parameter for strong inversion region
M0 ^(b)	-	1.0	0	-	Offset of non-saturation effect parameter for strong inversion region
C0 ^(b)	V	0	-	-	Lateral NUD1 voltage parameter
C0SI ^(b)	V	1.0	0	-	Correction factor for strong inversion used in Mnud1
C0SISAT ^(b)	V	1.0	0	-	Correction factor for saturation region used in Mnud1
QM0	-	1e-3	> 0.0	-	Charge centroid parameter - starting point for QME in inversion
ETAQM	-	0.0	0	-	Bulk charge coefficient for charge centroid in inversion

DLBIN	-	0.0	-	-	Length reduction parameter for binning
DWBIN	-	0.0	-	-	Width reduction parameter for binning
LMLT	-	1.0	> 0.0	-	Length shrinking factor
WMLT	-	1.0	> 0.0	-	Width shrinking factor

14 Both model and instance parameters

Name	Unit	Default	Min	Max	Description
DTEMP	K	0.0	-	-	Offset of Device Temperature
MULU0	$m^2/V/s$	1.0	-	-	Multiplication factor for low field mobility
DELVTO	V	0	-	-	Zero bias threshold voltage variation
IDS0MULT	-	1.0	-	-	Variability in drain current for miscellaneous reasons
XGW	m	0	0	-	Distance from gate contact center to device edge
NGCON	-	1	1	2	Number of gate contacts
EDGEFET(also an instance and model parameter)		1	-	-	Edge FET model Flag: 0: Disable 1: Enable
SSLMOD(also an instance and model parameter)		1	-	-	Sub-Surface Leakage Drain Current, 0: Turn off 1: Turn on

15 High-Speed/RF Model Parameters

Name	Description	Default
XRCRG1 (b)	Parameter for distributed channel-resistance effect for both intrinsic-input resistance and charge-deficit NQS models(Warning message issued if binned $XRCRG1 \leq 0.0$) distributed channel-resistance effect for both intrinsic-input resistance and charge-deficit NQS models(Warning message issued if binned $XRCRG1 \leq 0.0$)	12.0
XRCRG2 (b)	Parameter to account for the excess channel diffusion resistance for both intrinsic input resistance and charge-deficit NQS models	1.0
RBPB (Also an instance parameter)	Resistance connected between bNodePrime and bNode	50.0ohm
RBPD (Also an instance parameter)	Resistance connected between bNodePrime and dbNode (If less than 1.0e-3ohm, reset to 1.0e-3ohm)	50.0ohm
RBPS (Also an instance parameter)	Resistance connected between bNodePrime and sbNode (If less than 1.0e-3ohm, reset to 1.0e-3ohm)	50.0ohm
RBDB (Also an instance parameter)	Resistance connected between dbNode and bNode	50.0ohm
RBSB (Also an instance parameter)	Resistance connected between sbNode and bNode	50.0ohm
GBMIN	Conductance in parallel with each of the five substrate resistances to avoid potential numerical instability due to unreasonably too large a substrate resistance (Warning message issued if less than 1.0e-20 mho)	1.0e-12mho
RBPS0	Scaling prefactor for RBPS	50 Ohms
RBPSL	Length Scaling parameter for RBPS	0.0
RBPSW	Width Scaling parameter for RBPS	0.0
RBPSNF	Number of fingers Scaling parameter for RBPS	0.0

RBPD0	Scaling prefactor for RBPD	50 Ohms
RBDL	Length Scaling parameter for RBPD	0.0
RBDW	Width Scaling parameter for RBPD	0.0
RBDNF	Number of fingers Scaling parameter for RBPD	0.0
RBPBX0	Scaling prefactor for RBPBX	100 Ohms
RBPBXL	Length Scaling parameter for RBPBX	0.0
RBPBXW	Width Scaling parameter for RBPBX	0.0
RBPBXNF	Number of fingers Scaling parameter for RBPBX	0.0
RBPBY0	Scaling prefactor for RBPBY	100 Ohms
RBPBYL	Length Scaling parameter for RBPBY	0.0
RBPBYW	Width Scaling parameter for RBPBY	0.0
RBPBYNF	Number of fingers Scaling parameter for RBPBY	0.0
RBSBX0	Scaling prefactor for RBSBX	100 Ohms
RBSBY0	Scaling prefactor for RBSBY	100 Ohms
RBDBX0	Scaling prefactor for RBDBX	100 Ohms
RBDBY0	Scaling prefactor for RBDBY	100 Ohms
RBSDBXL	Length Scaling parameter for RBSBX and RBDBX	0.0
RBSDBXW	Width Scaling parameter for RBSBX and RBDBX	0.0
RBSDBXNF	Number of fingers Scaling parameter for RBSBX and RBDBX	0.0
RBSDBYL	Length Scaling parameter for RBSBY and RBDBY	0.0
RBSDBYW	Width Scaling parameter for RBSBY and RBDBY	0.0
RBSDBYNF	Number of fingers Scaling parameter for RBSBY and RBDBY	0.0

16 Flicker and Thermal Noise Model Parameters

Parameter Name	Description	Default Value
NOIA	Flicker noise parameter A	$6.25e41(eV)^{-1}s^{1-EF}m^{-3}$ for NMOS; $6.188e40(eV)^{-1}s^{1-EF}m^{-3}$ for PMOS
NOIB	Flicker noise parameter B	$3.125e26(eV)^{-1}s^{1-EF}m^{-1}$ for NMOS; $1.5e25(eV)^{-1}s^{1-EF}m^{-1}$ for PMOS
NOIC	Flicker noise parameter C	$8.75(eV)^{-1}s^{1-EF}m$
NOIA3	Flicker noise parameter for extra tuning flexibility in sub-threshold region	$0(eV)^{-1}s^{1-EF}m^{-3}$
MPOWER	Sub-threshold to strong inversion transition slope Parameter	1.2
QSREF	Charge at threshold condition	$50m\text{ }Cm^{-2}$
SPFN	Smoothing Parameter for FN model	2
NOIA1	Flicker noise fitting parameter in strong inversion	0
NOIAX	Flicker noise fitting parameter in strong inversion for high VDS	1
NOIA2	Flicker noise parameter A for Halo model	NOIA
LH	Length of Halo	10nm
EM	Saturation field	$4.1e7V/m$
EF	Flicker noise frequency exponent	1.0
AFNS	Flicker noise exponent for source resistance	2.0
BFNS	Flicker noise frequency exponent for source resistance	1.0
KFNS	Flicker noise coefficient for source resistance	0
AFND	Flicker noise exponent for drain resistance	2.0
BFND	Flicker noise frequency exponent for drain resistance	1.0
KFND	Flicker noise coefficient for drain resistance	0
LINTNOI	Length Reduction Parameter Offset	0.0 m

NTNOI	Noise factor for short-channel devices for TNOIMOD=0 only	1.0
TNOIA	Coefficient of channel-length dependence of total channel thermal noise	1.5
TNOIB	Channel-length dependence parameter for channel thermal noise partitioning	3.5
TNOIC	Length dependent parameter for Correlation Coefficient	0
RNOIA	Thermal Noise Coefficient	0.577
RNOIB	Thermal Noise Coefficient	0.5164
RNOIC	Correlation Coefficient parameter	0.395
RNOIK	Exponential coeff. for enhanced correlated thermal noise	0.0
TNOIK	Empirical parameter for Leff trend of Sid at low Ids	0.0
TNOIK2	Empirical parameter for sensitivity of RNOIK	0.1

17 Layout-Dependent Parasitic Model Parameters

Parameter Name	Description	Default Value
DMCG	Distance from S/D contact center to the gate edge	0.0m
DMCI	Distance from S/D contact center to the isolation edge in the channel-length direction	DMCG
DMDG	Same as DMCG but for merged device only	0.0m
DMCGT	DMCG of test structures	0.0m
NF (instance parameter only)	Number of device fingers (Fatal error if less than one)	1
DWJ	Offset of the S/D junction width	DWC (in CVmodel)
MIN (instance parameter only)	Whether to minimize the number of drain or source diffusions for even-number fingered device	0 (minimize the drain diffusion number)
XGW(Also an instance and model parameter)	Distance from the gate contact to the channel edge	0.0m
XGL	Offset of the gate length due to variations in patterning	0.0m
XL	Channel length offset due to mask/ etch effect	0.0m
XW	Channel width offset due to mask/etch effect	0.0m
NGCON(Also an instance and model parameter)	Number of gate contacts (Fatal error if less than one; if not equal to 1 or 2, warning message issued and reset to 1)	1

18 Asymmetric Source/Drain Junction Diode Model Parameters

Parameter Name (separate for source and drain side as indicated in the names)	Description	Default Value
IJTHSREV IJTHDREV	Limiting current in reverse bias region	IJTHSREV = 0.1A, IJTHDREV = IJTHSREV
IJTHSFWD IJTHDFWD	Limiting current in forward bias region	IJTHSFWD = 0.1A, IJTHDFWD = IJTHSFWD
XJBVS XJBVD	Fitting parameter for diode breakdown	XJBVS = 1.0, XJBVD = XJBVS
BVS BVD	Breakdown voltage (If not positive, reset to 10.0V)	BVS = 10.0V, BVD = BVS
JSS JSD	Bottom junction reverse saturation current density	JSS= 1.0e-4A/m ² , JSD = JSS
JSWS JSWD	Isolation-edge sidewall reverse saturation current density	JSWS = 0.0A/m, JSWD = JSWS
JSWGS JSWGD	Gate-edge sidewall reverse saturation current density	JSWGS = 0.0A/m, JSWGD = JSWGS
JTSS JTSD	Bottom trap-assisted saturation current density	JTSS = 0.0A/m JTSD = JTSS
JTSSWS JTSSWD	STI sidewall trap-assisted saturation current density	JTSSWS = 0.0A/m ² JTSSWD = JTSSWS
JTSSWGS JTSSWGD	Gate-edge sidewall trap-assisted saturation current density	JTSSWGS = 0.0A/m JTSSWGD = JTSSWGS
JTWEFF	Trap-assistant tunneling current density width dependence	0.0
NJTS NJTSD	Non-ideality factor for JTSS and JTSD	NJTS = 20.0 NJTSD = NJTS

NJTSSW NJTSSWD	Non-ideality factor for JTSSWS and JTSSWD	NJTSSW = 20.0 NJTSSWD = NJTSSW
NJTSSWG NJTSSWGD	Non-ideality factor for JTSSWGS and JTSSWGD	NJTSSWG = 20.0 NJTSSWGD = NJTSSWG
XTSS, XTSD	Power dependence of JTSS, JTSD on temperature	XTSS = 0.02 XTSD = 0.02
XTSSWS, XTSSWD	Power dependence of JTSSWS, JTSSWD on temperature	XTSSWS =0.02 XTSSWD = 0.02
XTSSWGS, XTSSWGD	Power dependence of JTSSWGS, JTSS-WGD on temperature	XTSSWGS = 0.02 XTSSWGD = 0.02
VTSS VTSD	Bottom trap-assisted voltage dependent parameter	VTSS = 10V VTSD = VTSS
VTSSWS VTSSWD	STI sidewall trap-assisted voltage dependent parameter	VTSSWS =10V VTSSWD =VTSSWS
VTSSWGS VTSSWGD	Gate-edge sidewall trap-assisted voltage dependent parameter	VTSSWGS = 10V VTSSWGD =VTSS-WGS
TNJTS TNJTS	Temperature coefficient for NJTS and NJTSD	TNJTS=0.0 TNJTS =TNJTS
TNJTSSW TNJTSSWD	Temperature coefficient for NJTSSW and NJTSSWD	TNJTSSW= 0.0 TNJTSSWD =TNJTSSW
TNJTSSWG TNJTSSWGD	Temperature coefficient for NJTSSWG and NJTSSWG	TNJTSSWG =0.0 TNJTSSWGD = TNJTSSWG
CJS CJD	Bottom junction capacitance per unit area at zero bias	CJS=5.0e-4 F/m ² CJD=CJS
MJS MJD	Bottom junction capacitance grating coefficient	MJS=0.5 MJD=MJS
MJSWS MJSWD	Isolation-edge sidewall junction capacitance grading coefficient	MJSWS =0.33 MJSWD =MJSWS
CJSWS CJSWD	Isolation-edge sidewall junction capacitance per unit area	CJSWS= 5.0e-10 F/m CJSWD =CJSWS
CJSWGS CJSWGD	Gate-edge sidewall junction capacitance per unit length	CJSWGS =CJSWS CJSWGD =CJSWS

MJSWGS MJSWGD	Gate-edge sidewall junction capacitance grading coefficient	MJSWGS =MJSWS MJSWGD =MJSWS
PBS	Source-side bulk junction built-in potential	1.0V
PBD	Drain-side bulk junction built-in potential	PBD=PBS
PBSWS PB- SWD	Isolation-edge sidewall junction built-in potential	PBSWS =1.0V PBSWD =PBSWS
PBSWGS PB- SWG D	Gate-edge sidewall junction built-in potential	PBSWGS =PBSWS PB- SWG D =PBSWS

19 Temperature Dependence and Self Heating Parameters

Parameter Name	Description	Default Value
TNOM	Temperature at which parameters are extracted	27°C
DTEMP	Variability handle for temperature	0
UTE (b)	Mobility temperature exponent	-1.5
UCSTE(b)	Temperature coefficient of coulombic mobility	-4.775e-3
TDELTA	Temperature coefficient for DELTA	0.0
TGIDL (b)	Temperature coefficient for GIDL/GISL	0.0
IIT (b)	Temperature coefficient for BETA0	0.0
KT1 (b)	Temperature coefficient for threshold voltage	-0.11V
KT1EXP	Temperature exponent for threshold voltage	1.0
KT1L (b)	Channel length dependence of the temperature coefficient for threshold voltage	0.0Vm
KT2(b)	Body-bias coefficient of Vth temperature effect	0.022
UA1 (b)	Temperature coefficient for UA	1.0e-9m/V
UC1 (b)	Temperature coefficient for UC	0.0561/K for MOBMOD=1; 0.056e-91/K for MOBMOD=0 and 2
UD1 (b)	Temperature coefficient for UD	0.0(1/m) ²
EU1 (b)	Temperature coefficient for EU	0.0
AT (b)	Temperature coefficient for saturation velocity	3.3e4m/s
PTWGT	Temperature coefficient for PTWG	0.0K
PRT (b)	Temperature coefficient for Rds _w	0.0
PRTHV (b)	Temperature coefficient for drift resistance	0.0
IGT (b)	Temperature coefficient for Gate current	2.5
NJS, NJD	Emission coefficients of junction for source and drain junctions, respectively	NJS=1.0; NJD=NJS

XTIS, XTIID	Junction current temperature exponents for source and drain junctions, respectively	XTIS=3.0; XTIID=XTIS
TPB	Temperature coefficient of PB	0.0V/K
TPBSW	Temperature coefficient of PBSW	0.0V/K
TPBSWG	Temperature coefficient of PBSWG	0.0V/K
TCJ	Temperature coefficient of CJ	0.0K-1
TCJSW	Temperature coefficient of CJSW	0.0K-1
TCJSWG	Temperature coefficient of CJSWG	0.0K-1
TVFBSDOFF	Temperature coefficient of VFBSDOFF	0.0K-1
TNFACTOR(b)	Temperature coefficient of NFACTOR	0.0
TETA0	Temperature coefficient of ETA0	0.0
RTH0	Thermal resistance for self-heating calculation	$0.0K * m/W$
CTH0	Thermal capacitance for self-heating calculation	$1.0E-5W * s/m/K$
WTH0	Width-dependence coefficient for self heating calculation	0.0m

20 Stress Effect Model Parameters

Parameter Name	Description	Default Value
SA (Instance Parameter)	Distance between OD edge to Poly from one side (If not given or(≤ 0), stress effect will be turned off)	0.0m
SAEDGE	SA parameter for EDGEFET	SA
SB (Instance Parameter)	Distance between OD edge to Poly from other side (If not given or(≤ 0), stress effect will be turned off)	0.0m
SBEDGE	SB parameter for EDGEFET	SB
SD (Instance Parameter)	Distance between neighbouring fingers (For NF>1 :If not given or(≤ 0), stress effect will be turned off)	0.0m
SAre _f	Reference distance between OD and edge to poly of one side (>0.0)	1E-06[m]
SBre _f	Reference distance between OD and edge to poly of the other side (>0.0)	1E-06[m]
WL _{OD}	Width parameter for stress effect	0.0[m]
KU ₀	Mobility degradation/enhancement coefficient for stress effect	0.0[m]
KVSAT	Saturation velocity degradation/ enhancement parameter for stress effect ($1 \leq k_{vsat} \leq 1$)	0.0[m]
TKU ₀	Temperature coefficient of KU ₀	0.0
LKU ₀	Length dependence of ku ₀	0.0
WKU ₀	Width dependence of ku ₀	0.0
PKU ₀	Cross-term dependence of ku ₀	0.0
LL _{OD} KU ₀	Length parameter for u ₀ stress effect (>0)	0.0
WL _{OD} KU ₀	Width parameter for u ₀ stress effect (>0)	0.0
KVTH ₀	Threshold shift parameter for stress effect	0.0[Vm]
KVTH ₀ EDGE	KVTH ₀ parameter for EDGEFET	0.0[Vm]
LKVTH ₀	Length dependence of kvth ₀	0.0
WKVTH ₀	Width dependence of kvth ₀	0.0
PKVTH ₀	Cross-term dependence of kvth ₀	0.0

LLODVTH	Length parameter for Vth stress effect (>0)	0.0
WLODVTH	Width parameter for Vth stress effect (>0)	0.0
STK2	K2 shift factor related to Vth0 change	0.0[m]
STK2EDGE	STK2E parameter for EDGEFET	STK2[m]
LODK2	K2 shift modification factor for stress effect (>0)	0.0
STETA0	eta0 shift factor related to Vth0 change	0.0[m]
STETA0EDGE	STETA0 parameter for EDGEFET	0.0[m]
LODETA0	eta0 shift modification factor for stress effect (>0)	1.0

21 Well-Proximity Effect Parameters

Parameter Name	Description	Default Value
SCA (Instance Parameter)	Integral of the first distribution function for scattered well dopant (If not given , calculated)	0.0
SCB (Instance Parameter)	Integral of the second distribution function for scattered well dopant (If not given , calculated)	0.0
SCC (Instance Parameter)	Integral of the third distribution function for scattered well dopant (If not given , calculated)	0.0
SC (Instance Parameter)	Distance to a single well edge (If not given or ≤ 0.0 , turn off WPE)	0.0[m]
WEB	Coefficient for SCB (>0.0)	0.0
WEC	Coefficient for SCC (>0.0)	0.0
KVTH0WE(b)	Threshold shift factor for well proximity effect	0.0
K2WE (b)	K2 shift factor for well proximity effect	0.0
KVTH0EDGEWE(b)	Threshold shift factor in EDGEFET module for well proximity effect	0.0
K2EDGEWE (b)	K2 shift factor in EDGEFET module for well proximity effect	0.0
KU0WE (b)	Mobility degradation factor for well proximity effect	0.0
SCREF	Reference distance to calculate SCA, SCB and SCC (<0)	1e-6[m]

22 Parameters for Edge FET and Sub-Surface Leakage Current

Note: binnable parameters are marked as: ^(b)

Name	Unit	Default	Min	Max	Description
EDGEFET(also an instance and model parameter)		1	-	-	Edge FET model Flag: 0: Disable 1: Enable
NDEPEDGE ^(b)	m^{-3}	$1e24$	-	-	channel doping concentration for EDGEFET.
WEDGE	m	$10e^{-9}$	$1e^{-9}$	-	Edge FET Width
DGAMMA		0	-	-	Different in body-bias coefficient between Edge-FET and Main-FET
DGAMMAL		0	-	-	L dependence parameter for DGAMMA
DGAMMAEXP		1.0	-	-	Exponent of L dependence parameter for DGAMMA
DVTEDGE		0.0	-	-	Vth shift for Edge FET
NFACTOREDGE ^(b)		0	-	-	NFACTOR for Edge FET
CITEDGE ^(b)	F/m^2	0	-	-	CIT for Edge FET
CDSCDEDGE ^(b)	$F/m^2/V$	$1e^{-9}$	-	-	CDSCD for edge FET
CDSCBEDGE ^(b)	$F/m^2/V$	0	-	-	CDSCB for edge FET
ETA0EDGE ^(b)	-	0.08	-	-	DIBL parameter for edge FET
ETABEDGE ^(b)	$1/V$	-0.07	-	-	ETAB for edge FET
K2EDGE	V	0.0	-	-	Vth shift due to body bias
KT1EDGE ^(b)	V	-0.11	-	-	Temperature dependence parameter of threshold voltage for edge FET
KT1LEDGE ^(b)	$V * m$	0	-	-	Temperature dependence parameter of threshold voltage for edge FET
KT2EDGE ^(b)	-	0.022	-	-	Temperature dependence parameter of threshold voltage for edge FET
KT1EXPEDGE	-	1	-	-	Temperature dependence parameter of threshold voltage for edge device

TNFACTOREDGE ^(b)		0.0	-	-	Temperature dependence parameter of sub-threshold slope factor for edge
TETA0EDGE	-	0	-	-	Temperature dependence parameter of DIBL parameter for edge FET
DVT0EDGE	-	2.2	-	-	First coefficient of SCE effect on Vth for Edge FET
DVT1EDGE	-	0.53	-	-	Second coefficient of SCE effect on Vth for Edge FET
DVT2EDGE	$1/V$	0.0	-	-	Body-bias coefficient for SCE effect for Edge FET
SSLMOD(also an instance and model parameter)		1	-	-	Sub-Surface Leakage Drain Current, 0: Turn off 1: Turn on
SSL0	A/m	400	-	-	
SSL1	$1/m$	3.36E8	-	-	
SSL2	-	0.185	-	-	
SSL3	V	0.3	-	-	
SSL4	$1/V$	1.4	-	-	
SSLEXP1		0.490	-	-	
SSLEXP2		1.42	-	-	

23 Parameters for High Voltage Model

Name	Unit	Default	Min	Max	Description
HVMOD	-	0	0	1	Flag to turn on high voltage mode-set HVMOD=1 and RDSMOD=1.
RDLCW	$Ohm * um^{WR}$	100	0	-	Resistance of the Drain at Low Current
RDLCWCV	$Ohm * um^{WR}$	RDLCW	0	-	Resistance of the Drain at Low Current used in CV calculations
RSLCW	$Ohm * um^{WR}$	0	0	-	Resistance of the Source at Low Current
NDRIFTD	$1/m^2$	-	-	5e16	Drift region charge density
NDRIFTS	$1/m^2$	-	-	NDRIFTD	Drift region charge density
VDRIFT	m/s	2e5	> 0	-	Carrier velocity in the drift region
PTWGHV	-	0	-	-	VDRIFT variation with gate bias
PTWGHV1	-	0	-	-	VDRIFT variation with gate bias
PSATXHV	-	60.0	-	-	Fine tuning of PTWGHV effect
PDRWB	-	0	-	-	Body bias dependence of the drift region resistance
MDRIFT	-	1	> 0	< 4	Parameter for Id,lin to Id,sat transition in Id-Vd
DRB1	-	0.0	-	-	Parameter for body bias dependency
DRB2	-	0.0	-	-	Parameter for body bias dependency
RDVDS	-	8	-	-	Parameter for Idriftsat variation with drain voltage
GADRIFT	-	200	-	-	Parameter for Idriftsat variation with drain voltage
RBODYHVMOD	-	0	-	-	Set RBODYHVMOD=1 to turn on Drain-Body Diode partitioning
XPART	-	0.0	-	-	Drain-Body Diode partitioning parameter when RBODYHVMOD=1
HVCAP	-	0	0	1	Flag to turn on high voltage capacitance model
HVFACCTOR	-	1e-3	1e-4	1	
VFBOV	V	-1	-	-	Flat band voltage of the drift region.

LOVER	m	500n	-	-	Length of the drift region in inversion.
LOVERACC	m	LOVER	-	-	Length of the drift region in accumulation.
SLHV	-	0	0	-	Parameter for tuning Cgg slope in accumulation. Also a sg, set=1 to enable the model
SLHV1	-	0	0	-	Parameter for tuning Cgg slope in accumulation
NDR	$1/m^3$	NDEP	-	-	Doping of the drift region
ALPHADR	m/V	ALPHA0	0	-	First parameter of Iii in the drift region
BETADR	$1/V$	BETA0	0	-	Second parameter of Iii in the drift region
BETA1	$1/V$	0	0	-	Parameter of Iii in the intrinsic region for high drain bias
BETA2	-	0	0	-	Parameter of Iii in the intrinsic region for high drain bias
BETA3	-	1	0.1	10	Parameter of Iii in the intrinsic region for high drain bias
ALPHA1	$1/V$	0	0	-	Parameter of Iii for Vb dependence in the intrinsic region
ALPHA2	$1/V^2$	0	0	-	Parameter of Iii for Vb dependence in the intrinsic region
DRII3	-	1	0	-	drift region paramter - Vds dependency
DRII4	-	0	0	-	Parameter accounting voltage drop correction at the internal node di for conductivity modulation
ALPHADR1	$1/V$	0	0	-	Parameter of Iii for Vb dependence in the drift region
ALPHADR2	$1/V^2$	0	0	-	Parameter of Iii for Vb dependence in the drift region
CMD1	-	0	0	-	Conductivity modulation parameter for drain side

CMD2	-	1	0.5	5.0	Conductivity modulation parameter for drain side
CMS1	-	0	0	-	Conductivity modulation parameter for source side
CMS2	-	1	0.5	5.0	Conductivity modulation parameter for source side

24 Parameter equivalence between BSIM-BULK & BSIM4

The equivalent parameters are the closest match between two models. Their values may be different in two models.

Region	BSIM-BULK Parameter Name	BSIM4 Parameter Name	Comment
Core Parameters	GEOMOD RGEOMOD RDSMOD COVMOD L W XL XW LINT WINT DLC DWC TOXE TOXP NF NDEP NGATE VFB, VFBCV	GEOMOD RGEOMOD RDSMOD COVMOD L W XL XW LINT WINT DLC DWC TOXE TOXP NF NDEP VTH0/VTHO NGATE VFB, VFBCV	or
Material properties	EASUB NI0SUB EPSRSUB EPSROX	- - - -	Corresponds to BSIM4 mtrmod=1
Threshold Voltage	NDEPL1, NDEPLEXP1, NDEPL2, NDEPLEXP2	DVT0, DVT1, DVT2, LPE0	Length scaling

	NDEPW, NDEP-WEXP, NDEPWL, NDEPWLEXP K2W DVTP0, DVTP1, DVTP2, DVTP3, DVTP4, DVTP5 PHIN ETA0 ETAB DSUB K2 K2L, L2LEXP	DVT0W, DVT1W, DVT2W, K3, W0 K3B same as BSIM4 PHIN ETA0 ETAB DSUB K2 K1, LPEB	Width and Narrow-short Scaling
Subthreshold Swing	CIT NFACTOR CDSCD CDSCB NFACTOR	CIT CDSC CDSCD CDSCB NFACTOR	
Drain Saturation Voltage	VSAT, DELTA	VSAT, DELTA	
Mobility Model	U0 ETAMOB U0L U0LEXP UA EU UD UCS UC	U0 - UP LPA UA EU UD UCS UC	BSIM6 uses MOBMOD=3 from BSIM4 default value of 1 corresponds to BSIM4
Channel Length Modulation and DITS	PCLM	PCLM	

	PCLMG PSCBE1 PSCBE2 PDITS PDITSL PDITSD	PCLMG PSCBE1 PSCBE2 PDITS PDITSL PDITSD	
Velocity Saturation	VSAT PTWG PSAT PSATX PSATB	VSAT - - - -	
Rs, Rd parameter	XJ VFBSDOFF NRS/NRD MINZ NSD RSH PRWG PRWB WR RDSWMIN RSWMIN RDWMIN RDSW RSW RDW DMCG DMCI DMDG DMCGT	XJ VFBSDOFF NRS/NRD MINZ NSD RSH PRWG PRWB WR RDSWMIN RSWMIN RDWMIN RDSW RSW RDW DMCG DMCI DMDG DMCGT	BSIM6 uses RDSMOD=1 from BSIM4
Impact Ionization	ALPHA0, PHA0L, PHA0LEXP BETA0	AL- AL- BETA0	ALPHA0, ALPHA1

GIDL/GISL	AGIDL BGIDL CGIDL EGIDL AGISL BGISL CGISL EGISL	AGIDL BGIDL CGIDL EGIDL AGISL BGISL CGISL EGISL	
C-V Model	CF CFRCOEFF CFI CGSO CGDO CGBO CGSL CGDL CKAPPAS CKAPPAD ADOS, BDOS, QM0, ETAQM	CF - - CGSO CGDO CGBO CGSL CGDL CKAPPAS CKAPPAD ADOS, BDOS	Taken from BSIMSOI

25 Appendix A : Smoothing Function

25.1 Polynomial Smoothing

The polynomial smoothing is used for a smooth transition between boundaries, maintaining exact values at all the corner points. Consider the function

$$f(x) = \begin{cases} x & \text{if } x > \frac{\Delta x}{2} \\ k & \text{if } x < \frac{-\Delta x}{2} \end{cases} \quad (25.1)$$

$$= \begin{cases} k & \text{if } x < \frac{-\Delta x}{2} \end{cases} \quad (25.2)$$

where k is some constant. The function is undefined for the region $\frac{-\Delta x}{2} < x < \frac{\Delta x}{2}$. If this region is approximated by a polynomial function, the complete function and even derivatives can be made continuous. Now consider the more generalized case

$$f(x) = \begin{cases} x & \text{if } x > x_1 \end{cases} \quad (25.3)$$

$$= \begin{cases} k & \text{if } x < x_2 \end{cases} \quad (25.4)$$

To express (25.4) in the form of (25.2), x is linearly transformed into z . Defining

$$x_0 = \frac{x_1 + x_2}{2} \quad (25.5)$$

$$\Delta x = x_1 - x_2 \quad (25.6)$$

then the boundary points becomes

$$x_1 = x_0 + \frac{\Delta x}{2} \quad (25.7)$$

$$x_2 = x_0 - \frac{\Delta x}{2} \quad (25.8)$$

Let $z = \frac{x-x_0}{\Delta x}$. Thus the above boundary points in z domain becomes,

$$z_1 = \frac{x_1 - x_0}{\Delta x} = \frac{1}{2} \quad (25.9)$$

$$z_2 = \frac{x_2 - x_0}{\Delta x} = -\frac{1}{2} \quad (25.10)$$

so that the function becomes

$$f(z) = z \cdot \Delta x - x_0 \quad \text{if } z > \frac{1}{2} \quad (25.11)$$

$$= k \quad \text{if } z < -\frac{1}{2} \quad (25.12)$$

the region $-\frac{1}{2} \leq z \leq \frac{1}{2}$ is modeled by the polynomial function whose order depends on the number of boundary conditions. For example, to have continuous derivatives upto third order, we need seventh order polynomial as there are 8 boundary conditions.

$$f(z) = a.z^7 + b.z^6 + c.z^5 + d.z^4 + e.z^3 + f.z^2 + g.z + 1 \quad (25.13)$$

Then boundary conditions can be applied to derivatives to determine the polynomial coefficients. For the case of continuous third order derivatives, we found that

$$f(x) = x_0 + \Delta x \cdot \left[\frac{5}{64} + \frac{z}{2} + z^2 \cdot \left[\frac{15}{16} - z^2 \cdot \left(\frac{5}{4} - z^2 \right) \right] \right] \quad (25.14)$$

while for continuous second order derivative

$$f(x) = x_0 + \Delta x \cdot \left[\frac{3}{32} + \frac{z}{2} + z^2 \cdot \left[\frac{3}{4} - z^2 \cdot \left(\frac{3}{4} - \frac{z^2}{2} \right) \right] \right] \quad (25.15)$$

with $z = \frac{x-x_0}{\Delta x}$. Figure 21 illustrate the concept of polynomial smoothing.

An Example : Let the function be given as

$$f(x) = x \quad \text{if } x > -90 \quad (25.16)$$

$$= -100 \quad \text{if } x < -110 \quad (25.17)$$

with the condition that third derivative to exist. From (25.6)

$$x_0 = -100 \quad (25.18)$$

$$\Delta x = 20 \quad (25.19)$$

$$z = \frac{x + 100}{20} \quad (25.20)$$

and function becomes,

$$f(z) = 20.z + 100 \quad \text{if } z > \frac{1}{2} \quad (25.21)$$

$$= -100 \quad \text{if } z < -\frac{1}{2} \quad (25.22)$$

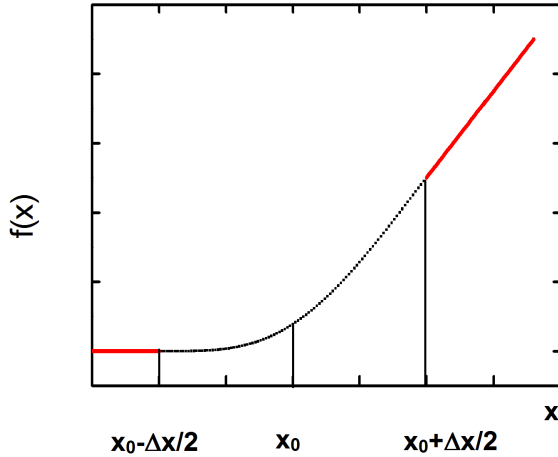


Figure 21: Illustration of Polynomial Smoothing

Boundary Conditions

$$f\left(\frac{1}{2}\right) = -90, f\left(-\frac{1}{2}\right) = -100 \quad (25.23)$$

$$f'\left(\frac{1}{2}\right) = 20, f'\left(-\frac{1}{2}\right) = 0 \quad (25.24)$$

$$f''\left(\frac{1}{2}\right) = 0, f''\left(-\frac{1}{2}\right) = 0 \quad (25.25)$$

$$f'''\left(\frac{1}{2}\right) = 0, f'''\left(-\frac{1}{2}\right) = 0 \quad (25.26)$$

We have 8 boundary conditions. So let

$$f(z) = a.z^7 + b.z^6 + c.z^5 + d.z^4 + e.z^3 + f.z^2 + g.z + 1 \quad (25.27)$$

Now we have 8 equations and 8 unknowns and hence all the coefficients can be derived. By substituting (25.23-25.26) in (25.27) we get

$$a = 0, b = 20, c = 0$$

$$d = -25, e = 0, f = \frac{75}{4} \quad (25.28)$$

$$g = 10, h = -\frac{6300}{64} \quad (25.29)$$

Thus

$$f(z) = 20.z^6 - 25.z^4 + \frac{75}{4}.z^2 + 10.z - \frac{6300}{64} \quad (25.30)$$

Figure:22 shows the above function. As can be seen that due to polynomial nature, the

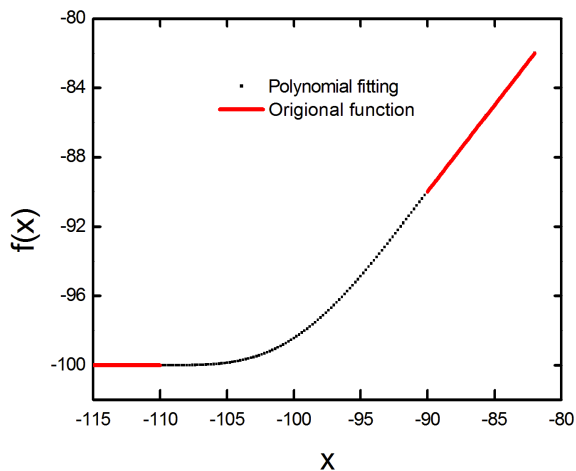


Figure 22: Polynomial Smoothing Function

approximated function undergoes smooth transitions around the boundary points.

26 Appendix B : Derivation of Bulk charge with poly-depletion effect

26.1 Bulk charge with polydepletion effect

Total Bulk Charge,

$$Q_B = W \cdot \int_0^L Q_b dx \quad (26.1)$$

Using charge balance equation, bulk charge density considering poly depletion effect is given by:

$$Q_b = -C_{ox} \cdot (V_G - V_{FB} - \Psi_S) - Q_i - \Delta Q_g \quad (26.2)$$

where ΔQ_g is the charge density due to polysilicon gate. Then using inversion charge linearization:

$$Q_i = n_q \cdot C_{ox} \cdot (\Psi_S - \Psi_P)$$

or

$$\Psi_S = \Psi_P + \frac{Q_i}{n_q C_{ox}}$$

Substituting this Ψ_S into (26.2):

$$Q_b = -C_{ox} \cdot (V_G - V_{FB} - \Psi_P) - Q_i \cdot \left(1 - \frac{1}{n_q}\right) - \Delta Q_g \quad (26.3)$$

Now, (26.1) reads:

$$Q_B = -W \cdot L \cdot C_{ox} \cdot \left((V_G - V_{FB} - \Psi_P) + \left(1 - \frac{1}{n_q}\right) \int_0^1 \frac{Q_i}{C_{ox}} d\xi + \int_0^1 \frac{\Delta Q_g}{C_{ox}} d\xi \right)$$

$$Q_B = -W \cdot L \cdot C_{ox} \cdot \left((V_G - V_{FB} - \Psi_P) + \left(1 - \frac{1}{n_q}\right) \int_0^1 \frac{Q_i}{C_{ox}} d\xi \right) - W \cdot L \cdot \int_0^1 \Delta Q_g d\xi$$

$$Q_B = -W.L.C_{ox} \cdot \left((V_G - V_{FB} - \Psi_P) + \left(1 - \frac{1}{n_q}\right) \int_0^1 \frac{Q_i}{C_{ox}} d\xi \right) - \Delta Q_G \quad (26.4)$$

where $\Delta Q_G = W \cdot \int_0^L \Delta Q_g dx$

$$Q_B = -W.L.C_{ox} \cdot (V_G - V_{FB} - \Psi_P) - W.L.2.n_q.C_{ox} \cdot \left(1 - \frac{1}{n_q}\right) \int_0^1 \frac{Q_i}{2.n_q.C_{ox}} d\xi - \Delta Q_G$$

Normalizing the bulk charge to $-W.L.C_{ox}.V_t$,

$$\begin{aligned} q_B &= \frac{Q_B}{-W.L.C_{ox}.V_t} \\ &= (v_g - v_{fb} - \psi_p) + 2.n_q \cdot \left(1 - \frac{1}{n_q}\right) \int_0^1 \frac{Q_i}{2.n_q.C_{ox}V_t} d\xi - \frac{\Delta Q_G}{-W.L.C_{ox}.V_t} \end{aligned}$$

Now,

$$\Delta q_G = \frac{-\Delta Q_G}{W.L.C_{ox}.V_t} \quad \& \quad q = \frac{-Q_i}{2.n_q.C_{ox}.V_t}$$

The above equation reads following:

$$q_B = (v_g - v_{fb} - \psi_p) - 2.(n_q - 1) \cdot \int_0^1 q d\xi - \Delta q_G$$

$$q_B = q_{B1} - \Delta q_G \quad (26.5)$$

$$\text{where, } q_{B1} = (v_g - v_{fb} - \psi_p) - 2.(n_q - 1) \cdot \int_0^1 q d\xi$$

Now, gate charge in the poly Si is given by [2]:

$$Q_{poly} = \Delta Q_g = \sqrt{2q\epsilon_s N_{poly}} \sqrt{\Psi_{poly}}$$

$$\frac{\Delta Q_g}{C_{ox}} = \gamma_g \sqrt{\Psi_{poly}}$$

Using potential balance $\frac{\Delta Q_g}{C_{ox}} = \Psi_{ox} = (V_G - V_{FB} - \Psi_s - \Psi_{poly})$

$$\{(V_G - V_{FB} - \Psi_s) - \Psi_{poly}\}^2 = \gamma_g^2 \cdot \Psi_{poly}$$

$$\frac{\Psi_{poly}}{\{(V_G - V_{FB} - \Psi_s) - \Psi_{poly}\}^2} = \frac{1}{\gamma_g^2}$$

$$\frac{\{(V_G - V_{FB} - \Psi_s) + \Psi_{poly}\}^2}{\{(V_G - V_{FB} - \Psi_s) - \Psi_{poly}\}^2} - 1 = \frac{4.(V_G - V_{FB} - \Psi_s)}{\gamma_g^2}$$

$$\frac{(V_G - V_{FB} - \Psi_s) + \Psi_{poly}}{(V_G - V_{FB} - \Psi_s) - \Psi_{poly}} = \sqrt{1 + \frac{4.(V_G - V_{FB} - \Psi_s)}{\gamma_g^2}}$$

$$\Psi_{poly} = (V_G - V_{FB} - \Psi_s) \cdot \frac{\sqrt{1 + \frac{4.(V_G - V_{FB} - \Psi_s)}{\gamma_g^2}} - 1}{\sqrt{1 + \frac{4.(V_G - V_{FB} - \Psi_s)}{\gamma_g^2}} + 1}$$

$$\Delta Q_g = -C_{ox} \cdot (V_G - V_{FB} - \Psi_s) \cdot \frac{\sqrt{1 + \frac{4.(V_G - V_{FB} - \Psi_s)}{\gamma_g^2}} - 1}{\sqrt{1 + \frac{4.(V_G - V_{FB} - \Psi_s)}{\gamma_g^2}} + 1}$$

$$\Delta Q_g = -C_{ox} \cdot \left(V_G - V_{FB} - \Psi_P - \frac{Q_i}{n_q \cdot C_{ox}} \right) \frac{\sqrt{1 + (\frac{2}{\gamma_g})^2 \cdot (V_G - V_{FB} - \Psi_P - \frac{Q_i}{n_q \cdot C_{ox}})} - 1}{\sqrt{1 + (\frac{2}{\gamma_g})^2 \cdot (V_G - V_{FB} - \Psi_P - \frac{Q_i}{n_q \cdot C_{ox}})} + 1}$$

$$\Delta Q_G = W \cdot \int_0^L \Delta Q_g \, dx = W.L \cdot \int_0^1 \Delta Q_g \, d\xi$$

$$\Delta Q_G = -W.L.C_{ox}.9ex_0^1 \left(V_G - V_{FB} - \Psi_P - \frac{Q_i}{n_q \cdot C_{ox}} \right) \frac{\sqrt{1 + (\frac{2}{\gamma_g})^2 \cdot (V_G - V_{FB} - \Psi_P - \frac{Q_i}{n_q \cdot C_{ox}})} - 1}{\sqrt{1 + (\frac{2}{\gamma_g})^2 \cdot (V_G - V_{FB} - \Psi_P - \frac{Q_i}{n_q \cdot C_{ox}})} + 1} \, d\xi$$

$$\Delta q_G = \frac{-\Delta Q_G}{W.L.C_{ox}.V_t}$$

$$\Delta q_G = 9ex_0^1 \left(v_g - v_{fb} - \psi_p + 2.q \right) \frac{\sqrt{1 + (\frac{2}{\gamma_g})^2 \cdot (v_g - v_{fb} - \psi_p + 2.q)} - 1}{\sqrt{1 + (\frac{2}{\gamma_g})^2 \cdot (v_g - v_{fb} - \psi_p + 2.q)} + 1} \, d\xi \quad (26.6)$$

where $(\gamma'_g)^2 = (\gamma_g)^2/V_t$

Now, (17) of [1] reads:

$$\xi_m - \xi = s \cdot \frac{(s + H_q)}{\Delta q \cdot H_q} \quad \text{where} \quad H_q = (1 + 2q_{ia}/D_{vsat})$$

where ξ_m is obtained by noting that at source end, $\xi = 0$ and $s = s_s = \Delta q/2$. Substituting back ξ_m above gives:

$$\xi = \frac{1}{2 \cdot H_q} \left(\frac{\Delta q}{2} + H_q \right) - \frac{s \cdot (s + H_q)}{\Delta q \cdot H_q}$$

$$d\xi = -\frac{(2 \cdot s + H_q)}{\Delta q \cdot H_q} ds$$

After substituting these, (26.6) reads:

$$\begin{aligned} \Delta q_G &= -9ex^{\frac{-\Delta q}{2}} \left(v_g - v_{fb} - \psi_p + 2 \cdot q \right) \frac{\sqrt{1 + (\frac{2}{\gamma'_g})^2 \cdot (v_g - v_{fb} - \psi_p + 2 \cdot q)} - 1}{\sqrt{1 + (\frac{2}{\gamma'_g})^2 \cdot (v_g - v_{fb} - \psi_p + 2 \cdot q)} + 1} \frac{(2 \cdot s + H_q)}{\Delta q \cdot H_q} ds \\ \Delta q_G &= 9ex^{\frac{\Delta q}{2}} \left(F_g + 2 \cdot q \right) \frac{\sqrt{1 + A_g \cdot (F_g + 2 \cdot q)} - 1}{\sqrt{1 + A_g \cdot (F_g + 2 \cdot q)} + 1} \frac{(2 \cdot s + H_q)}{\Delta q \cdot H_q} ds \end{aligned} \quad (26.7)$$

where $F_g = (v_g - v_{fb} - \psi_p)$ and $A_g = (\frac{2}{\gamma'_g})^2$

Also, $q = s + q_{ia}$

$$\Delta q_G = 9ex^{\frac{\Delta q}{2}} \left(F_g + 2 \cdot (s + q_{ia}) \right) \frac{\sqrt{1 + A_g \cdot (F_g + 2 \cdot (s + q_{ia}))} - 1}{\sqrt{1 + A_g \cdot (F_g + 2 \cdot (s + q_{ia}))} + 1} \frac{(2 \cdot s + H_q)}{\Delta q \cdot H_q} ds \quad (26.8)$$

$$\Delta q_G = 9ex^{\frac{\Delta q}{2}} \left(F_g + 2 \cdot (s + q_{ia}) \right) \frac{\left[\frac{\sqrt{1 + A_g \cdot (F_g + 2 \cdot (s + q_{ia}))} - 1}{A_g \cdot (F_g + 2 \cdot (s + q_{ia}))} \right]^2}{\frac{\sqrt{1 + A_g \cdot (F_g + 2 \cdot (s + q_{ia}))} - 1}{A_g \cdot (F_g + 2 \cdot (s + q_{ia}))}} \frac{(2 \cdot s + H_q)}{\Delta q \cdot H_q} ds$$

$$\Delta q_G = \frac{1}{A_g \cdot \Delta q \cdot H_q} 9ex^{\frac{\Delta q}{2}} \left[\sqrt{1 + A_g \cdot (F_g + 2 \cdot (s + q_{ia}))} - 1 \right]^2 (2 \cdot s + H_q) ds$$

$$\Delta q_G = \frac{1}{A_g \cdot \Delta q \cdot H_q} 9 \operatorname{ex}_{\frac{-\Delta q}{2}}^{\frac{\Delta q}{2}} \left[2 + A_g \cdot (F_g + 2 \cdot (s + q_{ia})) - 2 \cdot \sqrt{1 + A_g \cdot (F_g + 2 \cdot (s + q_{ia}))} \right] (2 \cdot s + H_q) ds \quad (26.9)$$

Let $t^2 = 1 + A_g \cdot [F_g + 2 \cdot (s + q_{ia})]$ so that $ds = \frac{t}{A_g} dt$ & $2 \cdot s = \frac{t^2 - 1 - A_g \cdot (F_g + 2 \cdot q_{ia})}{A_g}$
So, $s = \frac{-\Delta q}{2}$ corresponds to $t = t_1 = 1 + A_g \cdot [F_g + 2 \cdot (q_{ia} - \frac{\Delta q}{2})]$

And, $s = \frac{\Delta q}{2}$ corresponds to $t = t_2 = 1 + A_g \cdot [F_g + 2 \cdot (q_{ia} + \frac{\Delta q}{2})]$

Now, using this (26.9) reads:

$$\begin{aligned} \Delta q_G &= \frac{1}{A_g \cdot \Delta q \cdot H_q} 9 \operatorname{ex}_{t_1}^{t_2} \left[1 + t^2 - 2 \cdot t \right] \left(\frac{t^2 - 1 - A_g \cdot (F_g + 2 \cdot q_{ia})}{A_g} + H_q \right) \cdot \frac{t}{A_g} dt \\ \Delta q_G &= \frac{1}{A_g^3 \cdot \Delta q \cdot H_q} 9 \operatorname{ex}_{t_1}^{t_2} t \cdot \left[t^2 + 1 - 2 \cdot t \right] \left(t^2 - 1 + A_g \cdot \left[H_q - (F_g + 2 \cdot q_{ia}) \right] \right) .dt \end{aligned} \quad (26.10)$$

$$\begin{aligned} \Delta q_G &= \frac{1}{A_g^3 \cdot \Delta q \cdot H_q} 9 \operatorname{ex}_{t_1}^{t_2} t \cdot \left[t^2 - 2 \cdot t + 1 \right] \left(t^2 - 1 + A_g \cdot \left[H_q - (F_g + 2 \cdot q_{ia}) \right] \right) .dt \\ \Delta q_G &= \frac{1}{A_g^3 \cdot \Delta q \cdot H_q} 9 \operatorname{ex}_{t_1}^{t_2} \left[t^3 - 2 \cdot t^2 + t \right] \left(t^2 - 1 + B_g \right) .dt \end{aligned} \quad (26.11)$$

where $B_g = A_g \cdot \left[H_q - (F_g + 2 \cdot q_{ia}) \right]$

$$\Delta q_G = \frac{1}{A_g^3 \cdot \Delta q \cdot H_q} 9 \operatorname{ex}_{t_1}^{t_2} \left[t^5 - 2 \cdot t^4 + B_g \cdot t^3 + 2 \cdot t^2 \cdot (1 - B_g) - t \cdot (1 - B_g) \right] .dt \quad (26.12)$$

On integration, we have

$$\Delta q_G = \frac{1}{A_g^3 \cdot \Delta q \cdot H_q} \left[\frac{t^6}{6} - \frac{2 \cdot t^5}{5} + B_g \cdot \frac{t^4}{4} + 2 \cdot \frac{t^3}{3} \cdot (1 - B_g) - \frac{t^2}{2} \cdot (1 - B_g) \right]_{t_1}^{t_2} \quad (26.13)$$

$$\boxed{\Delta q_G = \frac{1}{A_g^3 \cdot \Delta q \cdot H_q} \left[\frac{R_1}{6} - \frac{2 \cdot R_2}{5} + B_g \cdot \frac{R_3}{4} + 2 \cdot \frac{R_4}{3} \cdot (1 - B_g) - \frac{R_5}{2} \cdot (1 - B_g) \right]} \quad (26.14)$$

where,

$$\boxed{R_1 = \left[1 + A_g \cdot \left[F_g + 2 \cdot \left(q_{ia} + \frac{\Delta q}{2} \right) \right] \right]^3 - \left[1 + A_g \cdot \left[F_g + 2 \cdot \left(q_{ia} - \frac{\Delta q}{2} \right) \right] \right]^3} \quad (A.1)$$

Simplification:

$$\begin{aligned} R_1 &= \left[1 + A_g \cdot (F_g + 2 \cdot q_{ia}) + A_g \Delta q \right]^3 - \left[1 + A_g \cdot (F_g + 2 \cdot q_{ia}) - A_g \Delta q \right]^3 \\ R_1 &= \left[1 + A_g \cdot [F_g + 2 \cdot q_{ia}] \right]^3 \cdot \left\{ \left[1 + \frac{A_g \Delta q}{1 + A_g \cdot [F_g + 2 \cdot q_{ia}]} \right]^3 - \left[1 - \frac{A_g \Delta q}{1 + A_g \cdot [F_g + 2 \cdot q_{ia}]} \right]^3 \right\} \\ R_1 &= \left[1 + A_g \cdot [F_g + 2 \cdot q_{ia}] \right]^3 \cdot \left\{ \frac{2 \cdot A_g^3 \cdot \Delta q^3}{(1 + A_g \cdot [F_g + 2 \cdot q_{ia}])^3} + \frac{6 \cdot A_g \cdot \Delta q}{1 + A_g \cdot [F_g + 2 \cdot q_{ia}]} \right\} \\ R_1 &= 6 \cdot A_g \Delta q \left[1 + A_g \cdot [F_g + 2 \cdot q_{ia}] \right]^2 + 2 \cdot (A_g \Delta q)^3 \\ \boxed{\frac{R_1}{6} = A_g \Delta q \left[1 + A_g \cdot [F_g + 2 \cdot q_{ia}] \right]^2 + \frac{(A_g \Delta q)^3}{3}} &\quad (A.2) \end{aligned}$$

$$\boxed{R_2 = \left[1 + A_g \cdot \left[F_g + 2 \cdot \left(q_{ia} + \frac{\Delta q}{2} \right) \right] \right]^{5/2} - \left[1 + A_g \cdot \left[F_g + 2 \cdot \left(q_{ia} - \frac{\Delta q}{2} \right) \right] \right]^{5/2}} \quad (B.1)$$

Simplification:

$$\begin{aligned} R_2 &= \left[1 + A_g \cdot (F_g + 2 \cdot q_{ia}) + A_g \Delta q \right]^{5/2} - \left[1 + A_g \cdot (F_g + 2 \cdot q_{ia}) - A_g \Delta q \right]^{5/2} \\ R_2 &= \left[1 + A_g \cdot [F_g + 2 \cdot q_{ia}] \right]^{5/2} \cdot \left\{ \left[1 + \frac{A_g \Delta q}{1 + A_g \cdot [F_g + 2 \cdot q_{ia}]} \right]^{5/2} - \left[1 - \frac{A_g \Delta q}{1 + A_g \cdot [F_g + 2 \cdot q_{ia}]} \right]^{5/2} \right\} \end{aligned}$$

Since, $(1+x)^{5/2} - (1-x)^{5/2} = (1+x)^2 \cdot \sqrt{1+x} - (1-x)^2 \cdot \sqrt{1-x} = (1+x^2) \cdot (\sqrt{1+x} - \sqrt{1-x}) + 2x \cdot (\sqrt{1+x} + \sqrt{1-x})$

$$R_2 = \left[1 + A_g \cdot [F_g + 2 \cdot q_{ia}] \right]^{5/2} \cdot \left\{ \left[1 + \frac{(A_g \Delta q)^2}{(1 + A_g \cdot [F_g + 2 \cdot q_{ia}])^2} \right] \cdot \left(\sqrt{1 + \frac{A_g \Delta q}{1 + A_g \cdot [F_g + 2 \cdot q_{ia}]}} - \sqrt{1 - \frac{A_g \Delta q}{1 + A_g \cdot [F_g + 2 \cdot q_{ia}]}} \right) \right. \\ \left. + 2 \cdot \left(\frac{A_g \Delta q}{1 + A_g \cdot [F_g + 2 \cdot q_{ia}]} \right) \cdot \left(\sqrt{1 + \frac{A_g \Delta q}{1 + A_g \cdot [F_g + 2 \cdot q_{ia}]}} + \sqrt{1 - \frac{A_g \Delta q}{1 + A_g \cdot [F_g + 2 \cdot q_{ia}]}} \right) \right\}$$

$$\boxed{\frac{2R_2}{5} = \frac{2}{5} \cdot \left[1 + A_g \cdot [F_g + 2 \cdot q_{ia}] \right]^{5/2} \cdot \left\{ \left[1 + \frac{(A_g \Delta q)^2}{(1 + A_g \cdot [F_g + 2 \cdot q_{ia}])^2} \right] \cdot \left(\sqrt{1 + \frac{A_g \Delta q}{1 + A_g \cdot [F_g + 2 \cdot q_{ia}]}} - \sqrt{1 - \frac{A_g \Delta q}{1 + A_g \cdot [F_g + 2 \cdot q_{ia}]}} \right) + 2 \cdot \left(\frac{A_g \Delta q}{1 + A_g \cdot [F_g + 2 \cdot q_{ia}]} \right) \cdot \left(\sqrt{1 + \frac{A_g \Delta q}{1 + A_g \cdot [F_g + 2 \cdot q_{ia}]}} + \sqrt{1 - \frac{A_g \Delta q}{1 + A_g \cdot [F_g + 2 \cdot q_{ia}]}} \right) \right\}}$$

(B.2)

$$\boxed{R_3 = \left[1 + A_g \cdot [F_g + 2 \cdot (q_{ia} + \frac{\Delta q}{2})] \right]^2 - \left[1 + A_g \cdot [F_g + 2 \cdot (q_{ia} - \frac{\Delta q}{2})] \right]^2} \quad (\text{C.1})$$

Simplification:

$$R_3 = \left[1 + A_g \cdot (F_g + 2 \cdot q_{ia}) + A_g \Delta q \right]^2 - \left[1 + A_g \cdot (F_g + 2 \cdot q_{ia}) - A_g \Delta q \right]^2$$

$$R_3 = \left[1 + A_g \cdot [F_g + 2 \cdot q_{ia}] \right]^2 \cdot \left\{ \left[1 + \frac{A_g \Delta q}{1 + A_g \cdot [F_g + 2 \cdot q_{ia}]} \right]^2 - \left[1 - \frac{A_g \Delta q}{1 + A_g \cdot [F_g + 2 \cdot q_{ia}]} \right]^2 \right\}$$

$$R_3 = 4 \cdot \Delta q \cdot A_g \cdot \left[1 + A_g \cdot [F_g + 2 \cdot q_{ia}] \right]$$

$$B_g \cdot \frac{R_3}{4} = B_g \cdot \Delta q \cdot A_g \cdot \left[1 + A_g \cdot [F_g + 2 \cdot q_{ia}] \right]$$

Since, $B_g = A_g \cdot [H_q - (F_g + 2 \cdot q_{ia})]$

$$B_g \cdot \frac{R_3}{4} = A_g^2 \cdot \Delta q \cdot [H_q - (F_g + 2 \cdot q_{ia})] \left[1 + A_g \cdot [F_g + 2 \cdot q_{ia}] \right]$$

$$\boxed{B_g \cdot \frac{R_3}{4} = A_g^2 \cdot \Delta q \cdot [H_q - (F_g + 2 \cdot q_{ia})] \left[1 + A_g \cdot [F_g + 2 \cdot q_{ia}] \right]} \quad (\text{C.2})$$

$$R_4 = \left[1 + A_g \cdot \left[F_g + 2 \cdot \left(q_{ia} + \frac{\Delta q}{2} \right) \right] \right]^{3/2} - \left[1 + A_g \cdot \left[F_g + 2 \cdot \left(q_{ia} - \frac{\Delta q}{2} \right) \right] \right]^{3/2} \quad (\text{D.1})$$

Simplification:

$$R_4 = \left[1 + A_g \cdot (F_g + 2 \cdot q_{ia}) + A_g \Delta q \right]^{3/2} - \left[1 + A_g \cdot (F_g + 2 \cdot q_{ia}) - A_g \Delta q \right]^{3/2}$$

$$R_4 = \left[1 + A_g \cdot [F_g + 2 \cdot q_{ia}] \right]^{3/2} \cdot \left\{ \left[1 + \frac{A_g \Delta q}{1 + A_g \cdot [F_g + 2 \cdot q_{ia}]} \right]^{3/2} - \left[1 - \frac{A_g \Delta q}{1 + A_g \cdot [F_g + 2 \cdot q_{ia}]} \right]^{3/2} \right\}$$

$$\text{Since, } (1+x)^{3/2} - (1-x)^{3/2} = (1+x)\sqrt{1+x} - (1-x)\sqrt{1-x} = \sqrt{1+x} - \sqrt{1-x} + x \cdot \left(\sqrt{1+x} + \sqrt{1-x} \right)$$

$$\text{Also, } (1 - B_g) = [1 + A_g \cdot (F_g + 2 \cdot q_{ia}) - A_g \cdot H_q]$$

$$\frac{2R_4}{3} \cdot (1 - B_g) = \frac{2}{3} \cdot [1 + A_g \cdot (F_g + 2 \cdot q_{ia}) - A_g \cdot H_q] \left[1 + A_g \cdot [F_g + 2 \cdot q_{ia}] \right]^{3/2} \cdot \left\{ \sqrt{1 + \frac{A_g \Delta q}{1 + A_g \cdot [F_g + 2 \cdot q_{ia}]}} - \sqrt{1 - \frac{A_g \Delta q}{1 + A_g \cdot [F_g + 2 \cdot q_{ia}]}} + \left(\frac{A_g \Delta q}{1 + A_g \cdot [F_g + 2 \cdot q_{ia}]} \right) \cdot \left(\sqrt{1 + \frac{A_g \Delta q}{1 + A_g \cdot [F_g + 2 \cdot q_{ia}]}} + \sqrt{1 - \frac{A_g \Delta q}{1 + A_g \cdot [F_g + 2 \cdot q_{ia}]}} \right) \right\} \quad (\text{D.2})$$

$$R_5 = \left[1 + A_g \cdot \left[F_g + 2 \cdot \left(q_{ia} + \frac{\Delta q}{2} \right) \right] \right] - \left[1 + A_g \cdot \left[F_g + 2 \cdot \left(q_{ia} - \frac{\Delta q}{2} \right) \right] \right] \quad (\text{E.1})$$

Simplification:

$$R_5 = \left[1 + A_g \cdot (F_g + 2 \cdot q_{ia}) + A_g \Delta q \right] - \left[1 + A_g \cdot (F_g + 2 \cdot q_{ia}) - A_g \Delta q \right]$$

$$R_5 = \left[1 + A_g \cdot [F_g + 2 \cdot q_{ia}] \right] \cdot \left\{ \left[1 + \frac{A_g \Delta q}{1 + A_g \cdot [F_g + 2 \cdot q_{ia}]} \right] - \left[1 - \frac{A_g \Delta q}{1 + A_g \cdot [F_g + 2 \cdot q_{ia}]} \right] \right\}$$

$$\text{Since, } (1+x) - (1-x) = 2x$$

$$R_5 = \left[1 + A_g \cdot [F_g + 2 \cdot q_{ia}] \right] \cdot \left\{ \frac{2 \cdot A_g \cdot \Delta q}{1 + A_g \cdot [F_g + 2 \cdot q_{ia}]} \right\} = 2 \cdot A_g \cdot \Delta q$$

$$\text{Also, } (1 - B_g) = [1 + A_g \cdot (F_g + 2 \cdot q_{ia}) - A_g \cdot H_q]$$

$$\frac{R_5}{2} \cdot (1 - B_g) = A_g \cdot \Delta q \cdot \left[1 + A_g \cdot (F_g + 2 \cdot q_{ia}) - A_g \cdot H_q \right] \quad (\text{E.2})$$

To obtain the final simplified expression of 26.14, we first only consider terms (A.2), (C.2) and (E.2) of Δq_G .

$$\widetilde{\Delta q_G} = \frac{1}{A_g^3 \cdot \Delta q \cdot H_q} \left\{ \frac{R_1}{6} + B_g \cdot \frac{R_3}{4} - \frac{R_5}{2} \cdot (1 - B_g) \right\} \quad (26.15)$$

$$\widetilde{\Delta q_G} = \frac{1}{A_g^3 \cdot \Delta q \cdot H_q} \left\{ \left(A_g \Delta q \left[1 + A_g \cdot [F_g + 2 \cdot q_{ia}] \right]^2 + \frac{(A_g \Delta q)^3}{3} \right) + \left(A_g^2 \cdot \Delta q \cdot [H_q - (F_g + 2 \cdot q_{ia})] \left[1 + A_g \cdot [F_g + 2 \cdot q_{ia}] \right] \right) - \left(A_g \cdot \Delta q \cdot \left[1 + A_g \cdot (F_g + 2 \cdot q_{ia}) - A_g \cdot H_q \right] \right) \right\}$$

$$\widetilde{\Delta q_G} = \frac{1}{A_g^3 \cdot \Delta q \cdot H_q} \left\{ \left(A_g \Delta q \left[1 + A_g \cdot [F_g + 2 \cdot q_{ia}] \right]^2 + \frac{(A_g \Delta q)^3}{3} \right) + \left(A_g^2 \cdot \Delta q \cdot [H_q - (F_g + 2 \cdot q_{ia})] \left[1 + A_g \cdot [F_g + 2 \cdot q_{ia}] \right] \right) - \left(A_g \cdot \Delta q \cdot \left[1 + A_g \cdot (F_g + 2 \cdot q_{ia}) - A_g \cdot H_q \right] \right) \right\}$$

$$\widetilde{\Delta q_G} = \frac{1}{A_g^2 \cdot H_q} \left\{ \left[1 + A_g \cdot [F_g + 2 \cdot q_{ia}] \right]^2 + [A_g \cdot H_q - A_g \cdot (F_g + 2 \cdot q_{ia})] \left[1 + A_g \cdot [F_g + 2 \cdot q_{ia}] \right] - \left[1 + A_g \cdot (F_g + 2 \cdot q_{ia}) - A_g \cdot H_q \right] \right\} + \frac{1}{3} \cdot \frac{\Delta q^2}{H_q}$$

$$\widetilde{\Delta q_G} = \frac{1 + A_g \cdot [F_g + 2 \cdot q_{ia}]}{A_g^2 \cdot H_q} \left\{ \left[1 + A_g \cdot [F_g + 2 \cdot q_{ia}] \right] + [A_g \cdot H_q - A_g \cdot (F_g + 2 \cdot q_{ia})] - \left[1 - \frac{A_g \cdot H_q}{1 + A_g \cdot (F_g + 2 \cdot q_{ia})} \right] \right\} + \frac{1}{3} \cdot \frac{\Delta q^2}{H_q}$$

$$\widetilde{\Delta q_G} = \frac{1 + A_g \cdot [F_g + 2 \cdot q_{ia}]}{A_g^2 \cdot H_q} \left\{ A_g \cdot H_q + \frac{A_g \cdot H_q}{1 + A_g \cdot (F_g + 2 \cdot q_{ia})} \right\} + \frac{1}{3} \cdot \frac{\Delta q^2}{H_q}$$

$$\widetilde{\Delta q_G} = \frac{1 + A_g \cdot [F_g + 2 \cdot q_{ia}]}{A_g} \left\{ 1 + \frac{1}{1 + A_g \cdot (F_g + 2 \cdot q_{ia})} \right\} + \frac{1}{3} \cdot \frac{\Delta q^2}{H_q}$$

$$\widetilde{\Delta q_G} = \frac{2 + A_g \cdot (F_g + 2 \cdot q_{ia})}{A_g} + \frac{1}{3} \cdot \frac{\Delta q^2}{H_q} \quad (15.1)$$

Now, (26.14) can be written as:

$$\Delta q_G = \widetilde{\Delta q_G} + \frac{1}{A_g^3 \cdot \Delta q \cdot H_q} \left[2 \cdot \frac{R_4}{3} \cdot (1 - B_g) - \frac{2 \cdot R_2}{5} \right] \quad (26.16)$$

Let:

$$\frac{1}{A_g^3 \cdot \Delta q \cdot H_q} \left[2 \cdot \frac{R_4}{3} \cdot (1 - B_g) \right] = D \quad \& \quad \frac{1}{A_g^3 \cdot \Delta q \cdot H_q} \left[\frac{2 \cdot R_2}{5} \right] = B$$

so that,

$$\Delta q_G = \widetilde{\Delta q}_G + D - B \quad (26.17)$$

We now simplify D and B , and then obtain a simplified expression for $(D - B)$:

$$D = \frac{1}{A_g^3 \cdot \Delta q \cdot H_q} \left[2 \cdot \frac{R_4}{3} \cdot (1 - B_g) \right] \quad (17.1)$$

$$\begin{aligned} \frac{2 \cdot R_4}{3} \cdot (1 - B_g) &= \frac{2}{3} \cdot [1 + A_g \cdot (F_g + 2 \cdot q_{ia}) - A_g \cdot H_q] \left[1 + A_g \cdot [F_g + 2 \cdot q_{ia}] \right]^{3/2} \cdot \left\{ \sqrt{1 + \frac{A_g \Delta q}{1 + A_g \cdot [F_g + 2 \cdot q_{ia}]}} - \sqrt{1 - \frac{A_g \Delta q}{1 + A_g \cdot [F_g + 2 \cdot q_{ia}]}} + \right. \\ &\quad \left. \left(\frac{A_g \Delta q}{1 + A_g \cdot [F_g + 2 \cdot q_{ia}]} \right) \cdot \left(\sqrt{1 + \frac{A_g \Delta q}{1 + A_g \cdot [F_g + 2 \cdot q_{ia}]}} + \sqrt{1 - \frac{A_g \Delta q}{1 + A_g \cdot [F_g + 2 \cdot q_{ia}]}} \right) \right\} \end{aligned}$$

$$\begin{aligned} D &= \frac{2}{3 \cdot A_g^3 \cdot \Delta q \cdot H_q} \cdot [1 + A_g \cdot (F_g + 2 \cdot q_{ia}) - A_g \cdot H_q] \left[1 + A_g \cdot [F_g + 2 \cdot q_{ia}] \right]^{3/2} \cdot \left\{ \sqrt{1 + \frac{A_g \Delta q}{1 + A_g \cdot [F_g + 2 \cdot q_{ia}]}} - \sqrt{1 - \frac{A_g \Delta q}{1 + A_g \cdot [F_g + 2 \cdot q_{ia}]}} + \right. \\ &\quad \left. \left(\frac{A_g \Delta q}{1 + A_g \cdot [F_g + 2 \cdot q_{ia}]} \right) \cdot \left(\sqrt{1 + \frac{A_g \Delta q}{1 + A_g \cdot [F_g + 2 \cdot q_{ia}]}} + \sqrt{1 - \frac{A_g \Delta q}{1 + A_g \cdot [F_g + 2 \cdot q_{ia}]}} \right) \right\} \end{aligned}$$

$$D = \frac{2}{3 \cdot A_g^3 \cdot \Delta q \cdot H_q} \cdot [1 + A_g \cdot (F_g + 2 \cdot q_{ia}) - A_g \cdot H_q] \frac{\sqrt{1 + A_g \cdot [F_g + 2 \cdot q_{ia}]}}{\sqrt{1 + \frac{A_g \Delta q}{1 + A_g \cdot [F_g + 2 \cdot q_{ia}]}} + \sqrt{1 - \frac{A_g \Delta q}{1 + A_g \cdot [F_g + 2 \cdot q_{ia}]}}} \cdot \left\{ (2 \cdot A_g \cdot \Delta q) + A_g \cdot \Delta q \left(2 + 2 \cdot \sqrt{1 - \frac{(A_g \Delta q)^2}{(1 + A_g \cdot [F_g + 2 \cdot q_{ia}])^2}} \right) \right\}$$

$$D = \frac{4}{3 \cdot A_g^2 \cdot H_q} \cdot [1 + A_g \cdot (F_g + 2 \cdot q_{ia}) - A_g \cdot H_q] \frac{\sqrt{1 + A_g \cdot [F_g + 2 \cdot q_{ia}]}}{\sqrt{1 + \frac{A_g \Delta q}{1 + A_g \cdot [F_g + 2 \cdot q_{ia}]}} + \sqrt{1 - \frac{A_g \Delta q}{1 + A_g \cdot [F_g + 2 \cdot q_{ia}]}}} \cdot \left\{ 2 + \sqrt{1 - \frac{(A_g \Delta q)^2}{(1 + A_g \cdot [F_g + 2 \cdot q_{ia}])^2}} \right\} \quad (17.2)$$

$$B = \frac{1}{A_g^3 \cdot \Delta q \cdot H_q} \left[\frac{2 \cdot R_2}{5} \right] \quad (17.3)$$

$$\begin{aligned} \frac{2 \cdot R_2}{5} &= \frac{2}{5} \cdot [1 + A_g \cdot [F_g + 2 \cdot q_{ia}]]^{5/2} \cdot \left\{ \left[1 + \frac{(A_g \Delta q)^2}{(1 + A_g \cdot [F_g + 2 \cdot q_{ia}])^2} \right] \cdot \left(\sqrt{1 + \frac{A_g \Delta q}{1 + A_g \cdot [F_g + 2 \cdot q_{ia}]}} - \sqrt{1 - \frac{A_g \Delta q}{1 + A_g \cdot [F_g + 2 \cdot q_{ia}]}} \right) \right. \\ &\quad \left. + 2 \cdot \left(\frac{A_g \Delta q}{1 + A_g \cdot [F_g + 2 \cdot q_{ia}]} \right) \cdot \left(\sqrt{1 + \frac{A_g \Delta q}{1 + A_g \cdot [F_g + 2 \cdot q_{ia}]}} + \sqrt{1 - \frac{A_g \Delta q}{1 + A_g \cdot [F_g + 2 \cdot q_{ia}]}} \right) \right\} \end{aligned}$$

$$\begin{aligned}
B &= \frac{2}{5} \cdot \frac{1}{A_g^3 \cdot \Delta q \cdot H_q} \cdot \left[1 + A_g \cdot [F_g + 2 \cdot q_{ia}] \right]^{5/2} \cdot \left\{ \left[1 + \frac{(A_g \Delta q)^2}{(1+A_g \cdot [F_g + 2 \cdot q_{ia}])^2} \right] \cdot \left(\sqrt{1 + \frac{A_g \Delta q}{1+A_g \cdot [F_g + 2 \cdot q_{ia}]}} - \sqrt{1 - \frac{A_g \Delta q}{1+A_g \cdot [F_g + 2 \cdot q_{ia}]}} \right) \right. \\
&\quad \left. + 2 \cdot \left(\frac{A_g \Delta q}{1+A_g \cdot [F_g + 2 \cdot q_{ia}]} \right) \cdot \left(\sqrt{1 + \frac{A_g \Delta q}{1+A_g \cdot [F_g + 2 \cdot q_{ia}]}} + \sqrt{1 - \frac{A_g \Delta q}{1+A_g \cdot [F_g + 2 \cdot q_{ia}]}} \right) \right\} \\
B &= \frac{2}{5 \cdot A_g^3 \cdot \Delta q \cdot H_q} \cdot \frac{\left(1 + A_g \cdot [F_g + 2 \cdot q_{ia}] \right)^{3/2}}{\sqrt{1 + \frac{A_g \Delta q}{1+A_g \cdot [F_g + 2 \cdot q_{ia}]}} + \sqrt{1 - \frac{A_g \Delta q}{1+A_g \cdot [F_g + 2 \cdot q_{ia}]}}} \cdot \left\{ \left[1 + \frac{(A_g \Delta q)^2}{(1+A_g \cdot [F_g + 2 \cdot q_{ia}])^2} \right] \cdot (2 \cdot A_g \cdot \Delta q) + 2 \cdot A_g \Delta q \cdot \left(2 + 2 \cdot \sqrt{1 - \frac{(A_g \Delta q)^2}{(1+A_g \cdot [F_g + 2 \cdot q_{ia}])^2}} \right) \right\} \\
B &= \frac{4}{5 \cdot A_g^2 \cdot H_q} \cdot \frac{\left(1 + A_g \cdot [F_g + 2 \cdot q_{ia}] \right)^{3/2}}{\sqrt{1 + \frac{A_g \Delta q}{1+A_g \cdot [F_g + 2 \cdot q_{ia}]}} + \sqrt{1 - \frac{A_g \Delta q}{1+A_g \cdot [F_g + 2 \cdot q_{ia}]}}} \cdot \left\{ 1 + \frac{(A_g \Delta q)^2}{(1+A_g \cdot [F_g + 2 \cdot q_{ia}])^2} + 2 + 2 \cdot \sqrt{1 - \frac{(A_g \Delta q)^2}{(1+A_g \cdot [F_g + 2 \cdot q_{ia}])^2}} \right\} \\
B &= \frac{4}{5 \cdot A_g^2 \cdot H_q} \cdot \frac{\left(1 + A_g \cdot [F_g + 2 \cdot q_{ia}] \right)^{3/2}}{\sqrt{1 + \frac{A_g \Delta q}{1+A_g \cdot [F_g + 2 \cdot q_{ia}]}} + \sqrt{1 - \frac{A_g \Delta q}{1+A_g \cdot [F_g + 2 \cdot q_{ia}]}}} \cdot \left\{ 3 + \frac{(A_g \Delta q)^2}{(1+A_g \cdot [F_g + 2 \cdot q_{ia}])^2} + 2 \cdot \sqrt{1 - \frac{(A_g \Delta q)^2}{(1+A_g \cdot [F_g + 2 \cdot q_{ia}])^2}} \right\}
\end{aligned} \tag{17.4}$$

$$\text{Let, } \alpha = \frac{1}{A_g^2 \cdot H_q} \cdot \frac{\sqrt{1 + A_g \cdot [F_g + 2 \cdot q_{ia}]}}{\sqrt{1 + \frac{A_g \Delta q}{1-A_g \cdot [F_g + 2 \cdot q_{ia}]}} + \sqrt{1 - \frac{A_g \Delta q}{1-A_g \cdot [F_g + 2 \cdot q_{ia}]}}}$$

Now, $D - B = \alpha \cdot \left\{ \frac{4}{3} \cdot \left[1 + A_g \cdot (F_g + 2 \cdot q_{ia}) - A_g \cdot H_q \right] \cdot \left(2 + \sqrt{1 - \frac{(A_g \Delta q)^2}{(1+A_g \cdot [F_g + 2 \cdot q_{ia}])^2}} \right) \right. \\ \left. - \frac{4}{5} \cdot (1 + A_g \cdot [F_g + 2 \cdot q_{ia}]) \left[3 + \frac{(A_g \Delta q)^2}{(1+A_g \cdot [F_g + 2 \cdot q_{ia}])^2} + 2 \cdot \sqrt{1 - \frac{(A_g \Delta q)^2}{(1+A_g \cdot [F_g + 2 \cdot q_{ia}])^2}} \right] \right\}$

$$\begin{aligned}
D - B &= \alpha \cdot \left\{ \frac{8}{3} \cdot \left[1 + A_g \cdot (F_g + 2 \cdot q_{ia}) \right] + \frac{4}{3} \cdot \left[1 + A_g \cdot (F_g + 2 \cdot q_{ia}) \right] \left(\sqrt{1 - \frac{(A_g \Delta q)^2}{(1+A_g \cdot [F_g + 2 \cdot q_{ia}])^2}} - \frac{8}{3} \cdot (A_g \cdot H_q) - \frac{4}{3} \cdot (A_g \cdot H_q) \cdot \left(\sqrt{1 - \frac{(A_g \Delta q)^2}{(1+A_g \cdot [F_g + 2 \cdot q_{ia}])^2}} \right) \right. \right. \\ &\quad \left. \left. - \frac{12}{5} \cdot (1 + A_g \cdot [F_g + 2 \cdot q_{ia}]) - \frac{4}{5} \cdot \frac{(A_g \Delta q)^2}{(1+A_g \cdot [F_g + 2 \cdot q_{ia}])^2} - \frac{8}{5} \cdot (1 + A_g \cdot [F_g + 2 \cdot q_{ia}]) \sqrt{1 - \frac{(A_g \Delta q)^2}{(1-A_g \cdot [F_g + 2 \cdot q_{ia}])^2}} \right) \right\}
\end{aligned}$$

$$\begin{aligned}
D - B &= \alpha \cdot \left\{ \frac{4}{15} \cdot \left[1 + A_g \cdot (F_g + 2 \cdot q_{ia}) \right] - \frac{4}{15} \cdot \left[1 + A_g \cdot (F_g + 2 \cdot q_{ia}) \right] \left(\sqrt{1 - \frac{(A_g \Delta q)^2}{(1+A_g \cdot [F_g + 2 \cdot q_{ia}])^2}} - \frac{8}{3} \cdot (A_g \cdot H_q) - \frac{4}{3} \cdot (A_g \cdot H_q) \cdot \left(\sqrt{1 - \frac{(A_g \Delta q)^2}{(1+A_g \cdot [F_g + 2 \cdot q_{ia}])^2}} \right) \right. \right. \\ &\quad \left. \left. - \frac{4}{5} \cdot \frac{(A_g \Delta q)^2}{(1+A_g \cdot [F_g + 2 \cdot q_{ia}])^2} \right) \right\}
\end{aligned}$$

$$D - B = \alpha \cdot \left\{ \frac{4}{15} \cdot \left[1 + A_g \cdot (F_g + 2 \cdot q_{ia}) \right] \left(1 - \sqrt{1 - \frac{(A_g \Delta q)^2}{(1 + A_g \cdot [F_g + 2 \cdot q_{ia}])^2}} \right) - \frac{4}{3} \cdot (A_g \cdot H_q) \left(2 + \sqrt{1 - \frac{(A_g \Delta q)^2}{(1 + A_g \cdot [F_g + 2 \cdot q_{ia}])^2}} \right) - \frac{4}{5} \cdot \frac{(A_g \Delta q)^2}{(1 + A_g \cdot [F_g + 2 \cdot q_{ia}])} \right\} \quad (17.5)$$

Now, with this simplification (26.17) reads as follows:

$$\Delta q_G = \frac{2 + A_g \cdot (F_g + 2 \cdot q_{ia})}{A_g} + \frac{1}{3} \cdot \frac{\Delta q^2}{H_q} + (D - B) \quad (26.18)$$

where, $(D - B)$ is given by (17.5)

$$\text{and, } \alpha = \frac{1}{A_g^2 \cdot H_q} \cdot \frac{\sqrt{1 + A_g \cdot [F_g + 2 \cdot q_{ia}]}}{\sqrt{1 + \frac{A_g \Delta q}{1 + A_g \cdot [F_g + 2 \cdot q_{ia}]}} + \sqrt{1 - \frac{A_g \Delta q}{1 + A_g \cdot [F_g + 2 \cdot q_{ia}]}}}$$

$$B_g = A_g \cdot \left[H_q - (F_g + 2 \cdot q_{ia}) \right] \quad ; \quad F_g = (v_g - v_{fb} - \psi_p) \quad ; \quad A_g = \left(\frac{2}{\gamma_g} \right)^2 \quad ; \quad (\gamma'_g)^2 = (\gamma_g)^2 / V_t$$

$$q_{ia} = \frac{q_s + q_d}{2} \quad ; \quad \Delta q = q_s - q_d \quad ; \quad H_q = (1 + 2q_{ia}/D_{vsat}) = 1 + \frac{q_s + q_d}{D_{vsat}}$$

Now, (26.5) reads as follows:

$$q_B = q_{B1} - \Delta q_G$$

where

$$q_{B1} = (v_g - v_{fb} - \psi_p) - 2 \cdot (n_q - 1) \cdot \int_0^1 q \, d\xi$$

Refer to (9.18) for q_{B1} derivation:

$$q_{B1} = F_g - \left\{ (n_q - 1) \left(q_s + q_d + \frac{1}{3} \cdot \frac{(q_s - q_d)^2}{1 + q_s + q_d} \right) \right\} \quad (26.19)$$

$$q_{B1} = F_g - 2 \cdot (n_q - 1) \left(q_{ia} + \frac{1}{6} \cdot \frac{(\Delta q)^2}{1 + q_s + q_d} \right) \quad (26.20)$$

Using this expression for q_{B1} in (26.18):

$$q_B = F_g - 2 \cdot (n_q - 1) \left(q_{ia} + \frac{1}{6} \cdot \frac{(\Delta q)^2}{1 + q_s + q_d} \right) - \frac{[2 + A_g \cdot (F_g + 2 \cdot q_{ia})]}{A_g} - \frac{1}{3} \cdot \frac{\Delta q^2}{H_q} - (D - B) \quad (26.21)$$

Upon rearranging:

$$q_B = F_g - 2 \cdot n_q \cdot \left(q_{ia} + \frac{1}{6} \cdot \frac{(\Delta q)^2}{H_q} \right) + 2 \cdot \left(q_{ia} + \frac{1}{6} \cdot \frac{(\Delta q)^2}{H_q} \right) - \frac{2}{A_g} - F_g - 2 \cdot q_{ia} - \frac{1}{3} \cdot \frac{\Delta q^2}{H_q} - (D - B)$$

$$q_B = -2 \cdot n_q \cdot \left(q_{ia} + \frac{1}{6} \cdot \frac{(\Delta q)^2}{H_q} \right) - \frac{2}{A_g} - (D - B) \quad (26.22)$$

$$\begin{aligned} q_B &= -2 \cdot n_q \cdot \left(q_{ia} + \frac{1}{6} \cdot \frac{(\Delta q)^2}{H_q} \right) - \frac{2}{A_g} - \alpha \cdot \left\{ \frac{4}{15} \cdot \left[1 + A_g \cdot (F_g + 2 \cdot q_{ia}) \right] \left(1 - \sqrt{1 - \frac{(A_g \Delta q)^2}{(1 + A_g \cdot [F_g + 2 \cdot q_{ia}])^2}} \right) \right. \\ &\quad \left. - \frac{4}{3} \cdot (A_g \cdot H_q) \left(2 + \sqrt{1 - \frac{(A_g \Delta q)^2}{(1 + A_g \cdot [F_g + 2 \cdot q_{ia}])^2}} \right) - \frac{4}{5} \cdot \frac{(A_g \Delta q)^2}{(1 + A_g \cdot [F_g + 2 \cdot q_{ia}])} \right\} \end{aligned}$$

$$\begin{aligned} q_B &= -2 \cdot n_q \cdot \left(q_{ia} + \frac{1}{6} \cdot \frac{(\Delta q)^2}{H_q} \right) - \frac{2}{A_g} - \alpha \cdot \left\{ \frac{4}{15} \cdot \left[1 + A_g \cdot (F_g + 2 \cdot q_{ia}) \right] \left(1 - \sqrt{1 - \frac{(A_g \Delta q)^2}{(1 + A_g \cdot [F_g + 2 \cdot q_{ia}])^2}} \right) \right. \\ &\quad \left. - \frac{4}{3} \cdot (A_g \cdot H_q) \left(2 + \sqrt{1 - \frac{(A_g \Delta q)^2}{(1 + A_g \cdot [F_g + 2 \cdot q_{ia}])^2}} \right) - \frac{4}{5} \cdot \frac{(A_g \Delta q)^2}{(1 + A_g \cdot [F_g + 2 \cdot q_{ia}])} \right\} \end{aligned}$$

$$\begin{aligned} q_B &= -n_q \cdot \left(q_s + q_d + \frac{1}{3} \cdot \frac{(q_s - q_d)^2}{1 + q_s + q_d} \right) - \frac{2}{A_g} - \alpha \cdot \left\{ \frac{4}{15} \cdot \left[1 + A_g \cdot (F_g + 2 \cdot q_{ia}) \right] \left(1 - \sqrt{1 - \frac{(A_g \Delta q)^2}{(1 + A_g \cdot [F_g + 2 \cdot q_{ia}])^2}} \right) \right. \\ &\quad \left. - \frac{4}{3} \cdot (A_g \cdot H_q) \left(2 + \sqrt{1 - \frac{(A_g \Delta q)^2}{(1 + A_g \cdot [F_g + 2 \cdot q_{ia}])^2}} \right) - \frac{4}{5} \cdot \frac{(A_g \Delta q)^2}{(1 + A_g \cdot [F_g + 2 \cdot q_{ia}])} \right\} \quad (26.23) \end{aligned}$$

$$\text{where, } \alpha = \frac{1}{A_g^2 \cdot H_q} \cdot \frac{\sqrt{1 + A_g \cdot [F_g + 2 \cdot q_{ia}]}}{\sqrt{1 + \frac{A_g \Delta q}{1 - A_g \cdot [F_g + 2 \cdot q_{ia}]}} + \sqrt{1 - \frac{A_g \Delta q}{1 - A_g \cdot [F_g + 2 \cdot q_{ia}]}}}$$

Now we proceed by defining following:

$$\delta_s = \frac{A_g}{4} \cdot (F_g + 2 \cdot q_s) = \frac{v_g - v_{fb} - \psi_p + 2 \cdot q_s}{(\gamma'_g)^2} = \frac{v_g - v_{fb} - \psi_p + q_s - q_d + q_s + q_d}{(\gamma'_g)^2}$$

$$\delta_s = \frac{v_g - v_{fb} - \psi_p + \Delta q + 2 \cdot q_{ia}}{(\gamma'_g)^2} \implies \boxed{\delta_s = \frac{A_g}{4} \cdot (F_g + 2 \cdot q_{ia} + \Delta q)}$$

$$\delta_d = \frac{v_g - v_{fb} - \psi_p + 2 \cdot q_{ia} - \Delta q}{(\gamma'_g)^2} \implies \boxed{\delta_d = \frac{A_g}{4} \cdot (F_g + 2 \cdot q_{ia} - \Delta q)}$$

$$\boxed{x = \frac{1}{4} + \delta_s} \quad \text{and} \quad \boxed{y = \frac{1}{4} + \delta_d}$$

In pursuit of expressing (26.23) in terms of x and y, we evaluate following terms:

$$(1 + A_g \cdot [F_g + 2 \cdot q_{ia}]) = 1 + 2 \cdot (\delta_s + \delta_d) = 2 \cdot \left[\frac{1}{2} + (\delta_s + \delta_d) \right] = 2 \cdot \left[\frac{1}{4} + \delta_s + \frac{1}{4} + \delta_d \right] = 2 \cdot (x + y)$$

$$1 + \frac{A_g \Delta q}{1 + A_g \cdot [F_g + 2 \cdot q_{ia}]} = \frac{1 + A_g \cdot [F_g + 2 \cdot q_{ia} + \Delta q]}{1 + A_g \cdot [F_g + 2 \cdot q_{ia}]} = \frac{1 + 4 \cdot \delta_s}{1 + 2 \cdot (\delta_s + \delta_d)} = \frac{\frac{1}{4} + \delta_s}{\frac{1}{4} + \frac{1}{2} \cdot (\delta_s + \delta_d)} = 2 \cdot \frac{x}{(x + y)}$$

$$1 - \frac{A_g \Delta q}{1 + A_g \cdot [F_g + 2 \cdot q_{ia}]} = \frac{1 + A_g \cdot [F_g + 2 \cdot q_{ia} - \Delta q]}{1 + A_g \cdot [F_g + 2 \cdot q_{ia}]} = \frac{1 + 4 \cdot \delta_d}{1 + 2 \cdot (\delta_s + \delta_d)} = \frac{\frac{1}{4} + \delta_d}{\frac{1}{4} + \frac{1}{2} \cdot (\delta_s + \delta_d)} = 2 \cdot \frac{y}{(x + y)}$$

$$\Delta q = \frac{2}{A_g} \cdot (\delta_s - \delta_d) = \frac{2}{A_g} \cdot (x - y) \quad \text{or} \quad A_g = \frac{2 \cdot (x - y)}{\Delta q}$$

Now, (26.23) reads as follows:

$$q_B = -n_q \cdot \left(q_s + q_d + \frac{1}{3} \cdot \frac{(q_s - q_d)^2}{1 + q_s + q_d} \right) - \frac{\Delta q}{(x - y)} - \alpha \cdot \left\{ \frac{8}{15} \cdot [x + y] \left(1 - \sqrt{\frac{2 \cdot x}{x+y} \cdot \frac{2 \cdot y}{x+y}} \right) - \frac{4}{3} \cdot \left(\frac{2 \cdot (x-y)}{\Delta q} \cdot H_q \right) \left(2 + \sqrt{\frac{2 \cdot x}{x+y} \cdot \frac{2 \cdot y}{x+y}} \right) - \frac{4}{5} \cdot \frac{[(x-y)]^2}{2 \cdot (x+y)} \right\} \quad (26.24)$$

$$\text{where, } \alpha = \frac{1}{\left[\frac{2 \cdot (x-y)}{\Delta q} \right]^2 \cdot H_q} \cdot \frac{\sqrt{2 \cdot (x+y)}}{\sqrt{2 \cdot \frac{x}{(x+y)}} + \sqrt{2 \cdot \frac{y}{(x+y)}}} = \frac{1}{\left[\frac{2 \cdot (x-y)}{\Delta q} \right]^2 \cdot H_q} \cdot \frac{\sqrt{(x+y)}}{\sqrt{\frac{x}{(x+y)}} + \sqrt{\frac{y}{(x+y)}}}$$

$$\text{Let, } \widetilde{q_B} = -n_q \cdot \left(q_s + q_d + \frac{1}{3} \cdot \frac{(q_s - q_d)^2}{1 + q_s + q_d} \right) - \frac{\Delta q}{(x - y)}$$

Then we can write:

$$q_B = \widetilde{q_B} - \frac{1}{4 \cdot \left[\frac{(x-y)}{\Delta q} \right]^2 \cdot H_q} \cdot \frac{\sqrt{(x+y)}}{\sqrt{\frac{x}{(x+y)}} + \sqrt{\frac{y}{(x+y)}}} \cdot \left\{ \frac{8}{15} \cdot [x + y] \left(1 - 2 \cdot \sqrt{\frac{x \cdot y}{(x+y)^2}} \right) - \frac{8}{3} \cdot \left(\frac{2 \cdot (x-y)}{\Delta q} \cdot H_q \right) \left(1 + \sqrt{\frac{x \cdot y}{(x+y)^2}} \right) - \frac{8}{5} \cdot \frac{[(x-y)]^2}{(x+y)} \right\} \quad (26.25)$$

Simplification:

$$q_B = \widetilde{q_B} - \frac{(\Delta q)^2 (x+y)}{4 \cdot (x-y)^2 \cdot H_q (\sqrt{x} + \sqrt{y})} \cdot \left\{ \frac{8}{15} \cdot [x + y] \left(1 - 2 \cdot \frac{\sqrt{x \cdot y}}{x+y} \right) - \frac{16}{3} \cdot \left(\frac{(x-y)}{\Delta q} \cdot H_q \right) \left(1 + \frac{\sqrt{x \cdot y}}{x+y} \right) - \frac{8}{5} \cdot \frac{[(x-y)]^2}{(x+y)} \right\}$$

$$q_B = \widetilde{q_B} - \frac{(\Delta q)^2 (x+y)}{(x-y)^2 \cdot H_q (\sqrt{x} + \sqrt{y})} \cdot \left\{ \frac{2}{15} \cdot \left(x + y - 2 \cdot \sqrt{x \cdot y} \right) - \left(\frac{4 \cdot (x-y) \cdot H_q}{3 \cdot \Delta q} \right) \left(\frac{x+y+\sqrt{x \cdot y}}{x+y} \right) - \frac{2}{5} \cdot \frac{[(x-y)]^2}{(x+y)} \right\}$$

$$\begin{aligned}
q_B &= \widetilde{q}_B - \frac{(\Delta q)^2(x+y)}{(x-y)^2 \cdot H_q(\sqrt{x}+\sqrt{y})} \cdot \left\{ \frac{2}{15} \cdot \left(x + y - 2 \cdot \sqrt{x \cdot y} \right) - \frac{2}{5} \cdot \frac{[(x-y)]^2}{(x+y)} \right\} + \left(\frac{4 \cdot \Delta q}{3 \cdot (x-y)} \right) \left(\frac{x+y+\sqrt{x \cdot y}}{(\sqrt{x}+\sqrt{y})} \right) \\
q_B &= \widetilde{q}_B - \frac{(\Delta q)^2}{(x-y)^2 \cdot H_q(\sqrt{x}+\sqrt{y})} \cdot \frac{2}{15} \cdot \left\{ \left(x^2 + y^2 + 2 \cdot x \cdot y - 2 \cdot (x+y) \cdot \sqrt{x \cdot y} \right) - 3 \cdot [x^2 + y^2 - 2 \cdot x \cdot y] \right\} + \frac{4 \cdot \Delta q}{3 \cdot (x-y)} \cdot \left(\frac{x+y+\sqrt{x \cdot y}}{(\sqrt{x}+\sqrt{y})} \right) \\
q_B &= \widetilde{q}_B + \frac{(\Delta q)^2}{(x-y)^2 \cdot H_q(\sqrt{x}+\sqrt{y})} \cdot \frac{4}{15} \cdot \left\{ x^2 + y^2 - 4 \cdot x \cdot y + (x+y) \cdot \sqrt{x \cdot y} \right\} + \frac{4 \cdot \Delta q}{3 \cdot (x-y)} \cdot \left(\frac{x+y+\sqrt{x \cdot y}}{(\sqrt{x}+\sqrt{y})} \right) \\
q_B &= \widetilde{q}_B + \frac{(\Delta q)^2}{(x-y)^2 \cdot H_q(\sqrt{x}+\sqrt{y})} \cdot \frac{4}{15} \cdot \left\{ (x-y)^2 - 2 \cdot x \cdot y + (x+y) \cdot \sqrt{x \cdot y} \right\} + \frac{4 \cdot \Delta q}{3 \cdot (x-y)} \cdot \left(\frac{x+y+\sqrt{x \cdot y}}{(\sqrt{x}+\sqrt{y})} \right) \\
q_B &= -n_q \cdot \left(q_s + q_d + \frac{1}{3} \cdot \frac{(q_s-q_d)^2}{1+q_s+q_d} \right) - \frac{\Delta q}{(x-y)} + \frac{(\Delta q)^2}{(x-y)^2 \cdot H_q(\sqrt{x}+\sqrt{y})} \cdot \frac{4}{15} \cdot \left\{ (x-y)^2 - 2 \cdot x \cdot y + (x+y) \cdot \sqrt{x \cdot y} \right\} + \frac{4 \cdot \Delta q}{3 \cdot (x-y)} \cdot \left(\frac{x+y+\sqrt{x \cdot y}}{(\sqrt{x}+\sqrt{y})} \right) \\
q_B &= -n_q \cdot \left(q_s + q_d + \frac{1}{3} \cdot \frac{(q_s-q_d)^2}{1+q_s+q_d} \right) - \frac{2}{A_g} + \frac{(\Delta q)^2}{(x-y)^2 \cdot H_q(\sqrt{x}+\sqrt{y})} \cdot \frac{4}{15} \cdot \left\{ x^2 + y^2 - 4 \cdot x \cdot y + (x+y) \sqrt{x \cdot y} \right\} + \frac{4 \cdot \Delta q}{3 \cdot (x-y)} \cdot \left(\frac{x+y+\sqrt{x \cdot y}}{(\sqrt{x}+\sqrt{y})} \right)
\end{aligned} \tag{26.26}$$

Let $\hat{q}_B = -n_q \cdot \left(q_s + q_d + \frac{1}{3} \cdot \frac{(q_s-q_d)^2}{1+q_s+q_d} \right)$ so that (26.26) reads:

$$q_B = -\frac{2}{A_g} + \frac{4 \cdot \Delta q}{3 \cdot (x-y)} \cdot \left(\frac{x+y+\sqrt{x \cdot y}}{(\sqrt{x}+\sqrt{y})} \right) + \frac{(\Delta q)^2}{(x-y)^2 \cdot H_q(\sqrt{x}+\sqrt{y})} \cdot \frac{4}{15} \cdot \left\{ x^2 + y^2 - 4 \cdot x \cdot y + (x+y) \sqrt{x \cdot y} \right\} + \hat{q}_B$$

$$q_B = -\frac{2}{A_g} + \frac{2}{A_g} \frac{4}{3} \cdot \left(\frac{x+y+\sqrt{x \cdot y}}{(\sqrt{x}+\sqrt{y})} \right) + \frac{(\Delta q)^2}{(x-y)^2 \cdot H_q(\sqrt{x}+\sqrt{y})} \cdot \frac{4}{15} \cdot \left\{ [x+y+3\sqrt{x \cdot y}] \cdot [x+y-2\sqrt{x \cdot y}] \right\} + \hat{q}_B \tag{26.27}$$

$$\text{Now, Let } \Theta = -\frac{2}{A_g} + \frac{2}{A_g} \frac{4}{3} \cdot \left(\frac{x+y+\sqrt{x \cdot y}}{(\sqrt{x}+\sqrt{y})} \right)$$

Rearranging:

$$\begin{aligned}
\Theta &= -\frac{2}{A_g} + \frac{2}{A_g} \frac{1}{3} \cdot \left(\frac{4x+4y+4\sqrt{x \cdot y}}{(\sqrt{x}+\sqrt{y})} \right) = -\frac{2}{A_g} + \frac{2}{A_g} \frac{1}{3} \cdot \left(\frac{3x+3y+6\sqrt{x \cdot y}+x+y-2\sqrt{x \cdot y}}{(\sqrt{x}+\sqrt{y})} \right) \\
\Theta &= -\frac{2}{A_g} + \frac{2}{A_g} \frac{1}{3} \cdot \left(\frac{3 \cdot (\sqrt{x}+\sqrt{y})^2 + (\sqrt{x}-\sqrt{y})^2}{(\sqrt{x}+\sqrt{y})} \right) = -\frac{2}{A_g} + \frac{2}{A_g} \cdot \left((\sqrt{x}+\sqrt{y}) + \frac{(\sqrt{x}-\sqrt{y})^2}{3 \cdot (\sqrt{x}+\sqrt{y})} \right) \\
\Theta &= \frac{2}{A_g} \cdot \left\{ \sqrt{x} + \sqrt{y} - 1 \right\} + \frac{2}{A_g} \cdot \left(\frac{(\sqrt{x}-\sqrt{y})^2}{3 \cdot (\sqrt{x}+\sqrt{y})} \right) = \frac{2}{A_g} \cdot \left\{ \sqrt{x} + \sqrt{y} - 1 \right\} + \frac{2}{A_g} \cdot \left(\frac{(\sqrt{x}+\sqrt{y})^2 \cdot (\sqrt{x}-\sqrt{y})^2}{3 \cdot (\sqrt{x}+\sqrt{y})^3} \right) \\
\Theta &= \frac{2}{A_g} \cdot \left\{ \sqrt{x} + \sqrt{y} - 1 \right\} + \frac{2}{A_g} \cdot \left(\frac{(x-y)^2}{3 \cdot (\sqrt{x}+\sqrt{y})^3} \right) = \frac{2}{A_g} \cdot \left\{ \sqrt{x} + \sqrt{y} - 1 \right\} + \frac{1}{3 \cdot (\sqrt{x}+\sqrt{y})^3} \cdot \left(\frac{2}{A_g} \right)^2 \cdot (x-y)^2 \cdot \frac{A_g}{2}
\end{aligned}$$

$$\boxed{\Theta = \frac{2}{A_g} \cdot \left\{ \sqrt{x} + \sqrt{y} - 1 \right\} + \frac{1}{3 \cdot (\sqrt{x} + \sqrt{y})^3} \cdot \left(\frac{2}{A_g} \right)^2 \cdot (x - y)^2 \cdot \frac{A_g}{2}} \quad (26.28)$$

$$\text{Now, } \frac{2}{A_g} \cdot \left((\sqrt{x} + \sqrt{y}) - 1 \right) = \frac{1}{A_g} \cdot \left(2 \cdot \sqrt{x} - 1 + 2 \cdot \sqrt{y} - 1 \right) = \frac{1}{A_g} \cdot \left(\frac{(1+2 \cdot \sqrt{x}) \cdot (2 \cdot \sqrt{x} - 1) \cdot (1+2 \cdot \sqrt{y}) + (1+2 \cdot \sqrt{x}) \cdot (2 \cdot \sqrt{y} - 1) \cdot (1+2 \cdot \sqrt{y})}{(1+2 \cdot \sqrt{x}) \cdot (1+2 \cdot \sqrt{y})} \right)$$

$$\frac{2}{A_g} \cdot \left((\sqrt{x} + \sqrt{y}) - 1 \right) = \frac{1}{A_g} \cdot \left(\frac{(4x - 1) \cdot (1+2 \cdot \sqrt{y}) + (1+2 \cdot \sqrt{x}) \cdot (4y - 1)}{(1+2 \cdot \sqrt{x}) \cdot (1+2 \cdot \sqrt{y})} \right) = \frac{1}{A_g} \cdot \left(\frac{4 \cdot \delta_s \cdot (1+2 \cdot \sqrt{y}) + (1+2 \cdot \sqrt{x}) \cdot 4 \cdot \delta_d}{(1+2 \cdot \sqrt{x}) \cdot (1+2 \cdot \sqrt{y})} \right)$$

$$\frac{2}{A_g} \cdot \left((\sqrt{x} + \sqrt{y}) - 1 \right) = \frac{1}{A_g} \cdot \left(\frac{4 \cdot \delta_s}{(1+2 \cdot \sqrt{x})} + \frac{4 \cdot \delta_d}{(1+2 \cdot \sqrt{y})} \right) = \left(\frac{F_g + 2 \cdot q_s}{(1+2 \cdot \sqrt{x})} + \frac{F_g + 2 \cdot q_d}{(1+2 \cdot \sqrt{y})} \right)$$

$$\boxed{\frac{2}{A_g} \cdot \left((\sqrt{x} + \sqrt{y}) - 1 \right) = \left(\frac{F_g + 2 \cdot q_s}{(1+2 \cdot \sqrt{x})} + \frac{F_g + 2 \cdot q_d}{(1+2 \cdot \sqrt{y})} \right) = A + B} \quad (26.29)$$

$$\boxed{\Theta = A + B + \frac{1}{3 \cdot (\sqrt{x} + \sqrt{y})^3} \cdot \left(\frac{2}{A_g} \right)^2 \cdot (x - y)^2 \cdot \frac{A_g}{2}} \quad (26.30)$$

Using (26.30), equation (26.27) reads:

$$q_B = A + B + \frac{1}{3 \cdot (\sqrt{x} + \sqrt{y})^3} \cdot \left(\frac{2}{A_g} \right)^2 \cdot (x - y)^2 \cdot \frac{A_g}{2} + \frac{(\Delta q)^2}{(x-y)^2 \cdot H_q(\sqrt{x} + \sqrt{y})} \cdot \frac{4}{15} \cdot \left\{ [x + y + 3\sqrt{xy}] \cdot [x + y - 2\sqrt{xy}] \right\} + \hat{q}_B \quad (26.31)$$

Rearranging:

$$q_B = A + B + \frac{1}{3 \cdot (\sqrt{x} + \sqrt{y})^3} \cdot (\Delta q)^2 \cdot \frac{A_g}{2} + \frac{(\Delta q)^2}{H_q(\sqrt{x} + \sqrt{y})} \cdot \frac{4}{15} \cdot \left\{ (x - y)^2 - 2 \cdot x \cdot y + (x + y) \cdot \sqrt{xy} \right\} + \hat{q}_B$$

$$q_B = A + B + \frac{1}{3 \cdot (\sqrt{x} + \sqrt{y})^3} \cdot (\Delta q)^2 \cdot \frac{A_g}{2} + \frac{(\Delta q)^2}{H_q(\sqrt{x} + \sqrt{y})} \cdot \frac{4}{15} \cdot \left\{ 1 - \frac{2 \cdot x \cdot y}{(x-y)^2} + \frac{(x+y) \cdot \sqrt{xy}}{(x-y)^2} \right\} + \hat{q}_B$$

$$q_B = A + B + \frac{1}{3 \cdot (\sqrt{x} + \sqrt{y})^3} \cdot (\Delta q)^2 \cdot \frac{A_g}{2} + \frac{(\Delta q)^2}{H_q(\sqrt{x} + \sqrt{y})} \cdot \frac{4}{15} \cdot \left\{ (\sqrt{x} + \sqrt{y})^2 - \frac{2 \cdot x \cdot y}{(\sqrt{x} - \sqrt{y})^2} + \frac{(x+y) \cdot \sqrt{xy}}{(\sqrt{x} - \sqrt{y})^2} \right\} + \hat{q}_B$$

$$q_B = A + B + \frac{1}{3 \cdot (\sqrt{x} + \sqrt{y})^3} \cdot (\Delta q)^2 \cdot \frac{A_g}{2} + \frac{(\Delta q)^2}{H_q(\sqrt{x} + \sqrt{y})} \cdot \frac{4}{15} \cdot \left\{ \frac{(x-y)^2 - 2 \cdot x \cdot y + (x+y) \cdot \sqrt{xy}}{(\sqrt{x} - \sqrt{y})^2} \right\} + \hat{q}_B$$

$$q_B = A + B + \frac{1}{3.(\sqrt{x}+\sqrt{y})^3} \cdot (\Delta q)^2 \cdot \frac{A_g}{2} + \frac{(\Delta q)^2}{H_q(\sqrt{x}+\sqrt{y})^3} \cdot \frac{4}{15} \cdot \left\{ \frac{(x+y+3\sqrt{x.y}).(\sqrt{x}-\sqrt{y})^2}{(\sqrt{x}-\sqrt{y})^2} \right\} + \hat{q}_B$$

$$q_B = A + B + \frac{1}{3.(\sqrt{x}+\sqrt{y})^3} \cdot (\Delta q)^2 \cdot \frac{A_g}{2} + \frac{(\Delta q)^2}{H_q(\sqrt{x}+\sqrt{y})^3} \cdot \frac{4}{15} \cdot \left\{ (x+y+3\sqrt{x.y}) \right\} + \hat{q}_B$$

$$q_B = A + B + \frac{(\Delta q)^2}{3.(\sqrt{x}+\sqrt{y})^3} \cdot \left\{ \frac{4}{5} \cdot (x+y+3\sqrt{x.y}) \cdot \frac{1}{H_q} + \frac{A_g}{2} \right\} + \hat{q}_B$$

$$q_B = A + B + \frac{(\Delta q)^2}{3.(\sqrt{x}+\sqrt{y})^3} \cdot \left\{ \frac{4}{5} \cdot (x+y+3\sqrt{x.y}) \cdot \frac{1}{H_q} + \frac{2}{(\gamma'_g)^2} \right\} + \hat{q}_B$$

$$q_B = A + B + \frac{(\Delta q)^2}{3.(\sqrt{x}+\sqrt{y})^3} \cdot \left\{ \frac{4}{5} \cdot \left((\sqrt{x}+\sqrt{y})^2 + \sqrt{x.y} \right) \cdot \frac{1}{H_q} + \frac{2}{(\gamma'_g)^2} \right\} + \hat{q}_B$$

$$q_B = A + B + \frac{(\Delta q)^2}{3.(\sqrt{x}+\sqrt{y})^3} \cdot \left\{ \frac{4}{5} \cdot \left((\sqrt{x}+\sqrt{y})^2 + \sqrt{x.y} \right) \cdot \frac{1}{H_q} + \frac{2}{(\gamma'_g)^2} \right\} - n_q \cdot \left(q_s + q_d + \frac{1}{3} \cdot \frac{(q_s - q_d)^2}{1 + q_s + q_d} \right) \quad (26.32)$$

$$q_B = A + B + \frac{1}{3} \cdot \frac{(\Delta q)^2}{C^3} \cdot \left\{ \frac{8}{10} \left(C^2 + P.Q \right) \cdot \frac{1}{1 + q_s + q_d} + \frac{2}{(\gamma'_g)^2} \right\} - n_q \cdot \left(q_s + q_d + \frac{1}{3} \cdot \frac{(q_s - q_d)^2}{1 + q_s + q_d} \right)$$

(26.33)

where $A = \frac{v_g - v_{fb} - \psi_p + 2.q_s}{1 + 2.\sqrt{x}}$ $B = \frac{v_g - v_{fb} - \psi_p + 2.q_d}{1 + 2.\sqrt{y}}$ $x = \frac{1}{4} + \frac{v_g - v_{fb} - \psi_p + 2.q_s}{(\gamma'_g)^2}$ $y = \frac{1}{4} + \frac{v_g - v_{fb} - \psi_p + 2.q_d}{(\gamma'_g)^2}$

$$\begin{aligned} P &= \sqrt{x} & Q &= \sqrt{y} \\ C &= P + Q \end{aligned}$$

The above equation (26.33) is same as (9.20).

References

- [1] Y. S. Chauhan, S. Venugopalan, M.-A. Chalkiadaki, M. Karim, H. Agarwal, S. Khandelwal, N. Paydavosi, J. Duarte, C. Enz, A. Niknejad, and C. Hu, “BSIM6: Analog and RF Compact Model for Bulk MOSFET,” *IEEE Trans. Electron Devices*, vol. 61, no. 2, pp. 234–244, 2014.
- [2] Y. Tsividis, *Operation and Modeling of the MOS Transistor 2nd ed.* Oxford, 1999.
- [3] Y. S. Chauhan, M. A. Karim, S. Venugopalan, S. Khandelwal, P. Thakur, N. Paydavosi, A. Sachid, A. B. and Niknejad, and C. Hu, “BSIM6:Symmetric Bulk MOSFET Model,” *Workshop on Compact Modeling, Santa Clara, USA*, June 2012.
- [4] J.-M. Sallese, M. Bucher, F. Krummenacher, and P. Fazan, “Inversion charge linearization in mosfet modeling and rigorous derivation of the ekv compact model,” *Solid-State Electronics*, vol. 47, no. 4, pp. 677–683, April 2003.
- [5] F. Pregaldiny, F. Krummenacher, B. Diagne, F. Pecheux, J.-M. Sallese, and C. Lallement, “Explicit modeling of the double-gate mosfet with vhdl-ams,” *International Journal of Numerical Modelling: Electronic Networks, Devices and Fields*, vol. 19, no. 3, pp. 239–256, May 2006.
- [6] C. K. Dabhi et al., “*BSIM4 4.8.1 MOSFET model*,” *Univ. California, Berkeley, Berkeley, CA, USA, Tech. Rep., 2017.* publisher = , URL = <http://www-device.eecs.berkeley.edu/bsim/>.
- [7] C. C. Hu, *Modern Semiconductor Devices for Integrated Circuits.* Pearson Education, 2010.
- [8] *MOS Model 11 manual.* [Online]. Available: <https://www.nxp.com/wcm-content/documents/models/mos-models/model-11/m1102.pdf>
- [9] H. Agarwal, C. Gupta, P. Kushwaha, C. Yadav, J. P. Duarte, S. Khandelwal, C. Hu, and Y. S. Chauhan, “Analytical Modeling and Experimental Validation of Threshold Voltage in BSIM6 MOSFET Model,” *IEEE Journal of the Electron Devices Society*, vol. 3, no. 3, pp. 240–243, 2015.
- [10] S. Khandelwal and H. Agarwal and J. P. Duarte and K. Chan and S. Dey and Y. S. Chauhan and C. Hu, “Modeling STI Edge Parasitic Current for Accurate Circuit Simulations,” *IEEE Transactions on Computer-Aided Design of Integrated Circuits and Systems*, vol. 34, no. 8, pp. 1291–1294, 2015.

- [11] Y. K. Lin, S. Khandelwal, A. Medury, H. Agarwal, H. C. Chang, Y. S. Chauhan, and C. Hu, “Modeling of Sub-surface Leakage Current in Low V_{th} Short Channel MOSFET at Accumulation Bias,” *appearin in IEEE Transactions on Electron Devices*, 2016.
- [12] K. K. Hung, P. Ko, and Y. C. Cheng, “A physics-based mosfet noise model for circuit simulator,” *IEEE Transaction on Electron Devices*, vol. 37, no. 5, pp. 1323–1333, 1990.
- [13] H. Agarwal, S. Khandelwal, S. Dey, C. Hu, and Y. S. Chauhan, “Analytical modeling of flicker noise in halo implanted mosfets,” *IEEE Journal of the Electron Devices Society*, vol. 3, no. 4, pp. 355–360, July 2015.
- [14] H. Agarwal, C. Gupta, S. Khandelwal, C. Hu, S. Dey, K. Chan, and Y. S. Chauhan, “Analysis and modeling of low frequency noise in presence of doping non-uniformity in mosfets,” in *International Conference on Emerging Electronics (ICEE)*. IEEE, 2016.
- [15] A. Sharma, Y. H. Zarkob, R. Goel, C. K. Dabhi, G. Pahwa, C. Hu, and Y. S. Chauhan, “Recent enhancements in the standard bsim-bulk mosfet model,” in *2022 IEEE International Conference on Emerging Electronics (ICEE)*, 2022, pp. 1–6.
- [16] A. J. Scholten, R. Langevelde, L. F. Tiemeijer, and D. B. M. Klaassen, “Compact modeling of noise in cmos,” in *CICC*, 2006.
- [17] H. Agarwal, S. Venugopalan, M.-A. Chalkiadaki, N. Paydavosi, J. P. Duarte, S. Agnihotri, C. Yadav, P. Kushwaha, Y. S. Chauhan, C. C. Enz, A. Niknejad, and C. Hu, “Recent enhancements in BSIM6 bulk MOSFET model,” in *IEEE Simulation of Semiconductor Processes and Devices*, 2013.
- [18] R. A. Bianchi, G. Bouche, and O. Roux-ditBuisson, “Accurate modeling of trench isolation induced mechanical stress effect on mosfet electrical performance,” in *2007 Symposium on VLSI Technology*, 2007.
- [19] T. Hook, J. Brown, P. Cottrell, E. Adler, D. Hoyniak, J. Johnson, and R. Mann, “Lateral ion implant straggle and mask proximity effect,” *IEEE Transaction on Electron Devices*, vol. 50, no. 9, pp. 1946–1951, 2003.
- [20] *Compact Model Council*. [Online]. Available: <http://www.geia.org/index.asp?bid=597>

- [21] H. Agarwal, C. Gupta, R. Goel, P. Kushwaha, Y. . Lin, M. . Kao, J. . Duarte, H. . Chang, Y. S. Chauhan, S. Salahuddin, and C. Hu, “Bsim-hv: High-voltage mosfet model including quasi-saturation and self-heating effect,” *IEEE Transactions on Electron Devices*, vol. 66, no. 10, pp. 4258–4263, Oct 2019.

27 Acknowledgements

We deeply appreciate the feedback we received from (in alphabetical order):

Shantanu Agnihotri(IIT Kanpur)

Maria Anna Chalkiadaki(EPFL)

Kaiman Chan (TI)

Brian Chen (Accelicon)

Sergey Cherepko (ADI)

Geoffrey Coram (ADI)

Krishnanshu Dandu (TI)

Anupam Dutta (IBM)

Christian Enz (EPFL)

Keith Green (TI)

Andre Juge (ST)

Tracey Krakowski (TI)

Francois Krummenacher (EPFL)

Pragya Kushwaha (IIT Kanpur)

Waikit Lee (TSMC)

Samuel Mertens (Agilent)

Saurabh Sirohi (IBM)

Jing Wang (IBM)

Joddy Wang (Synopsys)

Wenli Wang (Cadence)

Josef Watts (IBM)

Richard Williams (IBM)

Weimin Wu (TI)

Jane Xi (Synopsys)

Jushan Xie (Cadence)

Chandan Yadav(IIT Kanpur)

Fang Yu (Synopsys)
Fulong Zaho (Cadence)

Manual created: October 17, 2023